APRIL 2022

M.Sc. in Civil Engineering

Fulya GÖKSULAR

REPUBLIC OF TURKEY

HASAN KALYONCU UNIVERSITY

GRADUATE EDUCATION INSTITUTE

MAPPING GEOTECHNICAL PROPERTIES USING GEOGRAPHICAL INFORMATION SYSTEM: A CASE STUDY OF SİİRT CITY

M.Sc. THESIS

IN

CIVIL ENGINEERING

by

FULYA GÖKSULAR

2022

Mapping Geotechnical Properties Using Geographical Information System: A Case Study of Siirt City

M.Sc. Thesis

In

Civil Engineering

Hasan Kalyoncu University

Supervisor

Assist. Prof. Dr. Nurullah AKBULUT

by

Fulya GÖKSULAR

April 2022

GRADUATE EDUCATION INSTITUTE
M.Sc. ACCEPTANCE AND APPROVAL FROM

Civil Engineering Department, Civil Engineering Master programme student **Fulya Göksular** prepared and submitted the thesis titled **"Mapping Geotechnical Properties Using Geographical Information System: A Case Study of Siirt City"** defended successfully at the VIVA on the date of 12/04/2022 and accepted by the jury as a M.Sc. thesis.

Position	**Title, Name and Surname** **Department/University**	**Signature:**
Thesis Advisor	Assist. Prof. Dr. Nurullah AKBULUT Civil Engineering Department Hasan Kalyoncu University	
Jury Chair	Prof. Dr. Hanifi ÇANAKCI Civil Engineering Department Hasan Kalyoncu University	
Jury Member	Assoc. Prof. Dr. M. Eren GÜLŞAN Civil Engineering Department University of Gaziantep	

This thesis is accepted by the jury members selected by institute management board and approved by institute management board.

Prof. Dr. İbrahim Halil GÜZELBEY
Director

I hereby declare that all information in this document has been obtained and presented in accordance with academic rules and ethical conduct. I also declare that, as required by these rules and conduct, I have fully cited and referenced all materials and results that are not original to this work.

Fulya GÖKSULAR

ABSTRACT

MAPPING GEOTECHNICAL PROPERTIES USING GEOGRAPHICAL INFORMATION SYSTEM: A CASE STUDY OF SİİRT CITY

GÖKSULAR, Fulya
M.Sc. In Civil Engineering
Supervisor: Assist. Prof. Dr. Nurullah AKBULUT
April 2022
83 Pages

Siirt is one of the most important cities in the Southeastern Anatolian Region. The faults around the Southeast Anatolian and neighbouring has generated severe earthquakes in the study area. In this study, mapping of the geotechnical properties by Geographical Information System in Siirt Central District is aimed to be presented. The city center of Siirt is situated at 37^{o} 55' 38" North and 41^{o} 56' 31" East coordinates and is influenced by active faults connected to the Eastern Anatolian Fault Zone and Southeast Anatolian Thrust. The main goal was to provide ease of access to geotechnical data in the field of engineering, to support the workforce and to increase the efficiency. A total of 178 borehole points was obtained from the soil investigation reports of Siirt Environment and Urbanization Directorate. Geotechnical maps were created by transferring the field and laboratory test results which were obtained from the soil investigation reports to ArcGIS software by means of Geographic Information System. Calculations, mapping and analysis of SPT-N, bearing capacity, shear wave velocity, soil amplification, dominant vibration period and soil classifications according to NEHRP, EUROCODE8 and TBDY-2019 earthquake codes were made. Bearing capacity calculations were made in 4 different methods according to geophysical and geotechnical approaches. Both approaches have shown a great difference when have compared. Also, shear wave velocity values have been calculated and compared according to different scientist in the literature. Furthermore, many other maps and analysis were made, which will be available online in the Siirt Municipality. This analysis will save time and help the workforce in future studies.

Keywords: GIS, Siirt, geotechnical properties, mapping.

ÖZET

COĞRAFİ BİLGİ SİSTEMİYLE GEOTEKNİK VERİLERİN HARİTALANDIRILMASI: SİİRT İLİ ÖRNEĞİ

GÖKSULAR, Fulya
Yüksek Lisans İnşaat Mühendisliği
Danışman: Dr. Ögr.Üyesi Nurullah AKBULUT
Nisan 2022
83 Sayfa

Siirt, Güneydoğu Anadolu Bölgesi'nin en önemli şehirlerinden biridir. Güneydoğu Anadolu ve çevresindeki faylar çalışma alanında şiddetli depremlere neden olmuştur. Bu çalışmada Siirt Merkez ilçesindeki geoteknik özelliklerin Coğrafi Bilgi Sistemi ile haritalanması amaçlanmıştır. Siirt il merkezi 37^{o} 55' 38" Kuzey ve 41^{o} 56' 31" Doğu koordinatlarında yer almakta olup, Doğu Anadolu Fay Zonu ve Güneydoğu Anadolu Bindirmesi ile bağlantılı aktif faylardan etkilenmektedir. Tezin temel amacı mühendislik alanında geoteknik verilere erişim kolaylığı sağlamak, işgücünü desteklemek ve verimliliği arttırmaktır. Siirt Çevre ve Şehircilik Müdürlüğü'nün zemin etüt raporlarından toplamda 178 sondaj noktası elde edilmiştir. Zemin etüt raporlarından elde edilen saha ve laboratuvar deney sonuçlarının Coğrafi Bilgi Sistemi üzerinden ArcGIS yazılımına aktarılmasıyla geoteknik haritalar oluşturulmuştur. Zemin sınıflandırma haritaları; NEHRP, EUROCODE8 ve TBDY-2019 deprem kodlarına göre üretilmiş olup, SPT-N, taşıma kapasitesi, kayma dalga hızı, zemin büyütmesi ve hâkim titreşim periyodu haritaları, hesaplamaları ve analizleri yapılmıştır. Taşıma kapasitesi hesaplamaları jeofizik ve geoteknik yaklaşımlara göre dört farklı yöntemle yapılmıştır. Bu iki bilim dalının yaklaşımları kıyaslandığında önemli bir fark olduğu gözlemlenmiştir. Ayrıca literatürdeki farklı yaklaşım ve formasyonlar göre kayma dalga hızı değerleri hesaplanmış ve karşılaştırılmıştır. Gelecekteki çalışmalara zaman kazandırmak ve işgücüne yardımcı olmak amacıyla birçok harita ve analiz yapılarak literatüre katkı sağlanması hedeflenmiştir.

Anahtar Kelimeler: CBS, Siirt, geoteknik özellikler, haritalandırma.

My precious family…..

ACKNOWLEDGEMENTS

I would like to thank my academic advisor Assist. Prof. Dr. Nurullah AKBULUT, for guiding me, helping me complete my master's degree, and great support during the thesis preparation process.

I would like to thank my dear colleague Bahadır KARABAŞ, who contributed to my thesis with his suggestions and guidance, and helped with his constructive and guiding ideas in the preparation of my master's thesis.

I would like to thank the Siirt Municipality Directorate of Reconstruction and Urbanization, for enabling us to use the necessary resources to create the database, and to the geological engineer Muhammed Kutsal GÜLDOĞAN for transmitting the necessary data.

To my family who have always been with me in the preparation of this thesis; I would like to thank my father Adil GÖKSULAR, my mother Belgin GÖKSULAR, my sister Rana GÖKSULAR, and my brothers Ali GÖKSULAR and Ömer GÖKSULAR. I would also like to thank my friends for their support during the thesis phase.

TABLE OF CONTENTS

Page No

ABSTRACT v
ÖZET vi
ACKNOWLEDGEMENTS viii
TABLE OF CONTENTS ix
LIST OF TABLES xi
LIST OF FIGURES xii
ABBREVIATIONS OR SYMBOLS LIST xv
1 **INTRODUCTION** 1
1.1 General 1
1.2 Objectives of the Study 2
1.3 Research Area 2
2 **LITERATURE REVIEW** 5
2.1 General 5
2.2 GIS (Geographic Information System) 5
2.3 Case Studies Related to GIS 10
2.4 Introduction of the Study Area 16
2.4.1 Geomorphological and Environmental Information 16
2.4.2 Climate Information 17
2.4.3 Natural Disaster Hazards 17
2.4.3.1 Earthquake Status 17
2.4.3.1.1 Earthquake Hazard and Risk Analysis of the Siirt Region 18
2.4.3.2 Disaster Status 19
2.4.4 Hydrogeology 20
2.4.4.1 Streams 20
2.4.4.2 Groundwater 20
2.4.5 Geology 21
2.4.5.1 Regional Geology 21
2.4.5.1.1 Silvan Group: Lower Miocene 22
2.4.5.1.2 Gercüş Formation 23
2.4.5.1.3 Midyat Formation 24
2.4.5.1.4 Germik Formation 24
2.4.5.1.5 Young Sediments 25

2.4.5.1.6 Şelmo Formation: Upper Miocene 26
2.4.5.2 Structural Geology and Active Tectonics 27
2.4.6 Geophysical Studies 28
2.4.6.1 Shear Wave (Vs) Velocity by Multi-Channel Surface Wave Analysis Method (MASW-MAM) 29
3 **MATERİALS AND METHODS** 30
3.1 Standard Penetration Test 30
3.2 Bearing Capacity 31
3.2.1 Field Tests and Bearing Capacity Calculation Methods 32
3.2.1.1 Terzaghi and Peck (1967) Method 32
3.2.1.2 Meyerhof (1974) Method 33
3.2.2 Bearing Capacity Calculation Methods with Geophysical Methods 34
3.2.2.1 Keçeli Bearing Capacity Calculation 34
3.2.2.2 Tezcan et al. Bearing Capacity Calculation 34
3.3 Shear Wave Velocity 35
3.4 Soil Classification by NEHRP 36
3.5 Earthquake Hazard by Soil Amplification 37
3.6 Soil Dominant Vibration Period (To) 38
3.7 Soil Classifications Calculation According to Eurocode 8 39
3.8 Local Soil Class According to TBDY-2019 40
4 **RESULTS AND DISCUSSION** 41
4.1 SPT-N Calculation Analysis 41
4.2 Bearing Capacity Calculation Analysis 47
4.3 Shear Wave Velocity Calculation Analysis 53
4.3.1 Shear Wave Velocity Analysis 30 m 64
4.4 NEHRP (U.S.A.) Soil Classification Analysis According to Earthquake Code 66
4.5 Earthquake Hazard Level Analysis According to Soil Amplification Calculation 67
4.6 Dominant Vibration Period Analysis 69
4.7 Soil Classifications Analysis According to Eurocode 8 70
4.8 Local Soil Class According to TBDY-2019 72
5 **CONCLUSIONS AND RECOMMENDATIONS** 74
6 **REFERENCES** 78

LIST OF TABLES

Page No

Table 2.1 Siirt Province Climate Table 17
Table 2.2 Streams of Siirt Province 20
Table 3.1 The empirical correlation based on SPT-N and Vs 36
Table 3.2 Soil classification criteria according to NEHRP 37
Table 3.3 Soil classification criteria according to Eurocode8 39
Table 3.4 Local Soil Class According to TBDY-2019 40

LIST OF FIGURES

Page No

Figure 1.1 The Map of Siirt 3
Figure 2.1 Components of Geographic Information System 6
Figure 2.2 GIS Working 7
Figure 2.3 Geographic Information System 10
Figure 2.4 Turkey Earthquake Risk Map 18
Figure 2.5 The city of Siirt earthquake zone 19
Figure 2.6 Geological Map of Siirt and its Surroundings 22
Figure 2.7 Generalized stratigraphic column section of the Southeast Anatolian autochthon 23
Figure 2.8 Gercüş Formation (Pgg) 24
Figure 2.9 Germik Formation 25
Figure 2.10 Alluvium (Qal), Germik formation (Pgge) 26
Figure 2.11 Şelmo Formation 27
Figure 3.1 Sketch of Standard Penetration Test Instrumentation 30
Figure 3.2 Change of allowable bearing capacity according to foundation width and SPT-N 33
Figure 4.1 Study area 41
Figure 4.2 SPT-N in study area (1-3 m) 42
Figure 4.3 SPT-N in study area (3-5 m) 43
Figure 4.4 SPT-N in study area (5-7m 44
Figure 4.5 SPT-N in study area (7-9 m) 45
Figure 4.6 SPT-N in study area (9-11 m) 46
Figure 4.7 Comparison chart of SPT-N values according to boring depths 46
Figure 4.8 Bearing capacity map according to Keçeli method (1-3 m) 48
Figure 4.9 Bearing capacity map according to Tezcan et al. method (1-3 m) 48
Figure 4.10 Bearing capacity map according to Meyerhof method (1-3 m) 49
Figure 4.11 Bearing capacity map according to Terzaghi-Peck method ..... (1-3 m)…..... 50
Figure 4.12 Bearing capacity map according to Keçeli method (9-11 m) 51
Figure 4.13 Bearing capacity map according to Tezcan et al. method (9-11 m) 51
Figure 4.14 Bearing capacity map according to Meyerhof method (9-11 m) 52

Figure 4.15 Bearing capacity map according to Terzaghi-Peck method (9-11)..... 53
Figure 4.16 Comparison graph of shear wave velocity calculated results according to SPT-N values 1-3 m depth 54
Figure 4.17 Comparison graph of shear wave velocity according to seismic measurements and SPT-N values 1-3 m depth..... 55
Figure 4.18 Comparison graph of shear wave velocity calculated results according to SPT-N values 3-5 m depth 55
Figure 4.19 Comparison graph of shear wave velocity according to seismic measurements and SPT-N values 3-5 m depth..... 56
Figure 4.20 Comparison graph of shear wave velocity calculated results according to SPT-N values 5-7 m depth 56
Figure 4.21 Comparison graph of shear wave velocity according to seismic measurements and SPT-N values 5-7 m depth..... 57
Figure 4.22 Comparison graph of shear wave velocity calculated results according to SPT-N values 7-9 m depth 57
Figure 4.23 Comparison graph of shear wave velocity according to seismic measurements and SPT-N values 7-9 m depth..... 58
Figure 4.24 Comparison graph of shear wave velocity calculated results according to SPT-N values 9-11 m depth 58
Figure 4.25 Comparison graph of shear wave velocity according to seismic measurements and SPT-N values 9-11 m depth..... 59
Figure 4.26 Shear wave velocity map obtained from seismic measurements(1-3m)..... 60
Figure 4.27 Shear wave velocity map obtained from seismic measurements(3-5m)..... 61
Figure 4.28 Shear wave velocity map obtained from seismic measurements(5-7m)..... 62
Figure 4.29 Shear wave velocity map obtained from seismic measurements(7-9m)..... 63
Figure 4.30 Shear wave velocity map obtained from seismic measurements (9-11m)..... 64
Figure 4.31 Map of Shear wave velocity in 30m 65
Figure 4.32 Distribution of Vs_{30} values in the study area 65
Figure 4.33 Map of NEHRP soil classification..... 66
Figure 4.34 Distribution of soil classification values in the study area according to NEHRP..... 67
Figure 4.35 Hazard map according to soil amplification results..... 68
Figure 4.36 Distribution of hazard values in the study area according to soil amplification criteria 68
Figure 4.37 Map of dominant vibration period 69
Figure 4.38 Distribution of dominant vibration period 70
Figure 4.39 Soil classification map according to Eurocode 8 71
Figure 4.40 Distribution of soil classification values in the study area according to Eurocode 8 71

Figure 4.41 Local soil class map according to TBDY-2019 72
Figure 4.42 Distribution of local soil class values in the study area according to TBDY-2019 73

ABBREVIATIONS OR SYMBOLS LIST

A	Relative amplification coefficient
a_{maks}	Peak ground acceleration
ASTM	American society for testing and materials
BS	British standard
C_N	Overburden correction in SPT test
C_E	Stem bar energy ratio correction in SPT test
C_B	Borehole diameter correction in SPT test
C_R	Stem bar(rod) length correction in SPT test
C_S	Inner tube(sampler) correction in SPT test
D	Disturbed sample
Er	Stem bar energy ratio for SPT test
FS	Factor of safety
g	Gravity acceleration (cm/s^2)
NEHRP	National earthquake hazard reduction program
Pa	Atmospheric pressure 100 kPa
q_a	Allowable bearing capacity (kg/cm^2)
R	Radius of earth epicenter (km)
UD	Undisturbed sample
SPT	Standard penetration test
Vp	Compression wave velocity (m/sec)
Vs	Shear wave velocity (m/sec)
α, β	The coefficients to correct $(N_1)_{60}$ based on fine content values
τ_{av}	Average horizontal shear as a result of earthquake
To	Soil dominant vibration period (sec)
γ	Unit weight (kN/m^3)

CHAPTER 1

INTRODUCTION

1.1 General

New lives are constantly added to the ever-evolving and changing world order. Due to the ever-increasing human population, it is necessary to carry out new construction. The safety of human lives must be the priority when it comes to new construction. It is difficult to ensure this safety when it comes to a location where ground data is not available. That is why it is very important to know the soil on which the constructions will be carried out and act in accordance with their functions.

The soil is a layer that is constantly exposed to static and dynamic loads. Many parameters such as the structure of the soil, its classification, resistance, water flow between the soil layers and the active and passive soil pressures constitute the behaviour of the soil. Therefore, there are laboratory and field experiments in order to determine the type and behavior of the soil.

Nowadays, access to information transferred to digital media is very easy. When one wishes to access field and laboratory experimentsi the results can be presented to a small audience. Digitizing of the experiments performed can appeal to larger audiences by providing ease of access to the data.

A Geographic Information System (GIS) is a system of computer software, hardware and data, personnel that make it not impossible to enter, manipulate, analyze, and present data, and the information that is tied to a location on the earth's surface. This system comprises of Software, Hardware, Data, and Personnel that make it not impossible to enter, manipulate, analyze and present information that is tied to a location on the earth's surface. Definition of Geographic Information System (GIS)

There are various definitions for Geographic Information System, each developed from a different perspective or disciplinary origin. Some focus on the map connection, some stress the database or the software tool kit and others emphasis applications such as decision support. Defining a GIS can be done by either explaining what it can do or by looking at the components. Both are important to really understand a GIS and use it optimally. (Lemmens, 2011; Sarkar, 2019)

GIS finds its strongest applications in resources management, utilities management, telecommunications, urban and regional planning, vehicle routing and parcel delivery, and in all of the sciences that deal with the surface of the Earth. Geographic Information System is a system of hardware, software, data, people, organizations and institutional arrangements for collecting, storing, analyzing and disseminating information about areas of the earth. (Lemmens, 2011; Sarkar, 2019)

Using the established Geographical Information System, the aim is to transfer the ground data to the software and provide easy access to the soil information of the structures that will be built in the future.

1.2. Objectives of the Study

In this study, the bearing capacity of the soil, soil classification, shear wave velocity (Vs30), Standard Penetration Tests (SPT), were investigated with the data obtained from the studies conducted by the Municipality of Siirt.

The aim of the thesis is to produce color maps by transferring the drilling data in the soil survey reports obtained from the Siirt Municipality zoning department to a digital environment and processing them in the ArcGIS program. The ArcGIS software is a geographic information system. It is aimed to transfer the soil characteristics of Siirt province to digital media by making use of this system.

1.3. Research Area

Siirt province is located in the Southeastern Anatolia Region of Turkey, between 41^{o} – 42^{o} east longitudes and 37.45^{o} - 38.15^{o} northern latitudes. Siirt province has an area

of 6186 km 2 and a population of 332 thousand according to 2018 census data. (Doğruyol, 2021)

Although the surrounding area of Siirt province is surrounded by active fault lines, there is no effective earthquake focal point within the city limits. However, Southeastern Anatolia and its surroundings are a region where seismic activity is intense in general. The seismic activity of the region is caused by the relative movements of the Arabian and African plates to the north. These movements create a thrust effect in the region. The two important seismo-tectonic structures in the region are the Southeast Anatolian Wedge and the northward movement of the Arabian Plate and the Anatolian Plate, and the Southeast Anatolian Fault, located just north of the region. The deformation energy accumulated in the region is mostly released by earthquakes that develop through these two seismotectonic structures. For this reason, when evaluating the earthquake potential of any region, it is necessary to know the active fault and local soil characteristics that lead to an earthquake well. (SMDRU, 2020)

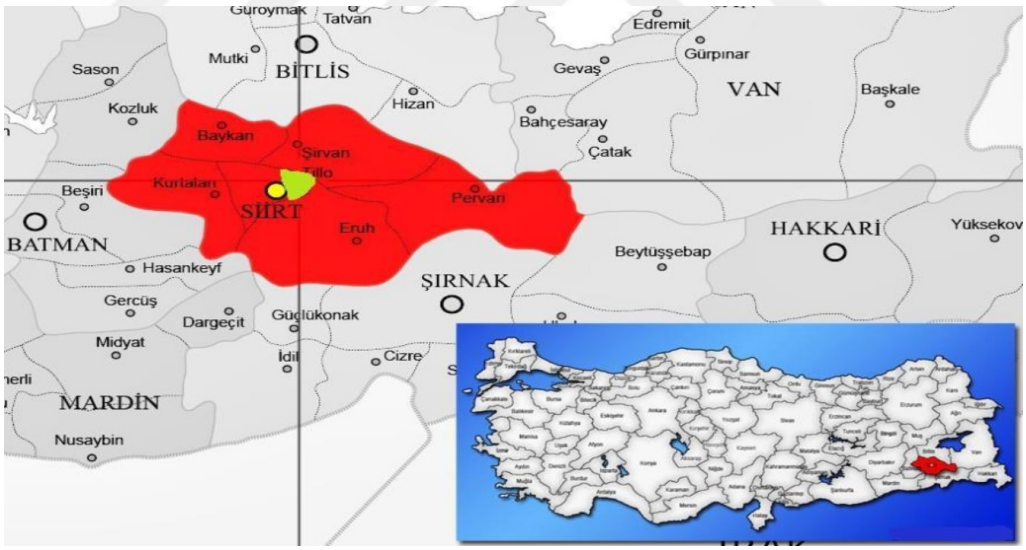

Figure 1.1 The Map of Siirt (Ege, 2019)

A large part of the territory of Siirt province is covered with mountains, and the terrain has a rugged and rolling structure. Continental climate characteristics are observed in the Southeastern Anatolia Region, Siirt province and its surroundings. Summers are very hot and dry, winters are cold and rainy. Siirt province is located at the northeastern end of the Southeastern Anatolia Region, it rises suddenly after the

plains of the region and therefore abundant precipitation is observed in the northern and eastern parts. The Siirt province area constitutes one of the important water catchment areas of the Tigris River. The Botan Stream flows from the east and south of Siirt and Kezer Stream flows from the west. The total annual average flow of these two headwaters is about 6.2 billion m3/year. The natural flow regimes of streams are very irregular. Maximum currents are 550-600 times the minimum currents. This leads to erosion and downstream flooding. (SMDRU, 2020)

CHAPTER 2

LITERATURE REVIEW

2.1. General

Data management holds an important position in this day and age. In data management, the point of origin of the data, the determination of its accuracy, its presentation and, in particular, its accessibility is considered. In this thesis, the data was presented to manking with the Geographical Information System. The Geographic Information System is used in many fields. In this study, other studies related to GIS were also examined.

2.2. GIS (Geographic Information System)

This mapping concept emerged for the first time in 1832 with the mapping of the cholera epidemic in Paris by Charles Picquet. Later, in 1854, when physician John Snow spatially analyzed the same cholera epidemic, the concept of spatial analysis also emerged. Finally, in the 1960s, when Canada used computers to collect natural resource data, the geographic information systems, which we now call GIS, emerged. (Yasobant, Vora and Upadhyay, 2019)

Geographical Information Systems (GIS) can be defined in different ways due to their use by very different disciplines. For example, while Geographic Information Systems may appear for reserve calculations for a mining engineer, it may be encountered for landscape planning in the eyes of a landscape architect. In other words, Geographic Information Systems, in some occupational groups, can be named as the transfer of geographical information to the system in a processable form, whereas in some occupational groups, it can be named as obtaining products by analyzing this processable data. However, despite these different interests and perspectives, if it is necessary to define Geographic Information Systems; 'It is a

system of hardware, software and methods that covers the scope, management, processing, analysis, modeling and display of the data located in a space designed to solve complex planning and management problems. (Töreyen et al., 2010)

Figure 2.1 Components of Geographic Information System (Töreyen et al, 2010)

In order for a system, an application, or any work to survive and function, there are certain requirements. Some requirements, components or elements are necessary in order for Geographic Information Systems to also function and benefit from the advantages it provides at the highest level:

Data: Operations cannot be performed without data in Geographic Information Systems. Because data is the essence of this system in a way and is one of the indispensable components of Geographical Information Systems.

Software: Data, one of the components of Geographic Information Systems, is not sufficient for this system to function. There is a need for software with which data can be processed and analyzed. Because of this requirement, another indispensable component of Geographic Information Systems is software.

Method: Successful operations in studies that will be carried out in Geographical Information Systems and are different from each other are realized by determining healthy methods. This method or methods to be determined must also be designed and planned very well so that the desired products can be produced both in the personal and institutional areas.

Hardware: Geographic Information Systems today can work on computers with very different hardware. However, in order to obtain maximum performance from the relevant software of Geographic Information Systems, computer hardware must also be of high quality.

People: Although the above-mentioned components in Geographical Information Systems are indispensable elements in the system, they have no function without the human component. Because GIS is a human oriented decision-support system. People prepare a plan for the work carried out as decision makers and system developers in solving problems. Therefore, in order for Geographic Information Systems to function, managers and personnel trained in this regard are required. (Töreyen et al, 2010)

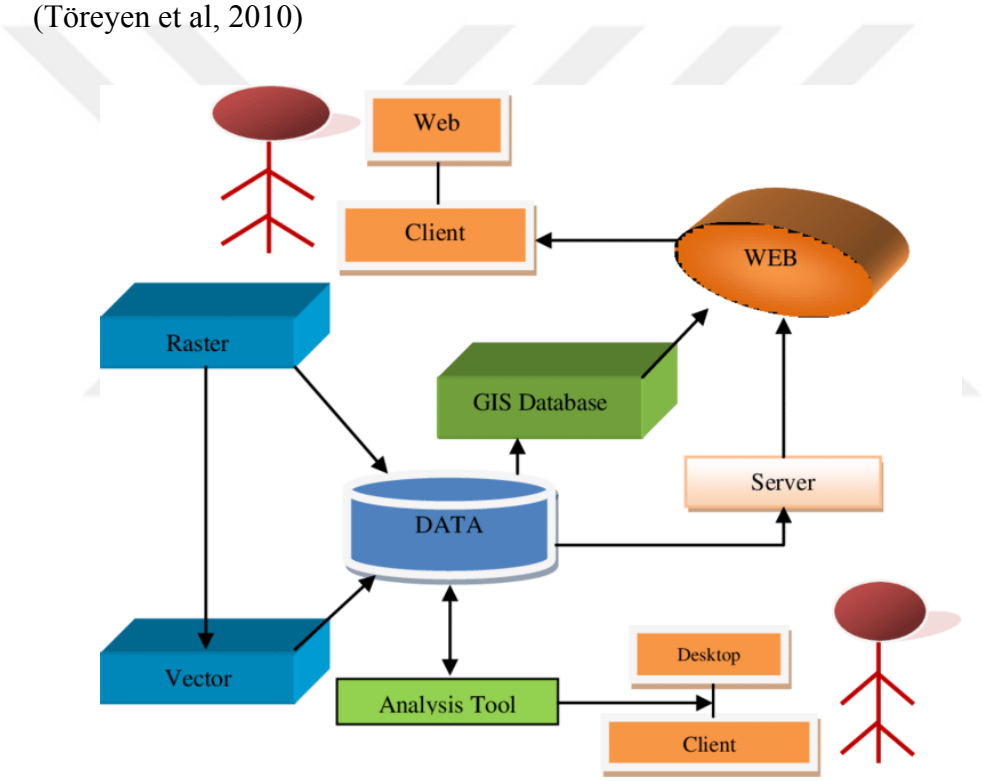

Figure 2.2 GIS system architecture (Qayum, 2015)

There are various definitions of geographic information and the systems that are used to store, retrieve, analyse and display data that are represented spatially or geographically. (Goodchild 1992, 2009, 2018).

From computer mapping to spatial analysis and then to geographic problem solving, GIS embraces ideas about how we use our cognition to understand spatial configurations and perceptions (Mark et al., 1999).

GIS has thus focused on three main aims: acquiring geographic information, studying geo-objects and their relationships and exploring advanced geographic rules that determine our spatiotemporal behaviour (Lin et al., 2013).

Computer mapping and related tools are basic GIS functions that have provided users with 2D/3D visual and digital images of the physical world, with extensions to 4D along the time dimension. (Crampton, 2011).

Combined with spatial statistics, spatial analysis has pushed GIS well beyond basic mapping applications to provide users with logic for understanding spatiotemporal distributions and relationships (Shaw et al., 2008).

Geographical analysis models, which play an important role in geographic simulation and experimentation, have been increasingly integrated into GIS for decision support and prediction, particularly for dynamic geographic processes, such as emergencies and disasters, and for detailing future scenarios in specific domains (Shi and Liu, 2014).

GIS includes many and important features such as database management, analysis and modeling capability, and decision support mechanism during studies. It is not easy to limit the benefits of Geographic Information Systems. However, a few examples can be given in terms of the benefits of GIS;

- It speeds up the flow of information.
- It provides more efficient production management.
- It increases work efficiency.
- It provides effective and accurate analysis.
- It provides ease of data updating.
- It increases the workforce.
- It prevents time wasting.

Nowadays, the number of areas where Geographical Information Systems are not used is quite small. The increase in the human population and the fact that cities are growing more and more each day also increases the amount of data that emerges.

GIS, which offers the opportunity to select and process the appropriate data among an intense data flow, is expanding its usage areas each and every day (Maptriks, 2020).

GIS focus on the acquisition, processing, storage and analysis of geographic data that are treated as core objects. Spatiotemporal data management and sharing have drawn considerable attention and have become relatively well developed. However, with the spread of professional applications and the increasing amount of attention paid to the analysis of the mechanisms and processes of comprehensive geographic phenomena, GIS with spatial data at its core and spatial analysis as its main function has a limited capacity for dynamic modelling and solving complex geographic problems. Therefore, GIS should translate beyond the loosely bounded 'information system' stage and evolve into an integrated and open geographic analysis systems (O'Sullivan and Unwin, 2010; Crooks and Castle, 2011).

If some of the usage areas are summarized as articles;

- Cartography
- Asset management and maintenance
- Community development through planning
- Water and sewerage distribution and network management
- Education
- Transportation management and planning
- Environmental impact analysis
- City planning and management
- Economy
- Industry
- Measurement and evaluation of land
- Municipality
- Health
- Disaster management and pre-disaster analysis, precautions
- Earth sciences

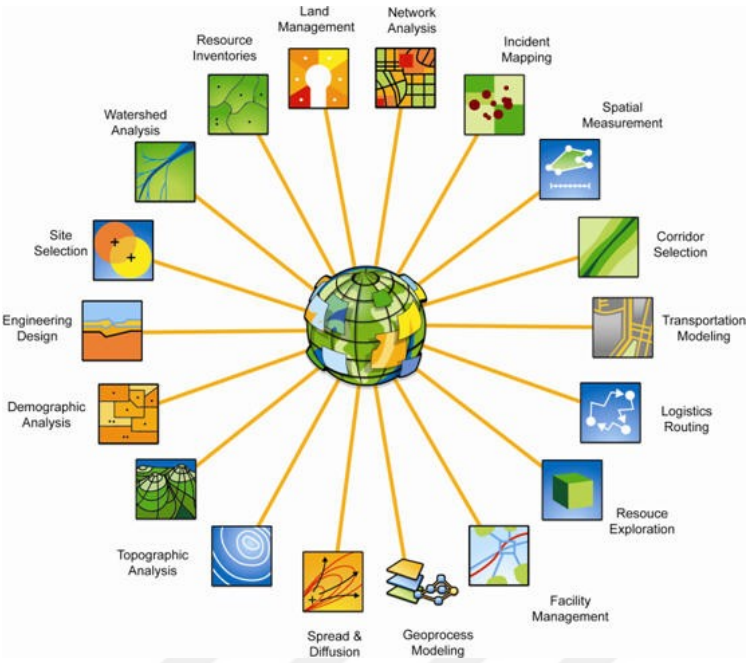

Figure 2.3 Geographic Information System (Grants Pass, 2022)

2.3 Case Studies Related to GIS

Consistency limits and plasticity of the soil are one of the basic soil parameters that reflect the physical properties of fine-grained soil sand provide important information about their engineering properties. It is extremely important to correctly define the consistency parameters that are in the standard input state of all soil survey and study programs. (Uzman et al., 2003) Modern Geographic Information Systems (GIS) are used to show the distribution of liquid limit, plastic limit, bearing capacity, liquefaction potential, spectral acceleration distribution, seismic microzonation, soil classifications, etc., which are extremely important in terms of Geotechnical Engineering, by taking advantage of the developments in today's technology. Thanks to Geographical Information Systems, it is possible to express the soil characteristics and parameters of the natural soil structure that differ at each point in its geographical location and to compare them depending on their geographical location. Because GIS has a wide range of applications, it is sometimes referred to by different names such as LIS (Land Information System), EIS (Engineering Information System, Environmental Information System), PIS (Planning Information System), RIS (Resource Information System). All these types can be named "Spatial-Based Information Systems". (Uzman et al., 2003) In this study (Uzman et al., 2003); by

using the consistency limit test results made with the samples taken from the drillings in Bakırköy district, they used "Modern Geographic Information System (GIS) technology to show the soil profile of the region under investigation, and by defining the drilling points of the region, liquid limit, plasticity index and soil class maps were produced with the help of GIS program.

Kuruoğlu (2004), in his doctoral dissertation, developed a soil dynamics database based on the geographical information system (GIS) and conducted one-dimensional dynamic analysis of local soil behavior for the northern coast of the Gulf of Izmir. They recorded a large number of geotechnical data in the soil dynamics database. They contributed to the development of DISO 7.0, the GIS-based dynamic interface software developed within the scope of a research project, and explained that they calculated the dynamic soil parameters necessary for local soil behavior analysis with DISO 7.0. They stated that they prepared surface models of dynamic parameters using ArcView 3D Analyst by examining the results of dynamic analysis within the framework of the national earthquake regulation.

In another study (Kuruoglu et al.), they prepared their scientific research on “Development of a soil dynamics database based on a Geographical Information System (GIS) and dynamic analysis of the soil of the northern coast of the Gulf of Izmir” in order to introduce and convey the results they have achieved. The aim of the study is to develop a method for the analysis of large-volume geotechnical findings obtained by conducting soil surveys, taking into account the principles of soil dynamics and basic engineering, and for their presentation using the possibilities of the Geographical Information System (GIS). The aim of the developed method is to apply it to the coastal areas of Karşıyaka and Bornova districts, which were selected as pilot regions in the study, located in the north of Izmir Province and which have a coast to the Gulf of Izmir. Geotechnical data obtained from a total of 238 drilling wells and 106 CPT experimental locations were collected in the “Geotechnical Features Database” developed in the Access environment. From the collected data, tables such as Geotechnical Properties Database Drilling Locations Table, SPT Data and Index Properties Table, Undisturbed Samples Data Table, CPT Locations Table, CPT Data Table were created. They have defined their own identification number for each drilling location and CPT location. They also carried out the process of connecting the soil data stored in the database to geographical

coordinates simultaneously. Thus, geotechnical data stored in the database is associated with geographical coordinates.

In the study, Özcep (2006) examined the regional and local seismicity using geophysical (seismological) and geological data. They emphasized that the soil/rock response should be developed at an advanced level using computer modeling, and used one-dimensional linear and nonlinear analysis, and two-three-dimensional analysis at this stage. In addition, they also used dynamic laboratory tests on soil samples for analysis at this stage.

In their study, Pekkan (2006) stated that they interpreted the results obtained from ground drilling, SCPT (Seismic Cone Penetration Test), field studies and laboratory experiments with the help of Geographical Information System (GIS) in his study. As a result of the study, they emphasized that the maps they created were geology map, soil grain size distribution map, soil type map, groundwater level map, N60 data maps, shear rate (Vs) map and liquefaction potential maps.

Alkaya et al. (2011), on the other hand, stated that the use of information technologies in urban management has become a necessity in order to ensure healthy urbanization. It was concluded that by using Geographical Information Systems in urbanization studies related to civil engineering such as zoning, infrastructure, land arrangement related to urbanization, and the establishment and continuous updating of the city information system will enable the city authorities to make the right decisions for the future, such as land planning and land production, and that the repetition of work will decrease due to the benefit of all institutions from the existing information infrastructure. 90% of the activities of local administrations and municipalities that are active in city administration are related to land and land use and planning. Land values are affected not only by the commercial structure of the city, but also by the geotechnical conditions that define the ground conditions of the city. Earthquake risk analysis in cities located within earthquake zones is an integral component of the city information system. It has been concluded that the city information system that will be established after the compilation of geotechnical data will be more useful in solving the problems of the city such as disaster planning, land use. (Alkaya et al., 2011)

Geotechnical results obtained from construction site and laboratory experiments are very important for the safe and economical design of building and infrastructure works in land development projects. Providing geotechnical data in formats useful for planners, land development specialists and engineers for processing provides convenience for the use of GIS. This article describes the use of GIS for storing, analyzing geotechnical data and presenting it to planners, architects and engineers in a format that will help them make better decisions and make safer and economical designs. (W.N.S. Wan-Mohamad and A.N. Abdul-Ghani, 2011). The study is based on the Seri Iskandar district of the Tengah Region of Perak. They conducted evaluations for a study in Seri Iskandar, Perak Tengah, Perak, Malaysia. Wan and Ghani (2011) conducted their studies in four field areas: Bandar Baru Seri Iskandar, UiTM Perak, Latihan Kemas Seri Iskender and Hükümet Neighbourhoods. Around fifteen boreholes were produced from these four field sites. Soil types were determined and tables were created by considering the standard penetration test for various depths from 3m, 5m, 10m, 20m and 25m. The data stored in the GIS systems are processed and made into maps with ground types and ground strengths (SPT values) at various depths. Thus, the data is always readily and rapidly available.

Geotechnics, which is a sub-branch of Civil Engineering, is an engineering discipline that deals with the determination of the physical and mechanical properties of the soil on which engineering structures are located. (Gündüz and Dağdeviren, 2009). Geotechnical data; is used to obtain information about the engineering properties of the soil before an earthquake and to determine the deformation forms such as liquefaction, loss of bearing capacity and settlement that may occur in the soil during an earthquake. In this study (Akdeniz et al., 2012), designed a geotechnical database of drilling and Seismic Cone Penetration Test (SCPT) data conducted on soils belonging to the Eskişehir region. Using this designed database, analyzes of soil problems such as liquefaction and loss of bearing capacity that may occur in the soil will also be performed. In addition, earthquake hazard maps can be created to determine geotechnically problematic soils. Within the scope of disaster damage mitigation studies, geotechnical characteristics of the soil of existing settlements or areas to be opened for new settlement should be determined and settlement suitability maps should be prepared. In order for these maps to be reliable, the engineering characteristics of the soil to be opened for settlement must be accurately

determined. In order for these specified properties to be used effectively, they must also be stored in a specific database. The database that will be created will be available to professional disciplines such as geology, geophysics, architecture, transportation, city planning and geotechnics.

Geographic Information Systems (GIS) have become a common method of analysis in civil engineering. GIS models, which process and compile positional data above or below the soil surface, have provided a powerful tool in civil engineering applications. (Priya, 2014) Realizing this, RMSI has created a broad range of services by providing a geotechnical GIS solution and services that are desktop geological applications, borehole survey, soil engineering, geotechnical engineering, environmental engineering, rural, city and regional planning. RMSI's core competency lies in providing solutions across the entire geospatial value chain – from data creation, conversion, and enhancement to software development, modeling, analytics, and consulting. Priya (2014) stated that Desktop Geotechnical GIS is a versatile system that can be used to assist in various preliminary geotechnical field assessments, execution and monitoring. To date, the system has been used to solve potential stability problems and to identify borehole logs of possible geological hazards, as well as to determine their various locations. It is used to guide field activities and combine field data with available information. This is provided by an accurate site model that allows for advanced site analysis. For example, road layout has been identified and cleared of potential problems which would prevent successful project completion early in the design process before significant design work is invested in it. (Pyria, 2014)

In another study, Akyol and Alkan (2015) used a multi-criteria decision-making technique. It has been noted that the multi-criteria decision-making technique comes to the fore as a common method for solving problems with many uncertainties and parameters. Experience is of great importance as well as knowledge in the method. These problems provide accurate and fast decisions using GIS when they contain positional information. The GIS-based multi-criteria decision-making technique is used in solving various geotechnical problems. (Akyol and Alkan, 2015) In this study, soil type, SPT blow number, shear wave velocity and groundwater level were used as geotechnical parameters. They analyzed the suitability of the neighborhoods within the borders of Denizli Municipality for settlement from a geotechnical point

of view with a multi-criteria decision-making technique.

Geographic Information Systems is a computer system that has been developed to collect all kinds of earth data with real coordinates in a database, to perform various analyzes on the desired data collection and to display the results in the form of maps, charts or graphics. (Bol et al., 2018). Bol et al. (2018), The outer borders of a medium-sized industrial site with typical terrain of the Adapazarı plain and the blocks it contains were digitized with the GIS software "MapInfo". All the data obtained from the CPT and the related geotechnical properties derived from this data was transferred to the database. The research was carried out with the data of the land cone penetration test (CPT). By establishing the necessary connections between the MapInfo software and the database, they prepared thematic maps showing the bearing capacity and liquefaction zones. At the end of the study, they made suggestions for strengthening the foundation where necessary with the help of thematic maps. They came to the conclusion that GIS accelerates decision-making processes in geotechnical terms in such environments and that the evaluations made reflect this more accurately.

In Kütahya, studies for the Geographical Information System have also been conducted. For GIS, the liquefaction potential of the Kütayha Central District has been discussed. Under cyclic loading conditions, the liquefaction of loose granular or alluvial soils with high groundwater levels causes irreparable damage to the superstructures. As a result, it is critical to create liquefaction risk maps prior to beginning construction in a specific region. (Şengül and Karabaş, 2021). According to the findings of this study for Kütahya, the liquefaction potential is high in loose alluvial soils where the groundwater level is close to the surface and the SPT-N values are low.

Another study was carried out for the province of Erzincan. Geotechnical characterizations are evaluated for contribution to IDW-based GIS. Efes et al. (2021), emphasizing that the preparation of maps for geotechnical characterization in earthquake-prone areas is very important for decision makers and local planners to reduce casualties, presented a series of maps for the city of Erzincan, which is mostly located in a deep alluvial basin near the North Anatolian Fault Zone (NAFZ). They obtained data from 92 boreholes in Erzincan.They prepared specific physical

properties of soil in the region using maps, field-based methods and geotechnical data to deal with Atterberg limits, classification, standard penetration test (SPT), shear wave velocity (Vs) and primary wave velocity (Vp) findings. (Çabalar et al, 2021)

2.4. Introduction of the Study Area

2.4.1. Geomorphological and Environmental Information

Siirt province consists mostly of high mountains and plateaus. The north and east of Siirt are high and steep areas. This mountain range, which is generally referred to as the Southeastern Taurus Mountains, draws a wide arc from east to southeast and merges with the Hakkari Mountains. The important mountains and their characteristics in this high and steep part of the Tigris Valley can be listed as follows: After the Muş Güneyi Mountains, in the east of the Bitlis Stream Valley, the mountains diverge to the south and cover the east of Siirt. These mountains, whose altitude decreases rapidly and intrude towards the Southeast Plains, unite with the Hakkari Mountains on the other hand. The mountains of the East of Siirt generally rise in individual bodies. These bodies are broken up by valleys opened by small streams that merge into the Tigris River. After the mountains, the most dominant landform in Siirt is the plateaus. These plateaus, most of which are in the form of high plains, are gathered on the slopes of the Doğruyol, Kurtalan, Kapılı and Yazlıca Mountains, which form the northern part of the Siirt Doğusu Mountains, overlooking the valleys split by the Botan Suyu and its branches. The main ones are Cemikari in Pervari, Ceman and Herekul Plateaus and Bacavan Plateau in Sirvan. The main ones are Cemikari in Pervari, Ceman and Herekul Plateaus and Bacavan Plateau in Sirvan. These plateaus, which receive abundant precipitation in summer and winter, are covered with rich meadows. The yield is lower in the plateaus at the foot of the mountains close to the steppe belt. Rainfall is more irregular and water resources are scarcer. The erosion is strong in this section, which is largely devoid of forest cover. The soil layer suitable for the formation of meadows has disappeared from place to place. The valleys running south and west from the mountainous areas in the north and east of the province are generally not very wide until they reach the eastern end of the Southeastern Anatolian Plains. Therefore, lowland areas are scarce in Siirt. (MAF, 2022)

2.4.2. Climate Information

Siirt is surrounded by plateaus covered with rich meadows that receive abundant precipitation in summer and winter. The continental climate prevails in Siirt and the four seasons are experienced with their most distinctive features. Winters are harsher and rainier in the eastern and northern regions, and warm in the south and southwest regions. In Siirt province, there is much more precipitation in winter than in summer. Precipitation is in the form of rain and snow in winter, and rain in spring and autumn. Summers are hot and dry. (MAF, 2022)

Table 2.1 Climate information about Siirt Province (Turkish State Meteorological Service, 2022)

	January	February	March	April	May	June	July	August	September	October	Nowember	December
Mean Temperature (°C)	2,70	4,3	8,4	13,8	29,5	26	30,7	30,4	25,5	18,2	10,5	4,8
Min Temperature (°C)	-0,5	0,6	4,1	9	13,7	19,1	23,5	23,3	18,8	12,8	6,4	1,7
Max Temperature (°C)	6,7	8,8	13,4	19,2	25,3	32,3	37,1	37	32,2	24,5	15,5	8,8
Precipitation (mm)	96,4	97,9	112,6	104,4	62,9	9,2	2,7	1,9	6,9	49,9	81,2	94,6

2.4.3. Natural Disaster Hazards

2.4.3.1. Earthquake Status

Earthquakes were first recorded instrumentally in 1880, with the advent of seismographs. In Turkey, it was established in 1934 with the registration process of the Kandilli Observatory. (BDTİM, 2018).

Siirt province is located in the Southeastern Anatolia Region of Turkey, between 41^{o} – 42^{o} east longitudes and 37.45^{o} - 38.15^{o} northern latitudes. (AFAD, 2018)

Although there has not been a significant earthquake disaster in the center of Siirt in recent years, a 7.2 magnitude earthquake occurred on November 23, 2011 with an epicentre of Erciş. In terms of earthquake risk, according to the earthquake map which entered into force in accordance with the Council of Ministers Decision 96/8109 dated April 18, 1996; Siirt is located in the 1st degree earthquake belt. The largest earthquake that occurred in the instrumental period on the EAB (Eastern

Anatolian Overthrust) was the Lice earthquake with a magnitude of M=6.6 on September 6, 1975, and the Erciş earthquake with a magnitude of 7.2 on November 23, 2011, in the west of the area. It is in the near east of the Şemdinli-Yüksekova Fault Zone. Two earthquakes with magnitudes Mw=7.4 and M=6.0 (Tan et al., 2008) were recorded outside the borders of our country in 1930. Apart from these, there are 11 earthquakes with a magnitude of M>6.0 recorded in the instrumental period in the study area. In the historical period, two major earthquakes (M=7.4 and M=7.0) that occurred in 1503 and 1884 (Tan et al., 2008) occurred in the south of Hakkari and north of Şırnak, respectively. Along with these, three medium-sized historical earthquakes are mentioned in the study area. Intensities and epicenters of the mentioned earthquakes are given. (SMDRU, 2020)

At the final project stage, the principles set out in the "Regulation on Structures to be Built in Disaster Zones" will be considered. The active fault map of Turkey, including the project area, and the Earthquake Map are given in the appendices. (Doğruyol, 2021)

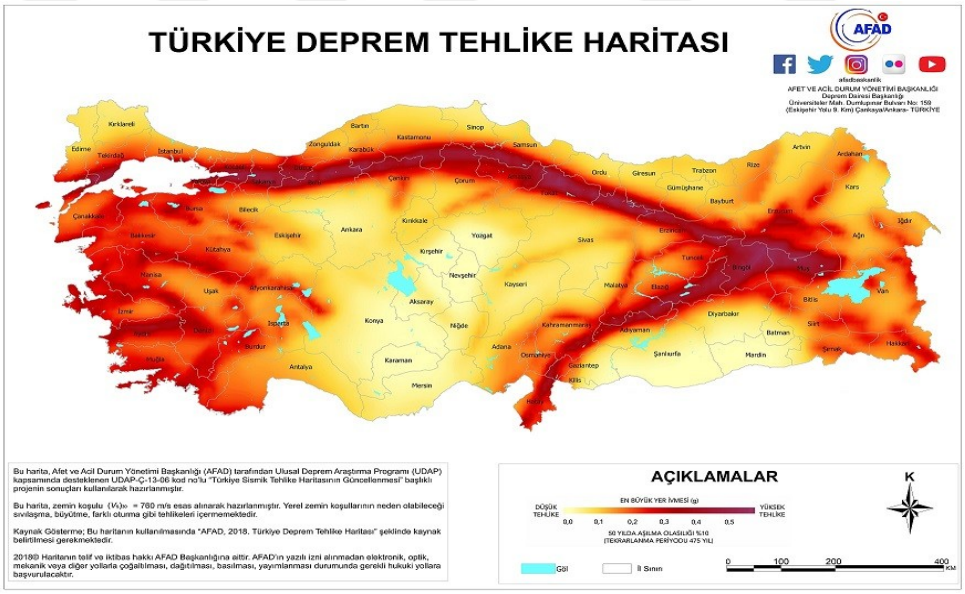

Figure 2.4 Turkey Earthquake Risk Map (AFAD, 2018)

2.4.3.1.1. Earthquake Hazard and Risk Analysis of the Siirt Region

Seismic risk or earthquake risk is the probability that an earthquake that can cause damage and loss of life will occur in a certain place and within a certain time frame.

This is the annual probability of exceeding the earthquake at a given magnitude, defined as the 'annual risk', or it can be considered as the "average conversion period" obtained by dividing it by one. The city of Siirt is located in a 1st degree earthquake zone. This feature and being close to very active fault lines put the city of Siirt in a risky position in terms of earthquakes. The frequent occurrence of earthquakes with a magnitude value greater than 4.5, which can be considered important in a radius circle 100 km from the city center of Siirt, showed that this area is active and significant in terms of earthquakes. It is seen that earthquakes with an instrumental magnitude higher than 4.5 are important in the vicinity of Siirt. Considering the magnitude of the recent Van and Erciş Earthquakes, these earthquakes pose a risk to the city of Siirt. In general, using seismicity data for the last hundred years, long-term earthquake forecasts are made, which will be the basis for short-term earthquake forecasting. The earthquake risk was calculated according to the earthquake magnitudes in Siirt and its surroundings in the last century. (SMDRU, 2020)

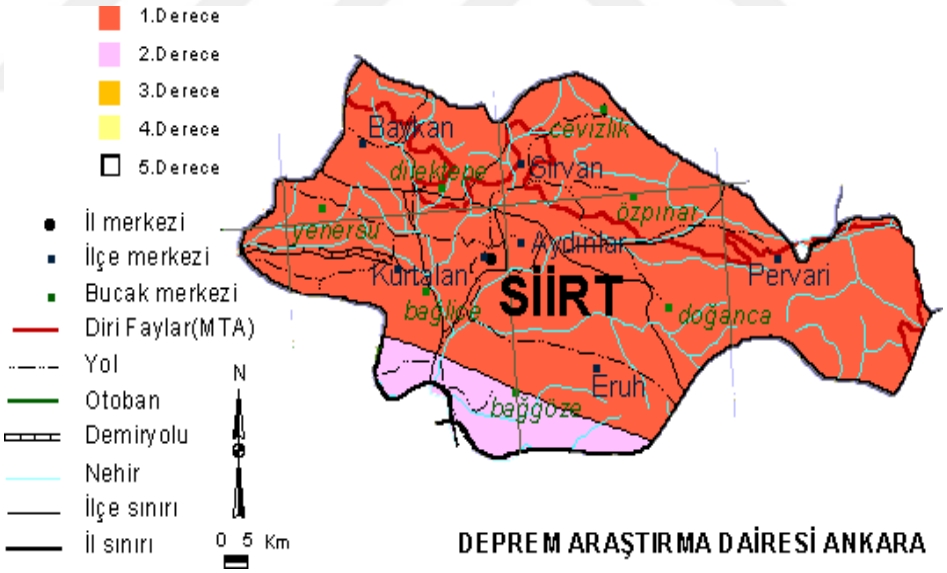

Figure 2.5 Siirt earthquake zones (AFAD, 2018)

2.4.3.2. Disaster Status

In the study area, apart from the earthquake, landslides, rockfalls, avalanches, floods which have occurred and possible disasters have not been observed. The fact that the number of snowy days in the region is limited to one or two days a year in the Şelmo

Formation, which forms the geological basis in the drilling and laboratory experiments, is an indication that it is not suitable for landslides as a result of the fact that the precipitation is low and the unit contains sandy levels. In addition, the slope in the field usually varies between 0-5%, and landslides cannot be expected to occur as a result of the settlement on the ground described above. No active faults were found in the study area and its immediate surroundings. The study area is not in a disaster area according to the geological reports based on the zoning plan. There are no sections in the field that require soil improvement such as flowing, swell and marshland originating from the ground. (SMDRU, 2020)

2.4.4. Hydrogeology

2.4.4.1. Streams

Siirt Province is located at the northeastern end of the Southeastern Anatolia Region. The region suddenly rises after the Southeastern Anatolian Plains, and the eastern and northern parts receive abundant precipitation. For this reason, the province area, surrounded by the Muş Güneyi Mountains from the north and the Siirt Doğusu Mountains to the east, constitutes one of the important water collection areas of the Tigris River. All of the province's territory enters the Tigris Basin. The basin is the fourth largest catchment area of the country after the Euphrates, Kızılırmak and Sakarya Basins. Important streams; Tigris River, Botan Stream (Uluçay), Garzan Stream, Kızılsu Stream and Behranca Stream. (MAF, 2022)

Table 2.2 Streams of Siirt Province (DSI, 2018)

NAME OF STREAM	Total length (km)	Length within the provincial border (km)	Flow rate (m3/s)	Tributary stream
Bitlis Stream	108,8	56,3	18,5	Botan Stream
Botan Stream	217,5	99	128,6	Dicle
Kezer Stream	105	40	19,5	Bitlis Stream
Zarova Stream	93,8	70		Botan Stream

2.4.4.2. Groundwater

Some of the drinking water needs of Siirt Center, Kurtalan, Tillo (Aydınlar) Districts and Kayabağlar, Gökçebağ and Atabağ Towns are supplied from the natural spring water called Hesko in the rural area of Şirvan District and the caisson wells located on the Botan Stream. In addition, there are underground water boreholes for

agricultural purposes, water boreholes opened to meet the domestic water needs of individual industrial facilities, and many registered or unregistered (without a groundwater use permit) water boreholes to meet the domestic and drinking water needs in rural areas (villages). According to the groundwater usage values recorded in the DSI records, the water levels for Siirt Merkez in 2017 are; depth 120-180 meters, static level 1-24 meters, dynamic level 50-100 meters and flow rate 0.5-2 liters / second. No findings related to groundwater were found in the field studies conducted. There are no water sources such as streams, etc. in the vicinity of the settlement. (SMDRU, 2020)

2.4.5. Geology

2.4.5.1. Regional Geology

Various sedimentary deposits from the Precambrian period to the present in the Southeastern Anatolia Region have been defined in group, formation and member stages. The stratigraphy and correlations of these units are observed along the northern and southern lines of the Southeastern Anatolia Region. The abundance and prevalence of Allochthonous units is also a feature due to the effective compression tectonism in the upper cretaceous and miocene periods. Cenozoic in Southeast Anatolia; It begins with Paleocene aged Upper Germav things, followed by Lower Eocene aged Becirman limestone and Gercüş clastic formation, overlain by Midyat limestones of Middle-Upper Eocene age (Kaya, 2008).

In the project area; from bottom to top,
There are Paleocene-Lower Eocene aged Gercüş Formation, Eocene aged Midyat Formation, Oligo-Miocene aged Germik Formation and Quaternary aged travertine, terrace set and alluvium. Due to the presence of typical outcrops in the Southeastern Anatolia region, many geologists (mainly oil company geologists) have conducted numerous geological surveys in the Amanos, around Adıyaman – Pendeği - Tut, in Karababa and Korudağ, in the Hazro region, around Mardin – Derik, in the Harbol-Hermis basins and around Hakkari.
Three tectonic events generally controlled the sedimentation in the region. These are;

- Epirogenic movements that caused sea surface changes in the Cambrian-Lower Cretaceous process.
- Upper Cretaceous compressional regime and nappe
- It can be summarized as Miocene compression regime and nappes. (SMDRU, 2020)

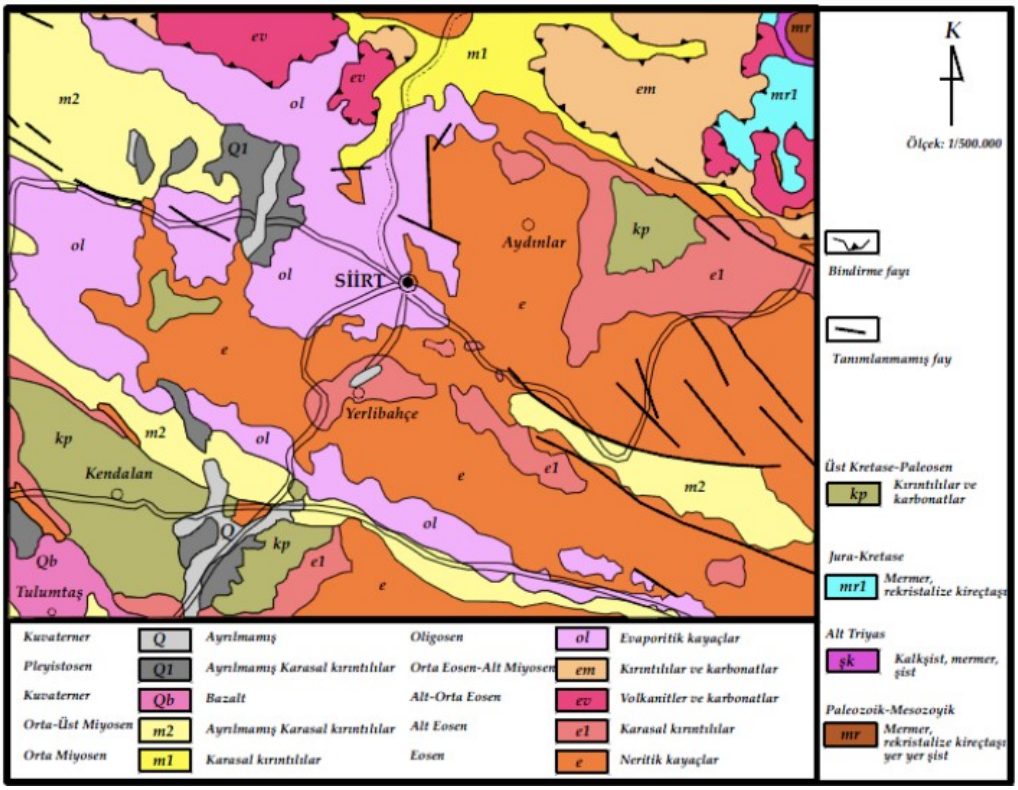

Figure 2.6 Geological Map of Siirt and its Surroundings (Alan and Aksay, 2002)

2.4.5.1.1. Silvan Group: Lower Miocene

Type Locality: Diyarbakir province Silvan district north and northeast
Hierarchy: The Silvan group is divided into three units from bottom to top as Kapıkaya, Euphrates and Lice Formations. The Kapıkaya Formation consists of conglomerate, evaporite interlayer shale, siltstone and sandstone; the Euphrates Formation consists of carbonate gravel limestone and reef limestone, and the Lice formation consists of flysch-characterized sandstone, marl, siltstone and limestone succession. In places where the formation's Touch relations outcrop in Southeastern Anatolia, it unconformably overlies the Midyat group units after an erosion and non-sedimentation phase (Duran et al.,1988 and 1989) In all areas, it unconformably overlies the Midyat group units by the Şelmo formation. (Duran et al.,1988 and

1989) In all areas, it is also unconformably covered by the ġelmo formation. It crops out in the north of the Batman-Siirt line, in front of the thrust.

In the project area; from bottom to top, there are Paleocene-Lower Eocene aged Gercüş Formation, Eocene aged Midyat Formation, Oligo-Miocene aged Germik Formation and Quaternary aged travertine, terrace set and alluvium (Duran et al.,1988 and 1989).

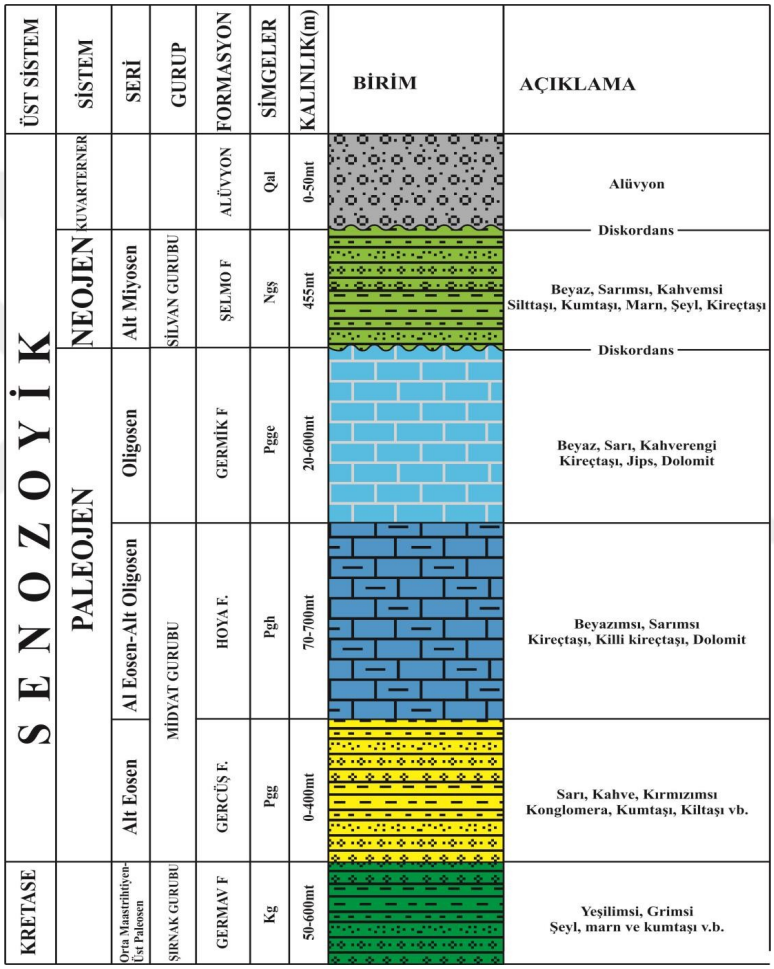

Figure 2.7 Generalized stratigraphic column section of the Southeast Anatolian autochthon (Dinç and Keskin, 2017)

2.4.5.1.2. Gercüş Formation

This formation is formed by alternation of reddish-brown claystone, mudstone, sandstone and conglomerate levels. There are vertical and lateral transitions between the mostly thick bedded levels. The Gercüş Formation is located on an outcrop in

structural uplift areas in the Botan Stream valley, south of the settlement area of Siirt province. (Duran et al., 1988)

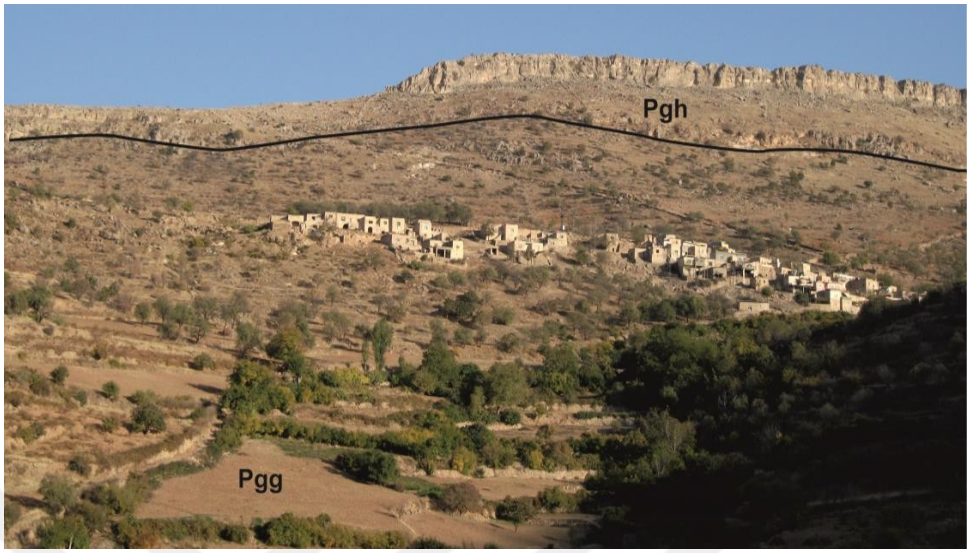

Figure 2.8 Gercüş Formation (Pgg) - (Dinç and Keskin, 2017)

2.4.5.1.3. Midyat Formation

This formation is composed of cream, light yellow clayey limestone, dark cream-colored massive porous limestone and whitish chalky clayey limestone levels. Almost all of the Midyat Formation, mostly the massive limestone level, has karstic cavities. The Midyat Formation, which is in harmony with the Gercüş Formation, is widely outcropped in the eastern and southern part of Siirt Province. (SMDRU, 2020)

2.4.5.1.4. Germik Formation

The Germik Formation is mostly composed of soluble rock types such as gypsum, anhydrite and limestone layers, wedges, lenses and blocks in reddish brown, gray, greenish and variegated claystone, mudstone, conglomerate layers present in the area. In most of the settlement area of Siirt, this formation is bedrock. Sulphated, brackish water is present in some of the water wells drilled in this formation. In the Germik Formation; except for the water reservoir within the scope of the Siirt Water Supply and Sewerage Project, all facilities are in bedrock. (Duran et al., 1988)

Figure 2.9 Germik Formation (Dinç and Keskin, 2017)

2.4.5.1.5. Young Sediments

There are young sediments such as Quaternary soil cover, slope wash, alluvium, terrace and travertine in the immediate vicinity of the settlement area of Siirt province. (SMDRU, 2020)

Travertine

It is outcropped in a narrow area under the terrace set on Cinhıttıyr Hill, southeast of Conkbayır Neighbourhood in Siirt. It must be the product of springs from pre-Quaternary fault zones. (SMDRU, 2020)

Terrace Set

At the summits of hills such as Cinhıttır, Şeyhinnacar, Şeyhşemu, Hedevris, Gerşabahçe and Kurt Tepe, which are at very high elevations in the study area, there are terrace set remains belonging to the periods when the pre-Quaternary Botan Stream flowed at these elevations. It is a hard, durable and stable conglomerate that is formed by the natural cementation of poorly sorted gravel, sand and silt grains originating from metamorphic rocks, whose pebbles are not easily separated from the cement by hammer blows, and can form slopes at 50-60^{o} steepness in exposed areas.

The water tank unit within the scope of Siirt Water Supply and Sewerage Project is on the terrace set unit. (SMDRU, 2020)

Alluvium

There is an alluvium consisting of sand and gravel of metamorphic rock origin with a thickness of more than 10.00 m in the bed of Botan and Kezer creeks. (Yıldırım and Karadoğan, 2005)

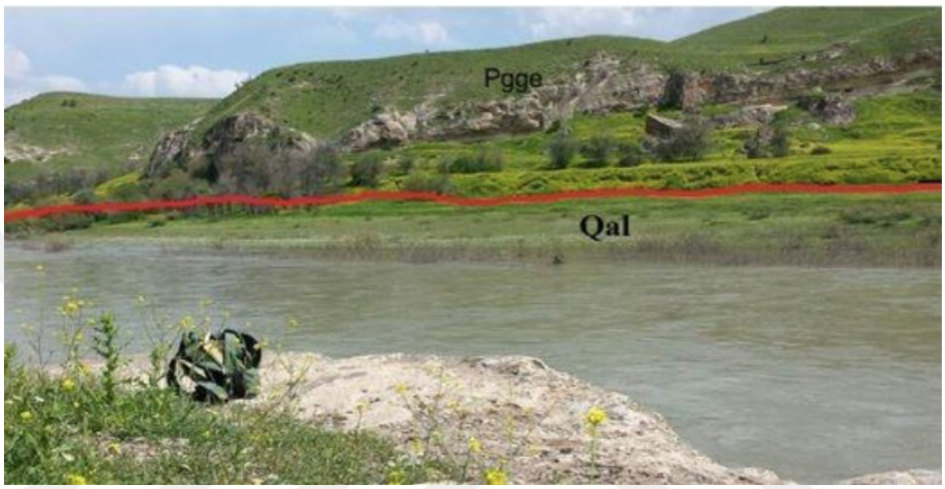

Figure 2.10 Alluvium (Qal), Germik formation (Pgge) (Dinç and Kekin 2017)

2.4.5.1.6. Şelmo Formation: Upper Miocene

Type Locality: Şelmo due to the village of Şelmo in the southwest of Sason district in Batman province. The name of the formation was first used by Bolgi (1961) around the provinces of Siirt and Batman. (SMDRU, 2020)

The Şelmo Formation, which is measured as 455.53 meters in total in the holostratype (in the Miocene type section of Başur Creek Valley), is in the form of grayish green, pink, brownish purple in places sandstone, Shale, sandy siltstone, locally gypsum interbedded, carbonate cemented, mollusc, poorly sorted, coarse textured, porous, thin bedded at the bottom, scattered limestone pebbles, thick and cross-bedded on the top, hard sandstone. (Duran et al., 1988)

Figure 2.11 Şelmo Formation (Dinç and Keskin, 2017)

2.4.5.2. Structural Geology and Active Tectonics

Although Siirt province is surrounded by active fault lines, there is no effective earthquake focal point within the city limits (Işık 2012). Since Siirt province is adjacent to the active EAF and SAB lines, it has been know that seismic movements are frequently experienced. (Doğruyol, 2021)

The African plate subducts under the Eurasian (or its part Anatolian) plate, in the so-called Hellenic-Cypriot arc in the Mediterranean. The Arabian plate, on the other hand, moves northward due to the opening in the Red Sea and compresses the Anatolian plate. As a result of this compression, the Bitlis Overthrust Zone was formed. As the compression still continues, the Anatolian plate moves westward along the fault lines in the north and south. The northern boundary of the Anatolian plate is the North Anatolian Fault, where the 17 August earthquake occurred. The southern border is formed by the Hellenic-Cypriot Arc and the Eastern Anatolian Fault (EAF). Again, due to the effect of this compression, there are many fractures in the region, most of which are not active in the East-West direction. Earthquakes occur in the Mediterranean Sea and in the Aegean Graben System as a result of the compression of the Arabian plate at the boundaries of the Anatolian plate sliding to the west and the subduction of the African plate under the Eurasian plate. However, since the compression of the Arabian plate cannot be fully compensated for by the

movement in these regions, earthquakes can also occur in the Central Anatolia and Eastern Anatolia regions due to the internal formation. (SMDRU, 2020)

Siirt is one of the important cities of the Southeastern Anatolia Region. Active faults in and around Southeast Anatolia have caused serious earthquakes in the past. In this study, the circular area within a radius of 200 km from the city center of Siirt with 37.55 north and 41.56 east coordinates of the city center, which is located in the region affected by the active fault lines of the Eastern Anatolian Fault Zone and the Southeast Anatolian Thrust , was chosen as the study area. (Doğruyol, 2021)

2.4.6. Geophysical Studies

In order to determine the geological structure and soil properties of the study areas, field observations and literature studies are made and morphological-structural features are compiled. Some studies were carried out to investigate the dynamic properties of the units in the area and groundwater. Seismic MASW (Multi Channel Analysis of Surface Waves) and MAM (Microtremor Array Measurements) tomography measurements are generally made on the field. The profile lengths are determined and the soil parameters up to the required meter depth are obtained. Before starting measurements in the field, field observations are made and measurement methods and locations are determined accordingly. Seismic measurement equipment is used in the study. (SMDRU, 2020)

With the help of these studies, an attempt was made to determine the physical and mechanical properties of the units and their behavioral characteristics. The geological characteristics of the site were determined by determining the horizontal and vertical changes of the lithological units in the area and the underground water level, and geotechnical modeling of the site was carried out by determining the mechanical elastic parameters of the units, and hazard analyses were carried out. With these studies, an attempt was made to determine the physical and mechanical properties of the units and the behavioral characteristicsand standards were taken into consideration. (SMDRU, 2020)

2.4.6.1. Shear Wave (Vs) Velocity by Multi-Channel Surface Wave Analysis Method (MASW-MAM)

The shear wave velocity profiles were measured using different geophysical methods, including a combined multichannel analysis of surface waves and microtremor array measurement (MASW-MAM) method and P-S waves. (Dejphumee, 2021)

MASW-MAM methods, which are a new method to obtain S wave velocities in construction-site investigations, as well as obtaining more information from the depths of the impact depth of the fracture method in narrow areas, also allows obtaining information from depths of 30 m and above, which is needed in urban studies where the signal/noise ratio is insufficient. Although 30m study depth is considered sufficient in regulations, it is also possible to determine the seismic velocities up to the layer with a velocity value of at least 760 m/s in order to determine the soil dominant period. In this way, Vs (30), local soil class, ground amplification and ground dominant period can also be calculated to a degree of high accuracy. In addition, measurements can be taken by ensuring a good connection on asphalt, concrete, pavement, stone floor, etc. environments without the need for a natural soil. (SMDRU, 2020)

Surface wave tests such as the multi-channel analysis of surface waves (MASW) and microtremor array measurements (MAM) offer a fast and convenient way of measuring the shear wave velocity (Vs) of the ground for geotechnical site investigation due to their non-intrusive nature. However, it has been widely reported that the accuracy and resolution of the Vs profile depend on the construction of the dispersion image and its interpretation. (Subramaniama et al., 2020)

CHAPTER 3

MATERIALS AND METHODS

3.1. Standard Penetration Test

Standard Penetration Test (SPT) is performed inside the borehole. At the very end, there are rods to which the standard sampler, known as the longitudinal slit tube sampler, is attached. A hammer weighing 63.5 kg is dropped on the rods repeatedly from a height of 76.2 cm and driven from the bottom of the borehole until a total penetration of 45 cm is reached, and the SPT-N values required are determined. Thanks to the slit tube driven into the soil, a sample is taken from the soil and it is possible to identify the soil accurately The mechanism and method of the experiment is simple. The experiment can be completed in a short period of time. Its widespread use in the world has allowed to create a rich knowledge base and database for the interpretation of the experiment (Erol and Çekinmez, 2014).

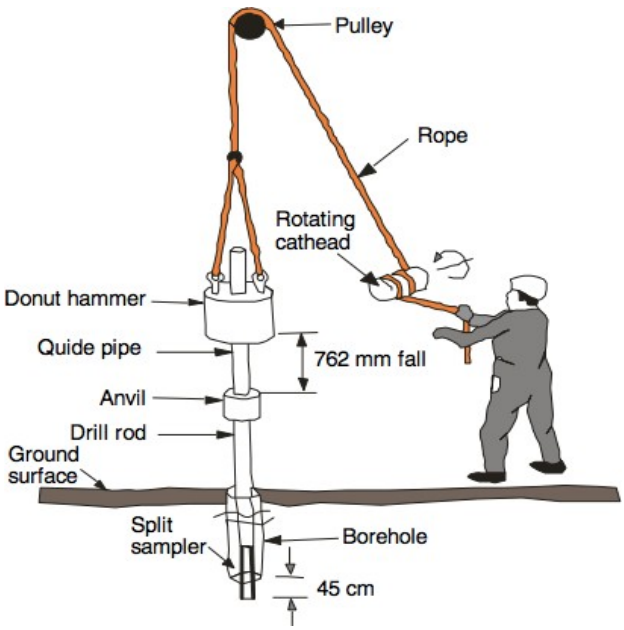

Figure 3.1 Sketch of Standard Penetration Test Instrumentation (Coduto, 1994)

The standard penetration test (SPT) is still one of the most commonly used in situ

test for site investigation. Empirical relation has been developed to estimate relative density, shear strength parameters. (Parmar and Sheth, 2021)

Some field experiments have been widely used for 40-50 years and some are developing with technology. The Standard Penetration Test (SPT) is one of the oldest field tests widely used in geotechnical engineering. SPT is a more advantageous test compared to other field experiments. (Nixon, 1982).

- The mechanical equipment used in SPT is generally more durable.
- Since SPT can be applied in the borehole during the drilling process, the cost is lower.
- One of the important advantages of SPT is that samples can be taken from boreholes.
- SPT can be applied in all soil groups and below the groundwater level.

Standard Penetration Test has advantages as well as disadvantages. In some cases, it can give misleading results. Misleading results can be observed in SPT applications on gravel or stone containing soils with an average diameter of more than 20mm. To eliminate this issue, the type of tip recommended for gravel soil can be used.

3.2. Bearing Capacity

The main purpose of geotechnical engineering is to physically and mechanically examine the soil on which structures will be built. For this reason, soil analyzes are carried out with various methods for the layers on which the structures will be built. The most important of these analyzes are the parameters that affect the bearing capacity.

Soil mechanics problems are divided into two as stability and elasticity (Settling) (Terzaghi, 1943). It is very important to know the maximum base pressure that the soil can withstand before collapse, which is one of the stability problems. The final bearing capacity of a foundation indicates the highest stress it can withstand without visibly collapsing into the ground (Sivrikaya, 2021).

There are many factors affecting the bearing capacity.

- Factors related to soil-soil profile;
  - ✓ Shear strength parameters of the soil (c and ϕ)
  - ✓ Soil unit weight (γ)
  - ✓ Groundwater level (YASS)
- Fundamental factors;
  - ✓ Foundation depth (D_f)
  - ✓ Basic shape (square, circular, rectangular)
  - ✓ Foundation dimensions (B, L)
  - ✓ Short side of foundation (B)
  - ✓ Roughness of the foundation base
- Factors related to loads;
  - ✓ Slope and eccentricity of the load (e)
  - ✓ If there is YASS, the time elapsed after the construction and installation of the foundation.

Bearing capacity failures (collapse); the shear stresses of the soil depend on the net base pressure and the size of the foundation. The shear stress of soils with large base pressure and small foundation size can exceed the shear strength of the soil. This may result in a bearing capacity collapse. (Sivrikaya, 2021)

Many methods are used to determine the bearing capacity.

- With Tables
- With Load Experiment
- With Other Field Tests (SPT, CPT, etc.)
- With Theoretical Approaches

3.2.1. Field Tests and Bearing Capacity Calculation Methods

3.2.1.1.Terzaghi and Peck (1967) Method

Two parameters are taken into account in the Terzaghi and Peck bearing capacity calculation method. Bearing capacity is calculated with foundation width and SPT-N values. (Bowles, 1996). The foundation width was chosen as 3 m.

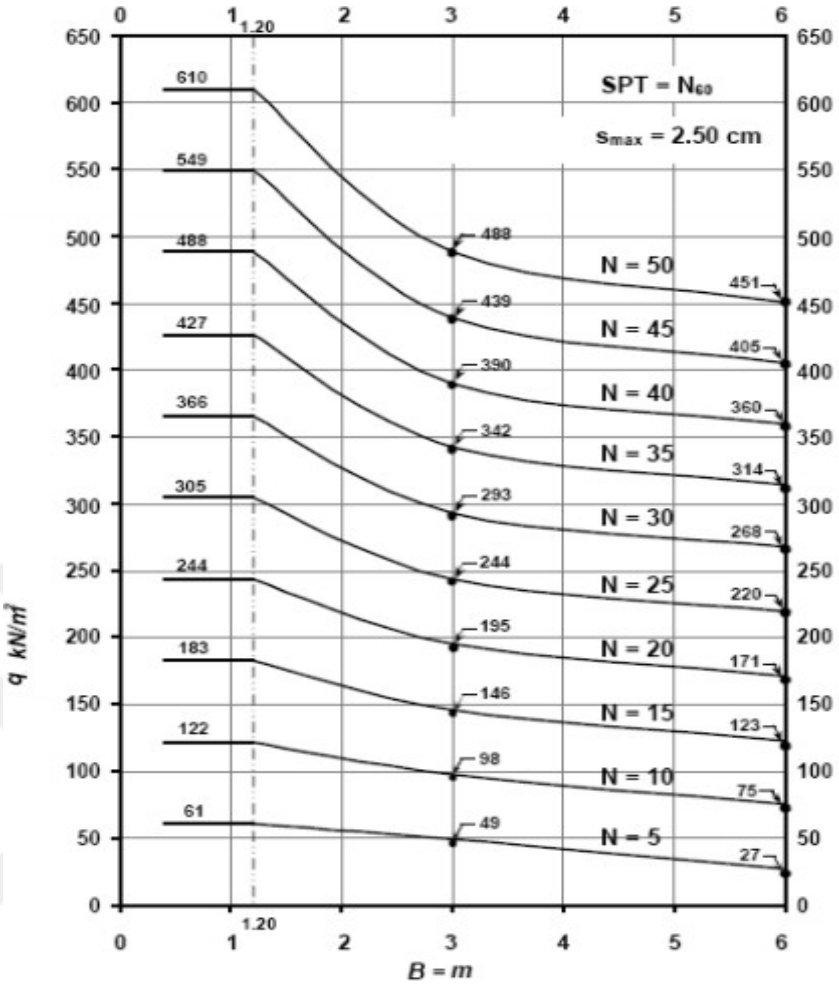

Figure 3.2 Change of allowable bearing capacity according to foundation width and SPT-N (Bowles, 1996).

3.2.1.2. Meyerhof (1974) Method

The Meyerhof bearing capacity calculation is obtained by using the SPT-N value. Similar to the studies conducted by Meyerhof, Terzaghi and Peck, it also limited settling to 25 millimeters (Bowles, 1996). The foundation width was chosen as 3m.

$$q = 12 * N * Kd \quad (3.1)$$

$$q = 8 * N * ((B + 0{,}3505) / B)^2 \quad (3.2)$$

$$Kd = 1 + 0{,}33 * D / B \leq 1{,}33 \quad (3.3)$$

Here;

q : Bearing capacity (kN / m^2)

N : SPT blow number

D : Foundation depth (m)

B : Foundation width (m)

3.2.2. Bearing Capacity Calculation Methods with Geophysical Methods:

3.3.2.1 Keçeli Bearing Capacity Calculation

Keçeli (1990) developed the formula presented below, assuming that the soil exhibits elastic behavior in the calculation of bearing capacity (Keçeli, 1990). The bearing capacity was calculated according to this formula.

$$q = \frac{T * Vp * \gamma}{40} \quad (3.4)$$

Here;

q : Bearing capacity (kN / m^2)

T : Soil dominant vibration period (sec)

Vp : Compression Wave Velocity (m / sec)

γ : The soil shows the unit weight (KN / m^3)

3.2.2.2. Tezcan et al. Bearing Capacity Calculation

Terzaghi and Peck (1967) took into account the foundation width-soil safety stress relationship in calculating the SPT-N value and the bearing capacity, and this was also adopted by Tezcan et al (2010) (Karabaş, 2019). In designs where the foundation width is between 0 and 12 meters, the bearing capacity is calculated using the β deceleration factor (Tezcan et al., 2010).
The foundation width was chosen as 3 m.

$$q = 0{,}1 * \gamma * Vs * \beta \quad (3.5)$$

Here;

q : Bearing capacity (kN / m^2)

Vs : Shear wave velocity (m / sec)

γ : The soil shows the unit weight (KN / m^3)

β : Reduction factor

B : Foundation width (m)

Relation of β reduction factor and B foundation width

$\beta = 1$ $\quad 0 \leq B \leq 1.2$ m (3.6)

$\beta = 1.13 - 0.11B$ $\quad 1.2$ m $\leq B \leq 3.00$ m (3.7)

$\beta = 0.83 - 0.01B$ $\quad 3.00$ m $\leq B \leq 12$ m (3.8)

3.3. Shear Wave Velocity

The velocity data determined by seismic waves is used to obtain the dynamic soil variables used in soil classification and understanding the engineering properties of the soil based on ground movements. Because of factors such as large depth of research, high accuracy, and resolution, the seismic method, which is one of the geophysics methods, is widely used in engineering studies. (Akkaya et al., 2017) One of the most important parameters used to determine the local ground effect is the shear wave velocity (Vs). Many measurement methods are used to determine the shear wave velocity "Vs (m/s)" (Hunter J.A. et al., 2002). Measurement methods for the shear wave velocity can be considered as methods obtained by seismic methods and their calculation by field experiments.

The shear wave velocity, the soils provide information about the rigidity. It is used in the analyzes to determine soil behavior. It is determined by measuring, it in situ or calculated (depend on SPT-N). However, in some soil classification systems and earthquake hazard analyzes, 30 m of average shear wave velocity information of the soil is used (Kurnaz, 2011).

Within the scope of measurement made in the field, surface fracture method is used. It is used to determine the parameters of the soil of the study area. This method, the

propagation of the waves coming from the interfaces with fraction and waves coming directly are recorded. As a seismic energy source, 8 kg weight sledgehammer is used. The energy in the S wave (shear wave) is obtained by hitting the plate placed perpendicular to the pit with 30-40 cm deep. S wave records are created. Geodetic geophones (detectors) are used in the transverse wave records. Seismograph with signal accumulation is used for precise measurement of S velocities. Vs is obtained by this method in the field. In situ measurement of the shear wave velocity can be disadvantageous in some cases, thus, shear wave velocities are often estimated from correlations associated with SPT-N numbers (Kurnaz, 2011). These correlations are given in Table 3.1.

Table 3.1 The empirical correlation based on SPT-N and Vs (Akın et al, 2011)

Researchers	Vs (m/s) (All type of soils)
Ohba and Trauma (1970)	$Vs= 84*N^{0.31}$
Imai and Yoshimura (1970)	$Vs=76*N^{0.33}$
Tsiambos and Sabatakakis (2011)	$Vs=105.7*N^{0.327}$
Vs: Shear wave velocity, N: Uncorrected SPT blow number	

3.4. Soil Classification by NEHRP

National Earthquake Hazard Reduction Program (NEHRP); it is aimed to increase the expected performances of important buildings during or after an earthquake in the United States of America. The soil class according to NEHRP is based on the average of the S-wave velocity up to 30 m depth, and these classes are given in Table 3.2 (Güzel, 2009).

Table 3.2 Soil classification criteria according to NEHRP (Güzel, 2009)

Soil	Description	Properties
A	Hard rock	Vs>1500
B	Rock	760 < Vs < 1500
C	Very dense soil/ soft rock	360 < Vs < 760
D	Stiff soil	180 < Vs < 360
E	Soft soil	Vs<180

3.5. Earthquake Hazard by Soil Amplification

Soft sedimentary rocks are known to strengthen soil movements during earthquakes and for this reason, the average damage caused is more severe than hard layers This means that sedimentary rocks are amplification factors for earthquake waves. (Tuladhar et al., 2004).

Constructions built on soft sediments easily suffer damage due to the amplification of earthquake waves. There are two reasons for the amplification of earthquake waves that can cause damage to constructions. First, there is a wave confined to in the soft layer (Tsutomu Sato, 2004), so that the wave occurs superposition between waves, if the wave has a relatively similar frequency, then the earthquake wave resonance process occurs. As a result of this resonance process, the waves are reciprocatively reinforcing. Second, there are similarities in natural frequencies between local geology and constructions (Roser and Gosar, 2010). This will cause resonance in constructions and local soil, which results in stronger ground vibrations in buildings. The amount of amplification can be forecasted from the impedance contrast between bedrock and surface sediment (Roser and Gosar, 2010).

Soil amplification is the increase in amplitude of seismic waves as they pass through soil layers closed to the surface. The reason for this is the low density, that the soil layers have. During the earthquake, in loose soils the earthquake waves grow at a considerable rate. These soils are known to have a huge role in damages caused by the earthquake (Kurnaz, 2011). Soil amplification was calculated from the following Midorikawa (1987) formula.

$$A=68V_1^{-0.6} \quad (V_1<1100 \text{ m/s}) \quad (3.9)$$

$$A=1 \quad (V_1>1100 \text{ m/s}) \quad (3.10)$$

Here;

A : Relative amplification coefficient

V_1 : Shear wave velocity for depth of 30 meters

Earthquake hazard level according to calculated soil amplification; for the amplification value of 0,0-2,0, hazard level C (low hazard), for the amplification value 2.0-4.0, hazard level B (medium hazard), for the amplification value of 4.0-6.5, hazard level A (high hazard) (Kurnaz, 2011).

3.6. Soil Dominant Vibration Period (To)

The soil dominant period is important for determining the frequency characteristics of ground movement. This period is specified as the vibration period corresponding to the max value of the amplitude spectrum. In addition, even for small vibrations, the soft soil layer on the solid rock layer has a dominant vibration period in nature (Kanai, 1983).

The period is expressed as the independent oscillation of the mass on the bedrock and depends on the dynamic properties of the soil layers. Soil dominant vibration period value of the soft soil layer cropping out on the bedrock (hard ground) is determined by utilizing the formula To = Σ(4H/Vs30) for small vibrations (Kanai, 1965)

$$To = \sum 4H / Vs \quad (3.11)$$

Here;

To : Dominant vibration period

H : Layer thickness (m)

Vs : Shear wave velocity (m/s)

Differences in soil layers and soil sections can be seen from one end to the other. Changes in earthquake waves can be seen depending on the characteristics, type, and thickness of the soil layers. At the same time, in earthquake resistant zoning plans, dynamic properties such as soil amplification and soil prevailing period should be defined. (Ansal et al., 1994)

3.7. Soil Classifications Calculation According to Eurocode 8

The Eurocode series are European Regulations relating to constructions. "Eurocode8: Design of structures for earthquake resistance" This regulation explains how constructions in earthquake zones should be designed. This regulation has been approved by the European Standards Committee. Eurocode 8 applies to the design and construction of buildings and other civil engineering works in seismic regions (Halaç, 2016).

Its purpose is to ensure that in the event of earthquakes: human lives are protected, damage is limited, structures important for civil protection remain operational. The soil class according to Eurocode8 is based on the average velocity (Vs_{30}) of the S-wave velocity up to 30 m depth, and these classes are given in Table 3.3

Table 3.3 Soil classification criteria according to Eurocode8 (Güzel,2009)

Soil	Description	Properties
A	Rock or other rock-like geological formation	Vs > 800
B	Very dense sand or gravel or very stiff clay	360 < Vs ≤ 800
C	Dense sand or gravel or stiff clay	180 < Vs ≤ 360
D	Loose to medium cohesionless soil or soft to firm cohesive soil	Vs < 180

3.8. Local Soil Class According to TBDY-2019

The updated Turkish seismic code “Building Earthquake Regulations-2019 (TBDY-2019)” includes radical changes in many aspects such as peer review and the earthquake hazard map hence, it brings new conditions into practical engineering. One of the most important conditions is the concept of "Site Response Analysis" for the soil type “ZF”. Local soil classes given in the updated new earthquake code are presented in Table 3.4 in this study. According to this table, the soil classes are divided into ZA, ZB, ZC, ZD, ZE and ZF according to the average shear wave velocities in the upper 30 meters.

Table 3.4 Local soil class according to TBDY-2019

Yerel Zemin Sınıfı	Zemin Cinsi	Üst 30 metrede ortalama		
		$(V_S)_{30}$ [m/s]	$(N_{60})_{30}$ [darbe /30 cm]	$(c_u)_{30}$ [kPa]
ZA	Sağlam, sert kayalar	> 1500	–	–
ZB	Az ayrışmış, orta sağlam kayalar	760 – 1500	–	–
ZC	Çok sıkı kum, çakıl ve sert kil tabakaları veya ayrışmış, çok çatlaklı zayıf kayalar	360 – 760	> 50	> 250
ZD	Orta sıkı – sıkı kum, çakıl veya çok katı kil tabakaları	180 – 360	15 – 50	70 – 250
ZE	Gevşek kum, çakıl veya yumuşak – katı kil tabakaları veya $PI > 20$ ve $w > \%40$ koşullarını sağlayan toplamda 3 metreden daha kalın yumuşak kil tabakası $(c_u < 25$ kPa$)$ içeren profiller	< 180	< 15	< 70
ZF	Sahaya özel araştırma ve değerlendirme gerektiren zeminler: 1) Deprem etkisi altında çökme ve potansiyel göçme riskine sahip zeminler (sıvılaşabilir zeminler, yüksek derecede hassas killer, göçebilir zayıf çimentolu zeminler vb.), 2) Toplam kalınlığı 3 metreden fazla turba ve/veya organik içeriği yüksek killer, 3) Toplam kalınlığı 8 metreden fazla olan yüksek plastisiteli (PI >50) killer, 4) Çok kalın (> 35 m) yumuşak veya orta katı killer.			

TBDY-2019 requires site-specific behavior analysis for ZF class soils and the use of site-specific earthquake ground motion spectrum. Site-specific soil behavior analyzes aim to determine the influence of local soil conditions on the ground surface. With this method, earthquake ground motions are first defined in the engineering bedrock. Soil layers are modeled in accordance with the ground conditions of the project site and the variation of the defined earthquake ground motion along the profile and the earthquake ground motion on the ground surface are obtaining. The estimation of the spectrum on the ground surface depending on the local soil properties is of great importance in terms of the design of new buildings and the evaluation of the performance of existing structures. (Chandler et al. 2002; Tsang et al. 2006)

CHAPTER 4

4. RESULTS AND DISCUSSION

4.1. SPT-N Calculation Analysis

SPT (Standard Penetration Test) is a widely used method among field experiments. Boring data was obtained from the soil survey reports of some regions of Siirt Central district. There are a total of 178 boring points in these soil survey reports. Data were obtained from these points and evaluations were made. Calculation analyzes are also evaluated from the SPT results. Figure 4.1 presents the visual of the study area.

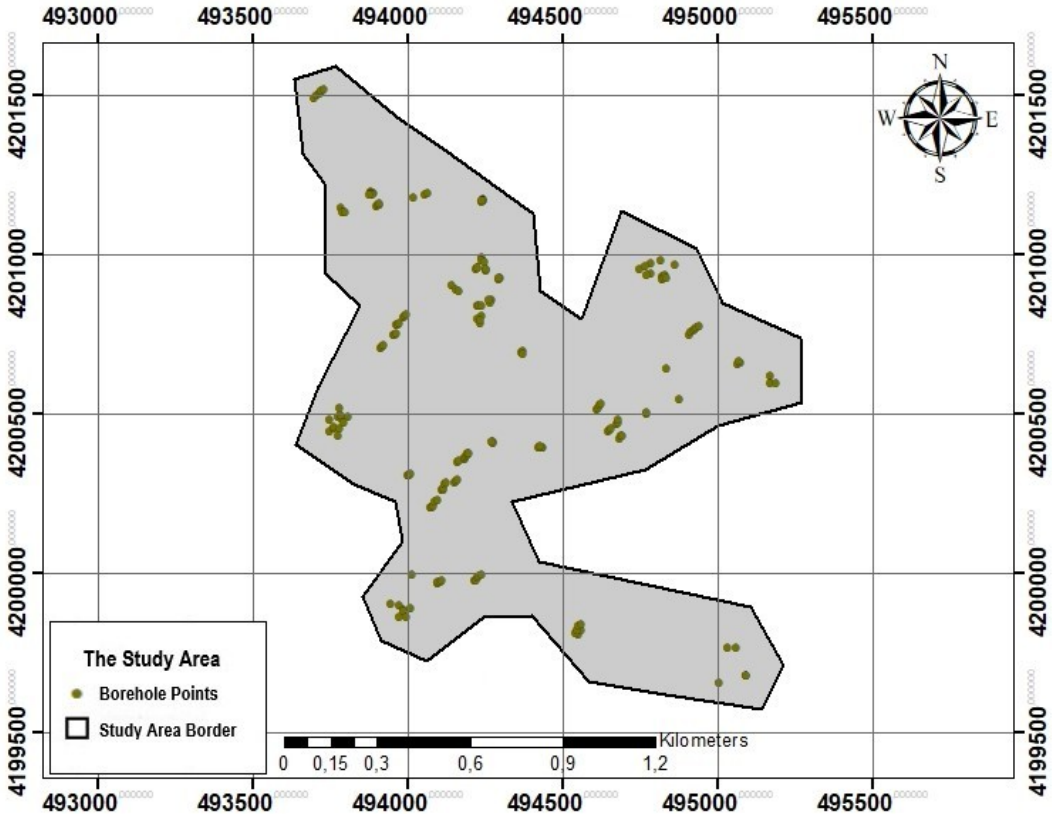

Figure 4.1 Study area

In the study area, maps were created for depths between 1-3 m, 3-5 m, 5-7 m, 7-9 m and 9-11 m in order to see the distribution of SPT values from the surface to a depth of 11 m and their change with the increase in depth. Estimated maps of SPT values were produced using ArcGis program and determined by using values between 1 and 50 while creating the maps.

It has been determined that 48% of the SPT-N data of 178 boring points between 1-3 m depth obtained from the study area are between 1-20, 41% between 21-30, 11% between 31-50. The prepared SPT-N map is presented in Figure 4.2. The SPT-N value of the blue colored area in the study area's Northwest region was found to be close to 50. While the SPT-N value of the blue colored area in the eastern region ranges from 31 to 50, the rest of the region's SPT-N value mostly ranges from 1 to 30.

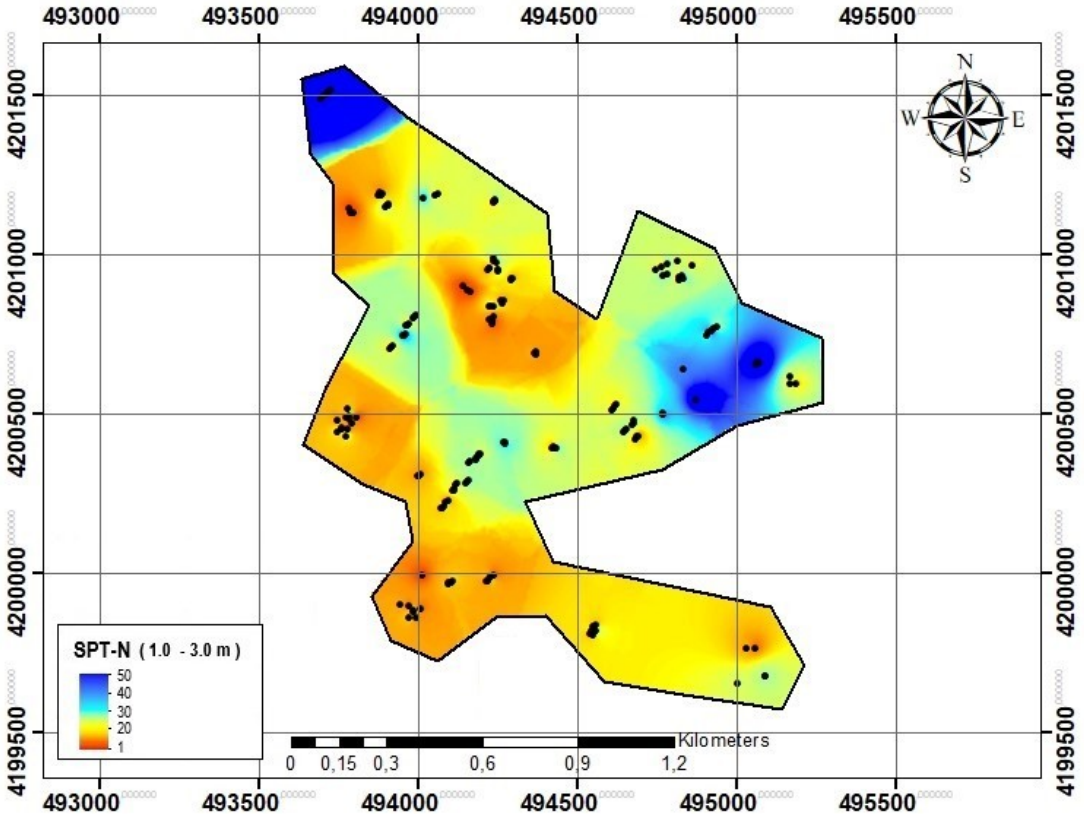

Figure 4.2 SPT-N in study area (1-3 m)

It was determined that 30% of the SPT-N data from 178 boring points between 3-5 m depth obtained from the study area are between 1-20, 37% are between 21-30, and 33% are between 31-50. The prepared SPT-N map is presented in Figure 4.3.

The SPT-N value of the blue colored area in the study area's Northwest region was found to be close to 50. While the SPT-N value of the blue-colored area in the eastern region varied between 31-50, the SPT-N value of the orange-colored region observed in the centre of the study area was observed to be between 1-20. The SPT-N value of the remaining yellow areas in the region was observed to be around 20.

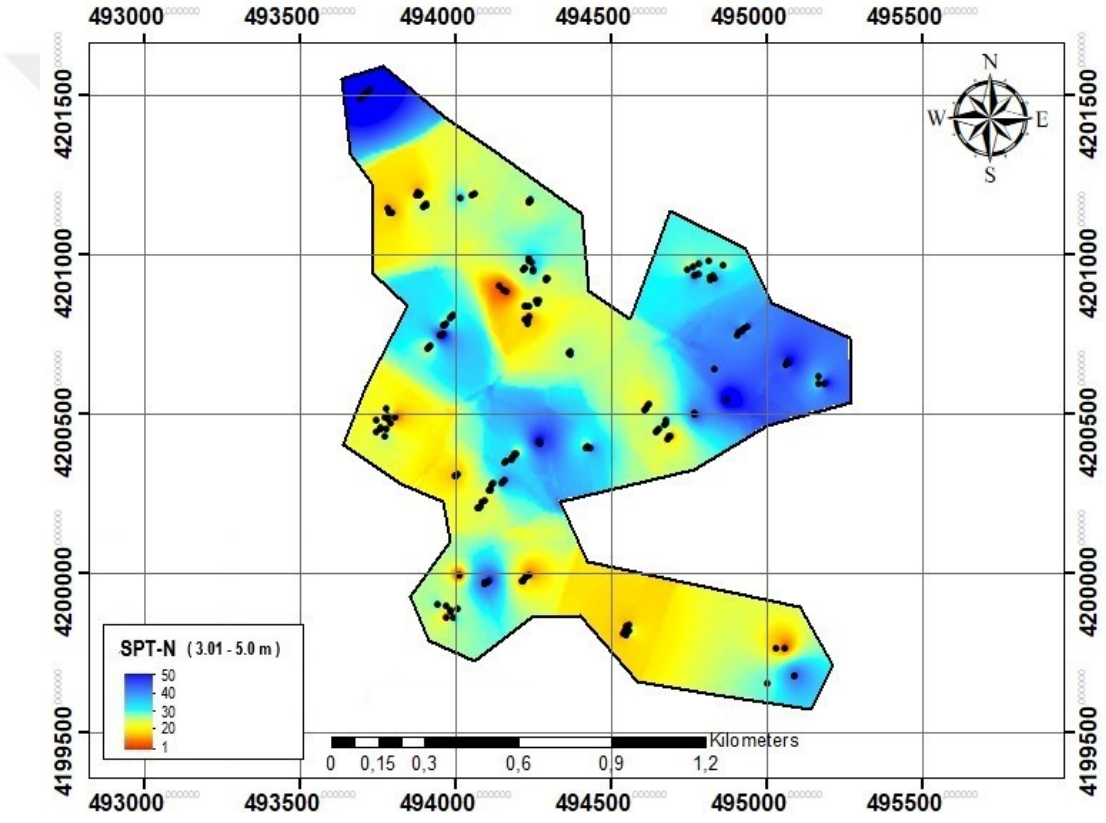

Figure 4.3 SPT-N in study area (3-5 m)

It was determined that 22% of the SPT-N data from 178 boring points between 5-7 m depth obtained from the study area are between 1-20, 31 between 21-30, and 47% between 31-50. The prepared SPT-N map is presented in Figure 4.4.

The SPT-N value of the dark blue regions in the study area was observed to be close to 50. The SPT-N value of the light blue regions covering a large part of the study

area was observed as 30-40. The SPT-N value of the small reddish region visible towards the middle of the study area was observed to be between 1 and 10. The SPT-N value of the remaining yellow regions was observed to be around 20.

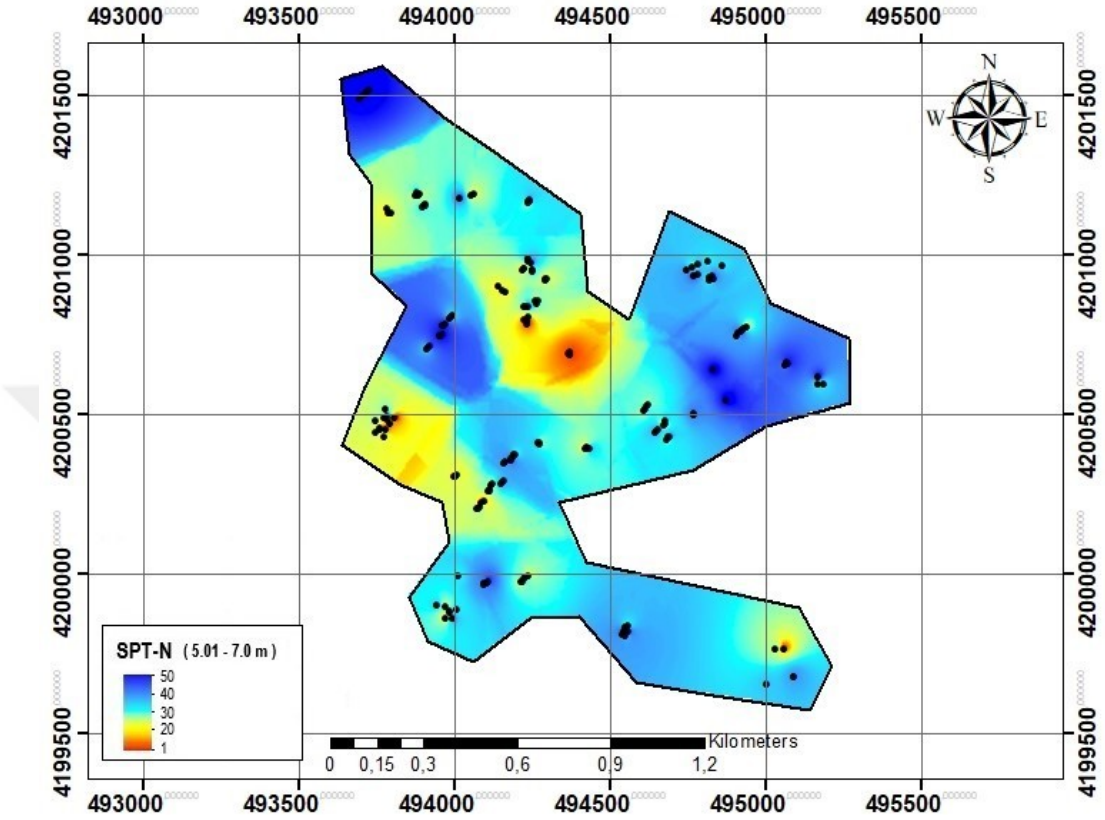

Figure 4.4 SPT-N in study area (5-7m)

It was determined that 10% of the SPT-N data from 178 boring points between 7-9 m depth obtained from the study area are between 1-20, 26% between 21-30, and 64% between 31-50. The prepared SPT-N map is presented in Figure 4.5.

The SPT-N value of the dark blue colored areas observed in the study area is 45-50. The SPT-N value of the light blue color that dominates the majority of the study area is between 30-45. The SPT-N value of the red colored area observed in the middle of the study area is between 1-10. The SPT-N value of the yellow areas observed in the central part of the region and a small part of the western part is between 20-30.

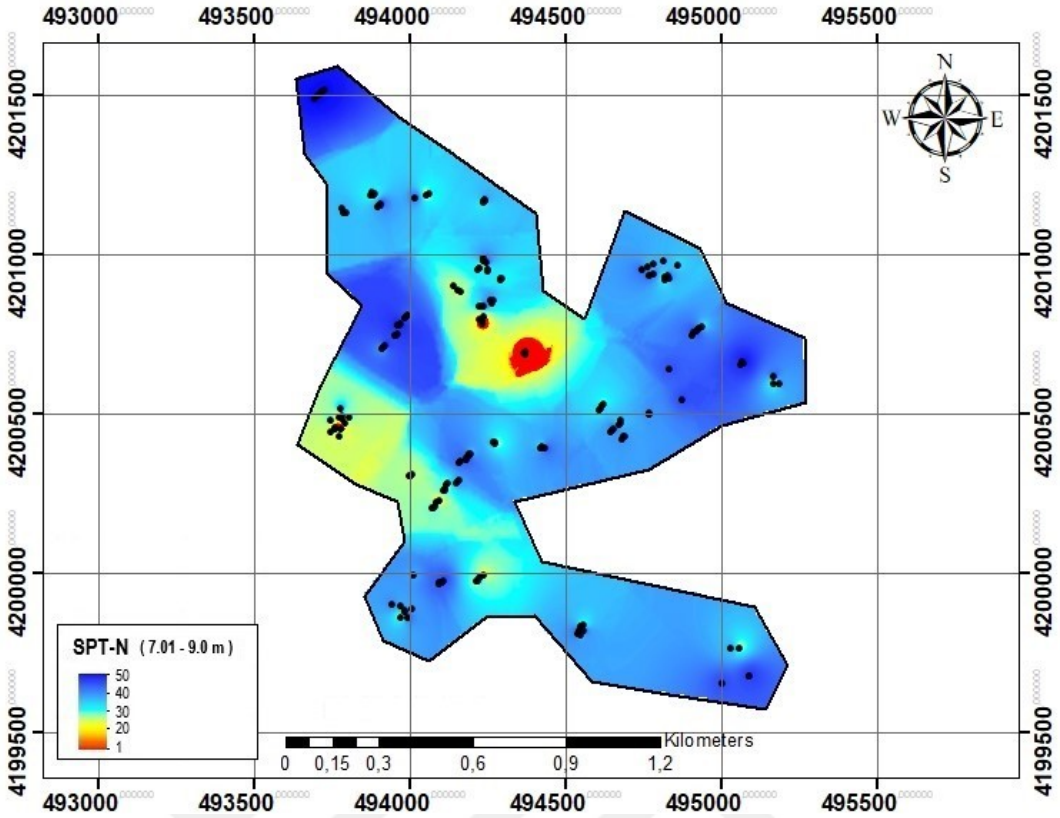

Figure 4.5 SPT-N in study area (7-9 m)

It was determined that 8% of the SPT-N data from 178 boring points between 9-11 m depth obtained from the study area are between 1-20, 21% between 21-30, and 71% between 31-50. The prepared SPT-N map is presented in Figure 4.6.

A large part of the study area is covered with blue color as observed, and the SPT-N value is between 30-50. The SPT-N values of two small red areas formed towards the middle of the study area were observed between 1-10. The SPT-N value of the remaining yellow regions was observed to be between 15-25.

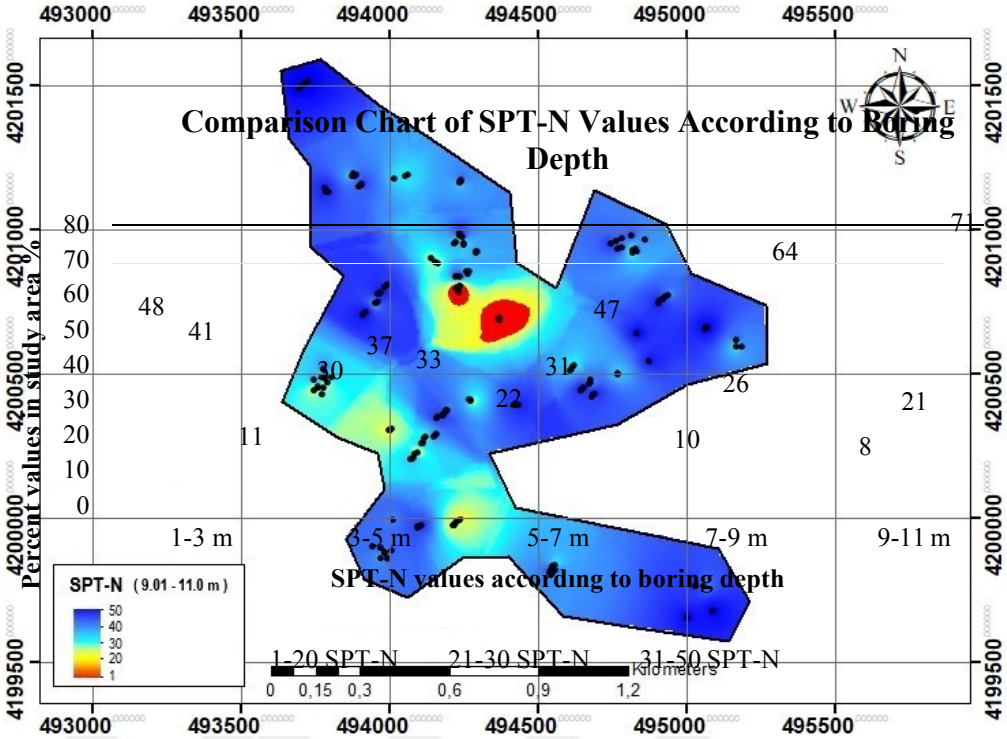

Figure 4.6 SPT-N in study area (9-11 m)

When we look at the results obtained from 1-3 m, 3-5 m, 5-7 m, 7-9 m, 9-11 m intervals in the borings; it was determined that 24% of the SPT-N data were between 1-20, 31% between 21-30, and 45% between 31-50. The graphic created in this context is presented in Figure 4.7.

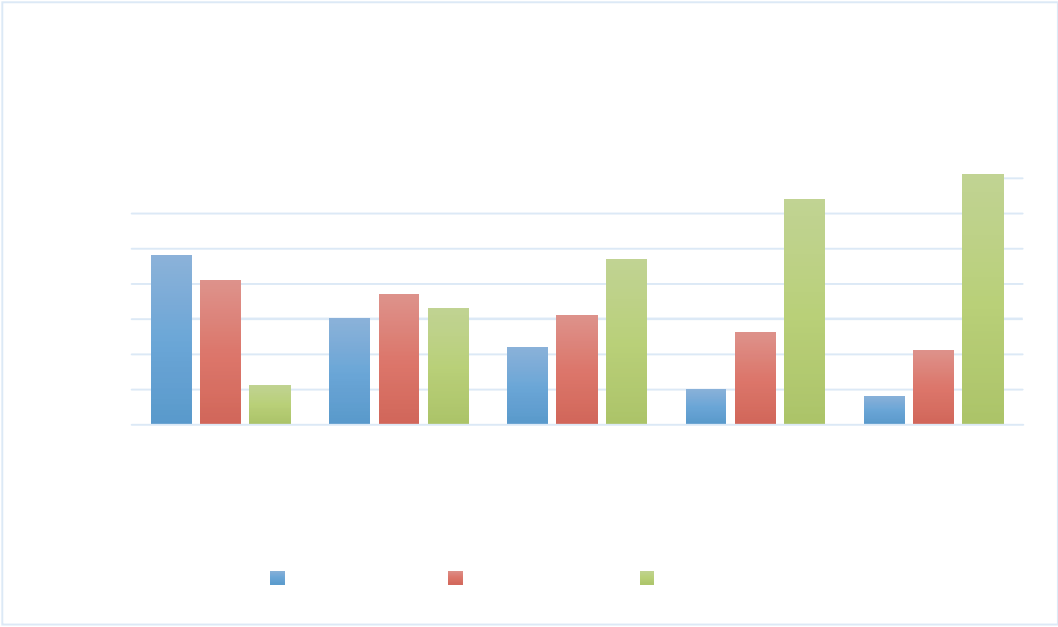

Figure 4.7 Comparison chart of SPT-N values according to boring depths

4.2 Bearing Capacity Calculation Analysis

Many methods are encountered when calculating the bearing capacity of an area. When these methods are classified, they can be considered as field experiments and geophysical methods. Data were obtained from 178 boring points in the study area. While these data were calculated by applying the Keçeli Method and Tezcan et al Method, which are geophysical methods, the bearing capacity was calculated using the Meyerhof Method and Terzaghi-Peck Method, which are the field tests.

For 178 boring points in the study area, the data obtained from the surface to a depth of 11 m were calculated among themselves. For depths between 1-3 m, 3-5 m, 5-7 m, 7-9 m, 9-11 m, maps were created using the Keçeli Method, Tezcan et al Method, Meyerhof Method and Terzaghi-Peck Method. The maps were obtained using the ArcGis program. Comparisons were made with the bearing capacity maps obtained from the depths between 1-3 m and 9-11 m in the study area.

By using geophysical methods, bearing capacity maps of depths in the range of 1-3 m were created. The maps of the data obtained by the Keçeli Method and Tezcan et al Method are given in Figure 4.8 and Figure 4.9.

In the data map obtained by the Keçeli Method, the bearing capacity is seen as approximately 60-150 kN/m^2 in the red-orange colored regions. The bearing capacity of the gray area in the south of the map is between 150-250 kN/m^2.

In the data map obtained by the Tezcan et al. method, the bearing capacity is between 200-300 kN/m^2 in the regions where gray and yellow colors intersect. While the bearing capacity is between 350-450 kN/m^2 in the green parts seen in some parts of the map, the bearing capacity of the pink colored region seen in the south of the map is between 500-565 kN/m^2.

The maximum bearing capacity is 242.5 kN/m^2 and the minimum bearing capacity is 63.2 kN/m^2 in the data map obtained by the Keçeli Method between 1-3 m depths. In the data map obtained by the Tezcan et al. method, the maximum bearing capacity is 563.5 kN/m^2, and the minimum bearing capacity is 210.9 kN/m^2.

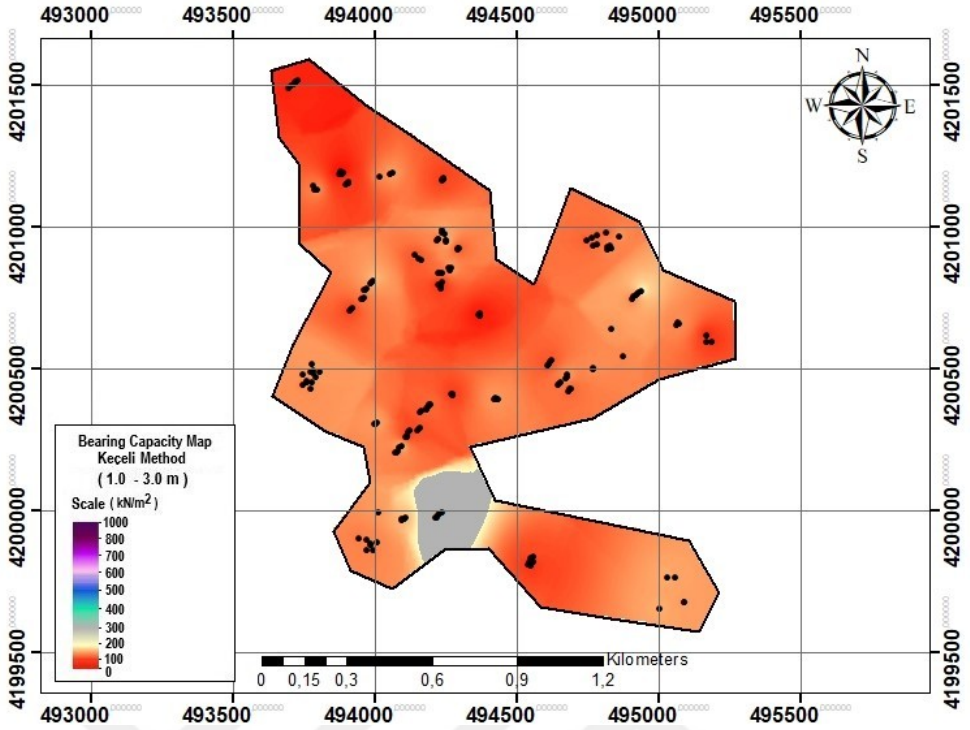

Figure 4.8 Bearing capacity map according to Keçeli (1990) method (1-3 m)

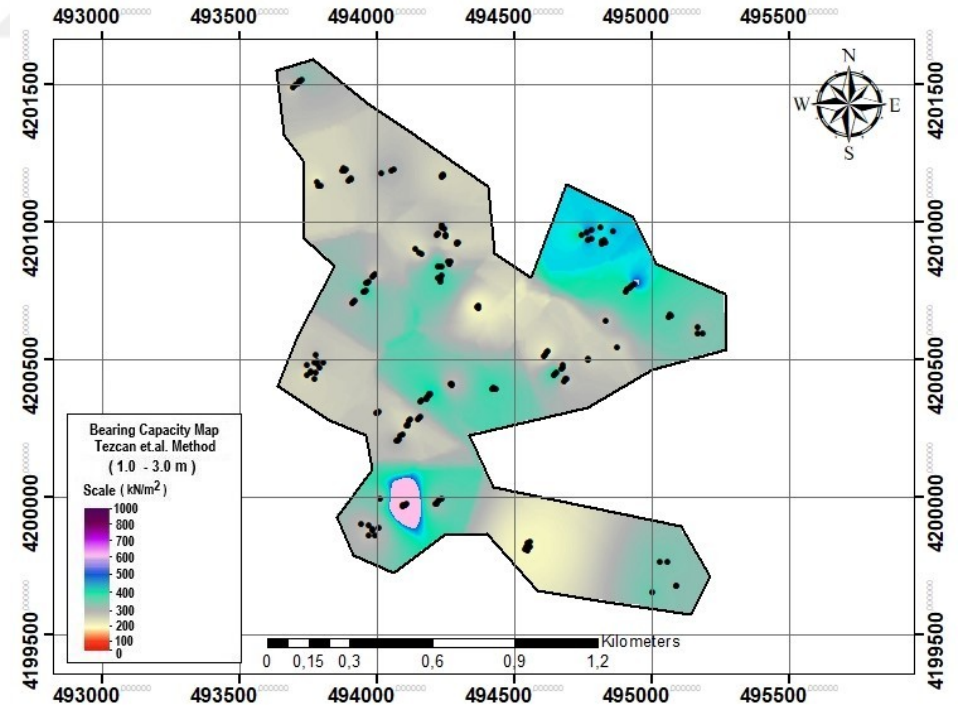

Figure 4.9 Bearing capacity map according to Tezcan et al. (2010) method (1-3 m)

By using field test methods, bearing capacity maps of depths in the range of 1-3 m were created. The maps of the data obtained by the Meyerhof Method and the Terzaghi-Peck Method are given in Figure 4.10 and Figure 4.11.

In the data map obtained by the Meyerhof Method, the bearing capacity is 110-250 kN/m^2 in the region with yellow-orange color distributions. It has been seen that the bearing capacity of the gray colored regions is 250-350 kN/m^2, while the bearing capacity of the green-blue colored regions is 350-500 kN/m^2. The bearing capacity range of the pink colored areas on the map is 500-570 kN/m^2.

In the data map obtained by Terzaghi-Peck Method, the bearing capacity of the regions dominated by orange-yellow colors is around 98-200 kN/m^2. The bearing capacity of the regions of the blue-green parts on the map is between 350-488 kN/m^2.

The maximum bearing capacity is 565.6 kN/m^2 and the minimum bearing capacity is 113.1 kN/m^2 in the data map obtained by the Meyerhof Method between 1-3 m depths. In the data map obtained by the Terzaghi-Peck method, the maximum bearing capacity is 488 kN/m^2, and the minimum bearing capacity is 98 kN/m^2.

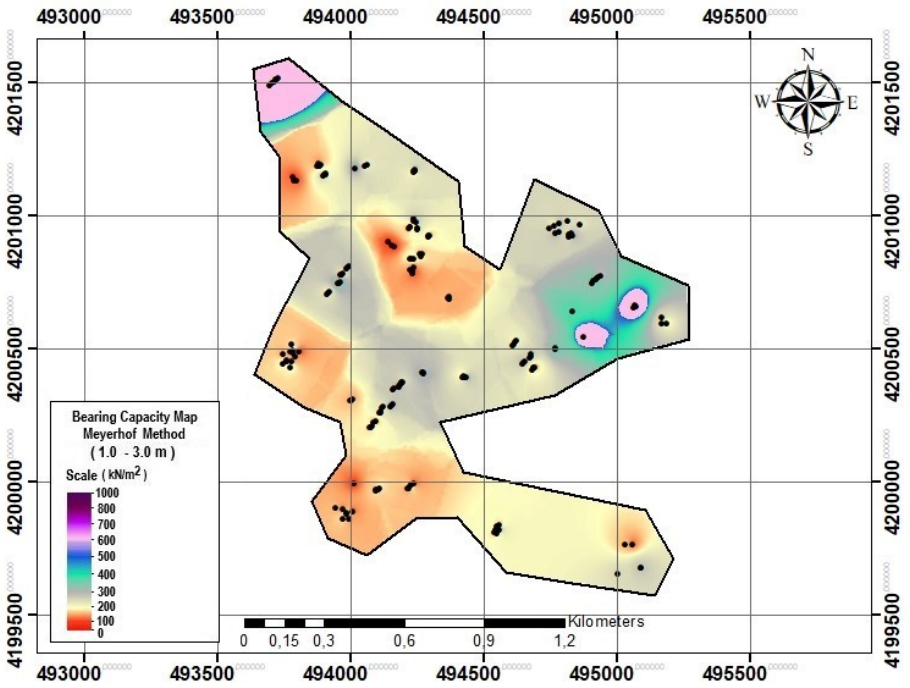

Figure 4.10 Bearing capacity map according to Meyerhof (1974) method (1-3 m)

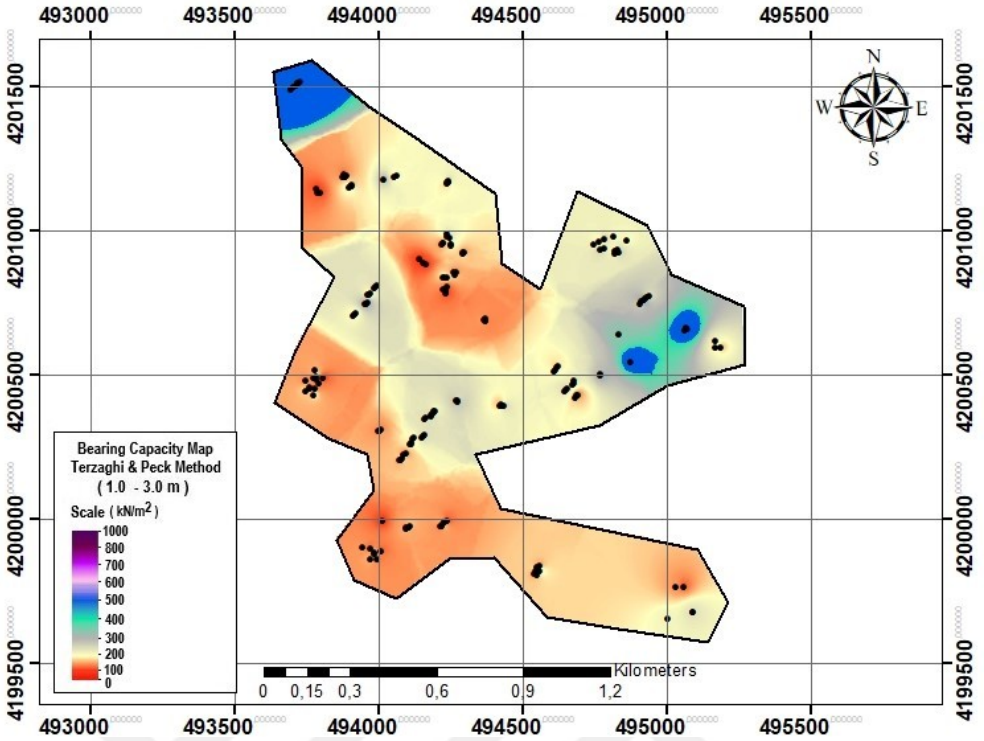

Figure 4.11 Bearing capacity map according to Terzaghi-Peck (1967) method (1-3 m)

By using geophysical methods, bearing capacity maps of depths in the range of 9-11 m were created. The maps of the data obtained by the Keçeli Method and Tezcan et al Method are given in Figure 4.12 and Figure 4.13.

In the data map obtained by Keçeli Method, the bearing capacity of the regions dominated by orange-yellow colors is around 85-100 kN/m^2. The bearing capacity of the regions with yellow-gray colors that dominate the map varies between 150-300 kN/m^2. In the green area on the map, the bearing capacity is observed as 300-385 kN/m^2.

In the data map obtained by Tezcan et al. Method, the bearing capacity of the regions dominated by blue-green colors is around 350-550 kN/m^2. The bearing capacity range of the pink colored areas on the map is 650-750 kN/m^2. The bearing capacity of the remaining purple area on the map varies between 750-975 kN/m^2.

The maximum bearing capacity is 381.2 kN/m^2 and the minimum bearing capacity is 88.7 kN/m^2 obtained by the Keçeli Method between 9-11 m depths. In the data map obtained by the Tezcan et al. method, the maximum bearing capacity is 971.2 kN/m^2, and the minimum bearing capacity is 264.7 kN/m^2.

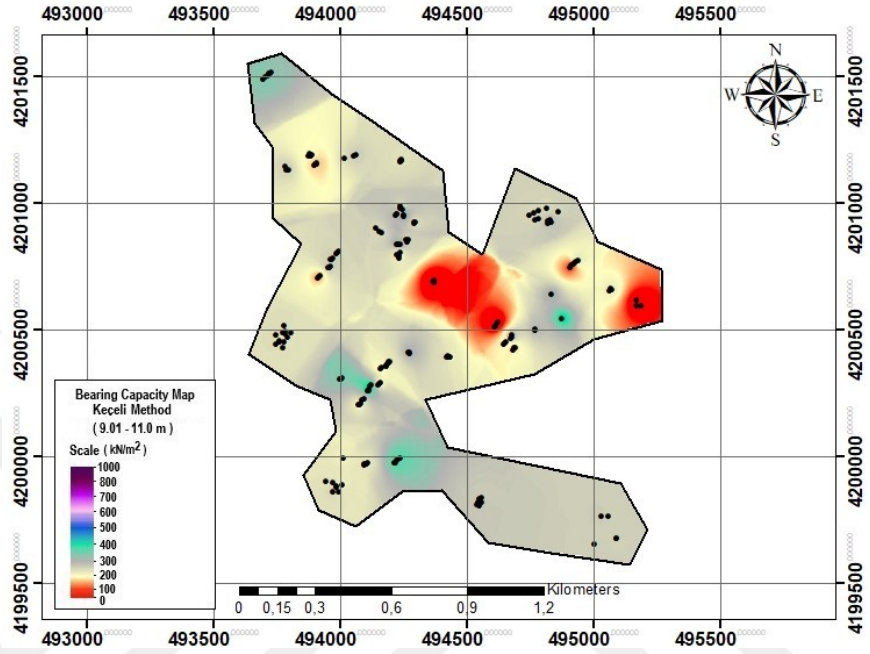

Figure 4.12 Bearing capacity map according to Keçeli (1990) method (9-11 m)

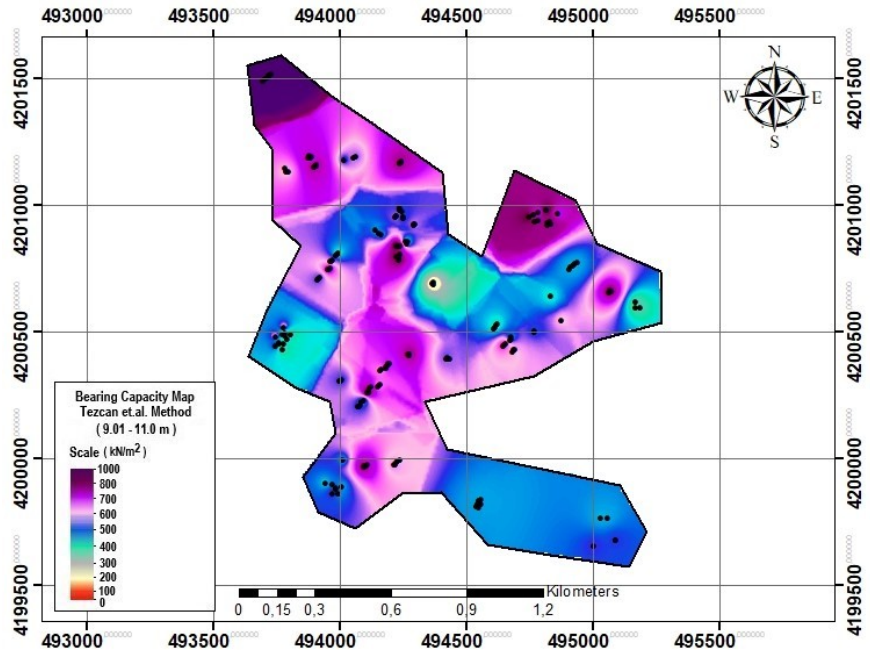

Figure 4.13 Bearing capacity map according to Tezcan et al.(2010) method (9-11 m)

By using field test methods, bearing capacity maps of depths in the range of 9-11 m were created. The maps of the data obtained by the Meyerhof Method and the Terzaghi-Peck Method are given in Figure 4.14 and Figure 4.15.

The bearing capacity of the red colored region in the Meyerhof Method data map was estimated to be around 150 kN/m^2. While the bearing capacity of the green-gray colored areas of the map is 350-450 kN/m^2, the bearing capacity of the blue colored regions is between 450-550 kN/m^2. It has been observed that the bearing capacity of the lilac colored areas on the map is 600-650 kN/m^2.

The bearing capacity of the red-colored region and the surrounding yellow-colored region in the Terzaghi-Peck data map is between 100 and 150 kN/m^2. The bearing capacity of the map's gray-green colored areas is 300-450 kN/m^2. The bearing capacity of the blue colored areas on the map has been determined to be 450-500 kN/m^2.

The maximum bearing capacity is 645.7 kN/m^2 and the minimum bearing capacity is 155 kN/m^2 in the data map obtained by the Meyerhof Method between 9-11 m depths. In the data map obtained by the Terzaghi-Peck method, the maximum bearing capacity is 488 kN/m^2, and the minimum bearing capacity is 118 kN/m^2.

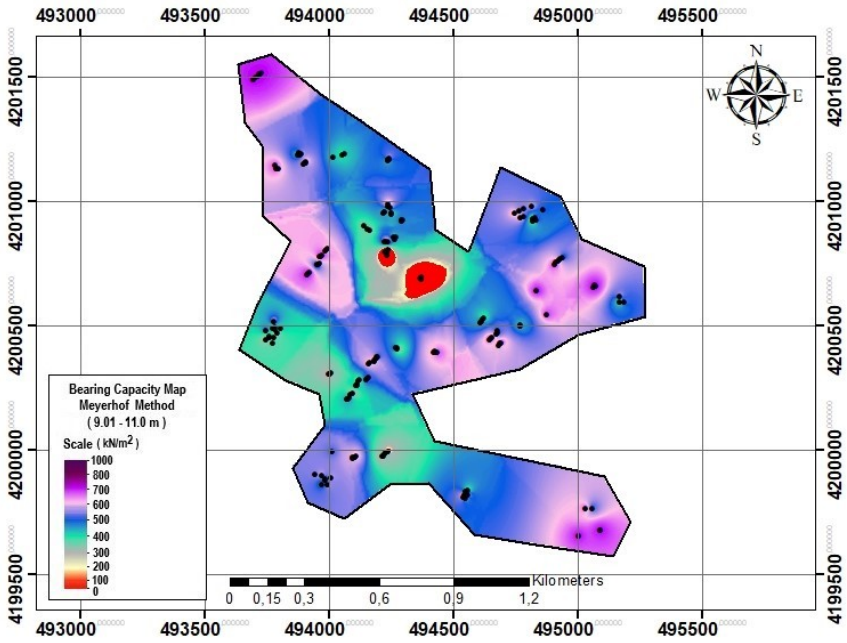

Figure 4.14 Bearing capacity map according to Meyerhof (1974) method (9-11 m)

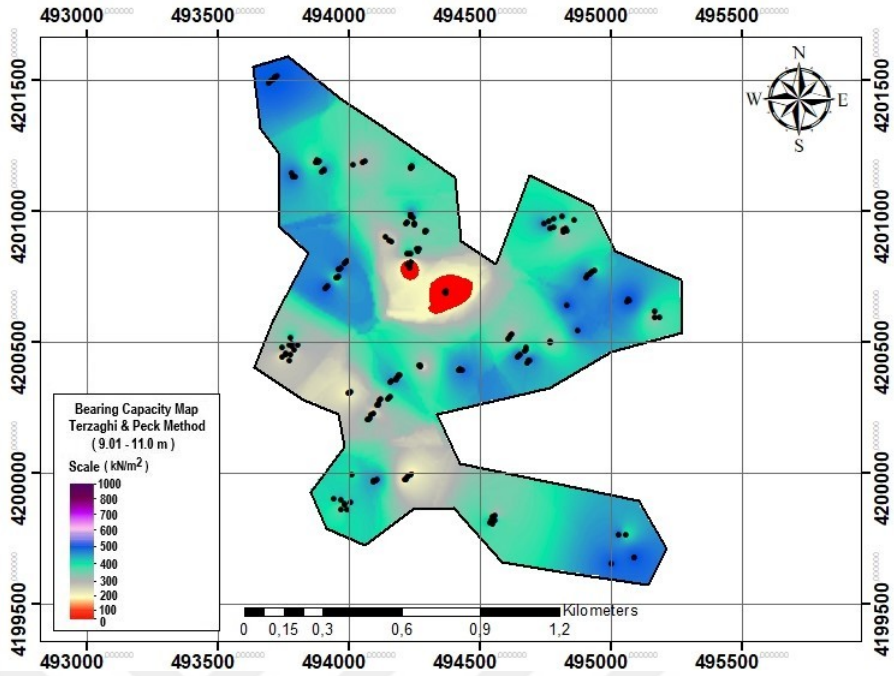

Figure 4.15 Bearing capacity map according to Terzaghi-Peck (1967) method (9-11 m)

4.3. Sheer Wave Velocity Calculation Analysis

The shear wave velocity (Vs), which is one of the dynamic properties of the soil, is one of the important ground properties in civil and earthquake engineering. The shear wave velocity can be determined directly by field and laboratory experiments. In addition, the shear wave velocity can be obtained by various formulas using the results of the field experiment. Shear wave velocities in the study area were determined using seismic measurements in our thesis study. Furthermore, other shear wave velocity results were obtained using methods developed using the SPT-N values obtained for the study area. Shear wave velocity maps and comparison graphs were created for the depths studied in the study area, which ranged from 1-3 m to 3-5 m, 5-7 m to 7-9 m, and 9-11 m. The ArcGIS program was used to create maps.

The results obtained in the calculation of shear wave velocity by field tests (SPT-N) and the data obtained from 178 boring points using the Ohba and Trauma Method, Imai and Yoshimura Method, Tsiambos and Sabatakakis Method are comparatively shown in Figure 4.16, Figure 4.18, Figure 4.20, Fig. 4.22 and Fig. 4.24.

In addition, the results obtained by measuring the shear wave velocity in the terrain (Seismic Methods) and ground suveys (SPT-N) and calculating data from 178 boring points using the Ohba and Trauma Method, Imai and Yoshimura Method, Tsiambos and Sabatakakis Method are shown comparatively in Figure 4.17, Figure 4.19, Figure 4.21, Figure 4.23, Figure 4.25.

Shear wave velocity was calculated for 1-3 m, 3-5 m, 5-7 m, 7-9 m, 9-11 m, considering Seismic Methods and SPT-N values obtained from 178 boring points. As a result of the calculation, the proximity sensitivity ranking of the results obtained by the seismic method was performed. The ranking is closely related to the Imai and Yoshimura Method, the Ohba and Trauma Method, the Tsiambos and Sabatakakis Method for the ranges of 1-3 m and 3-5 m. When the sequence is evaluated from near to far, seismic measurements for the 5-7 m range show a general spread. The sequence is as follows: Tsiambos and Sabatakakis Method, Ohba and Trauma Method, Imai and Yoshimura Method for 7-9 m and 9-11 m intervals from near to far.

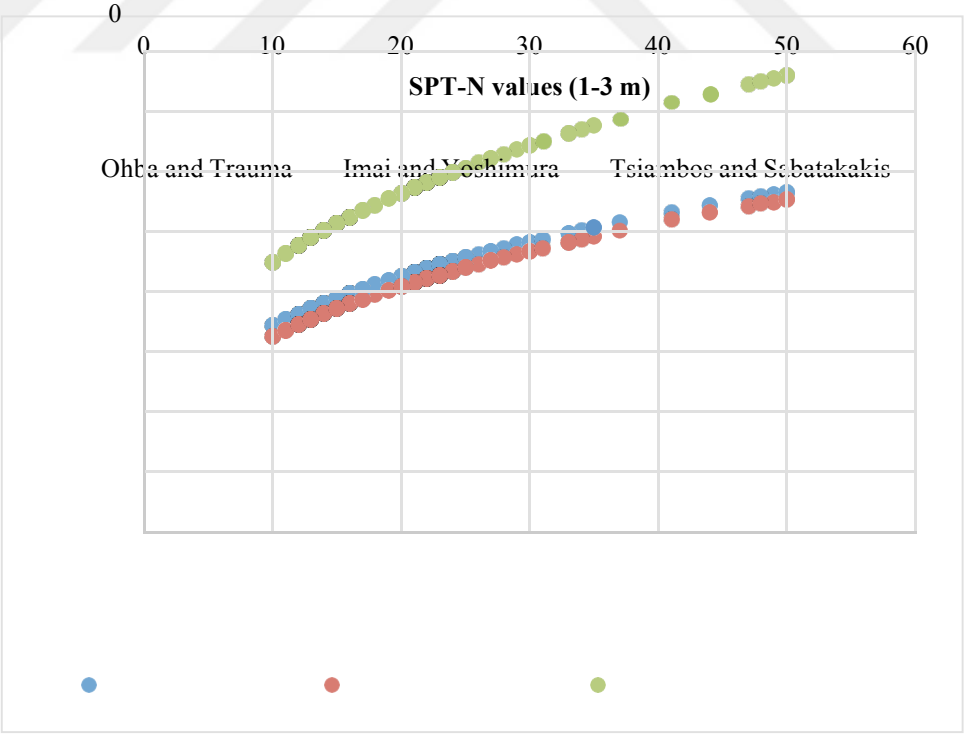

Figure 4.16 Comparison graph of shear wave velocity calculated results according to SPT-N values 1-3 m depth

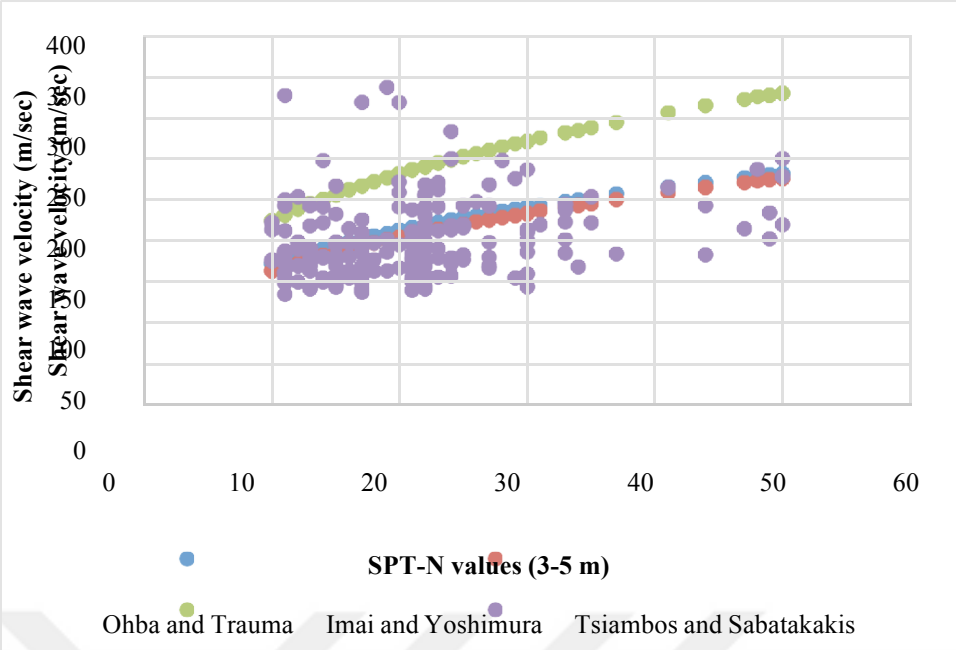

Figure 4.17 Comparison graph of shear wave velocity according to seismic measurements and SPT-N values 1-3 m depth

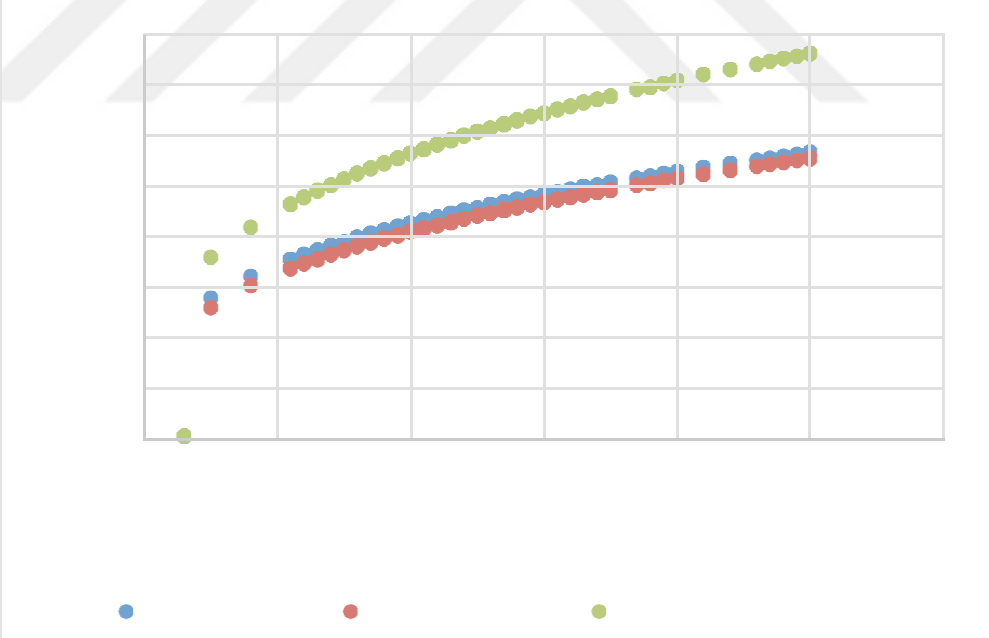

Figure 4.18 Comparison graph of shear wave velocity calculated results according to SPT-N values 3-5 m depth

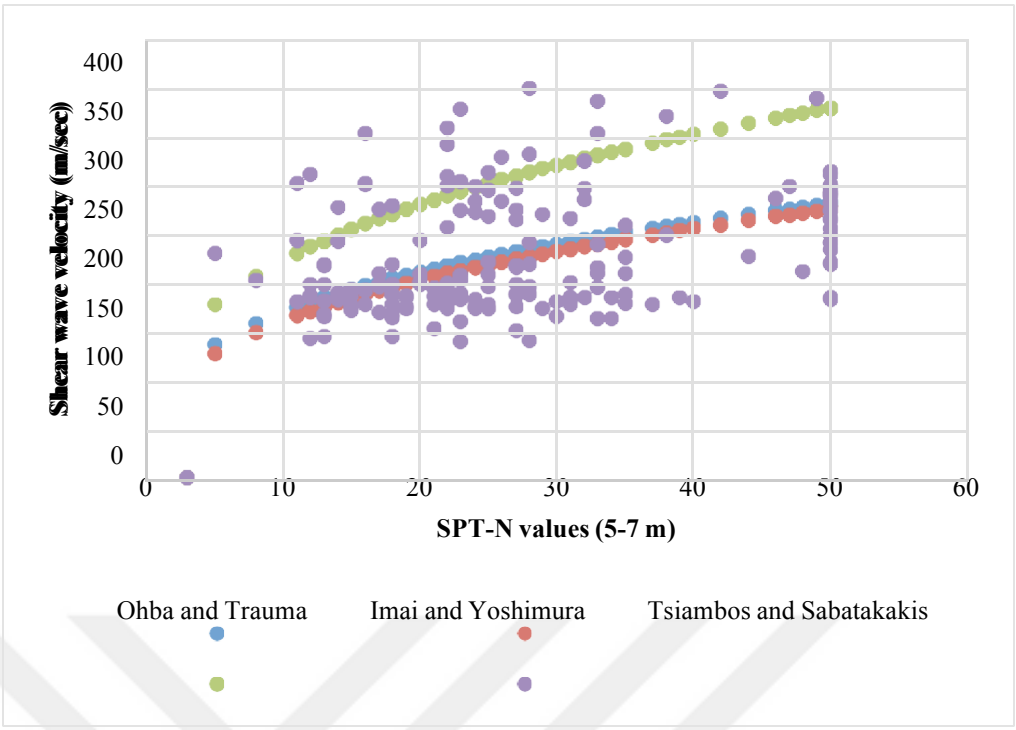

Figure 4.19 Comparison graph of shear wave velocity according to seismic measurements and SPT-N values 3-5 m depth

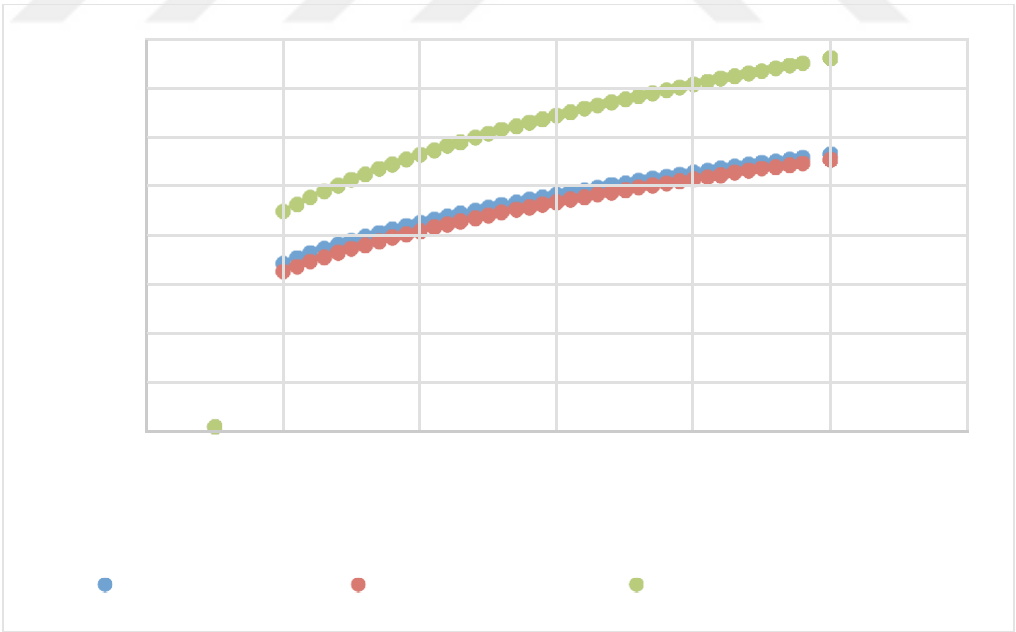

Figure 4.20 Comparison graph of shear wave velocity calculated results according to SPT-N values 5-7 m depth

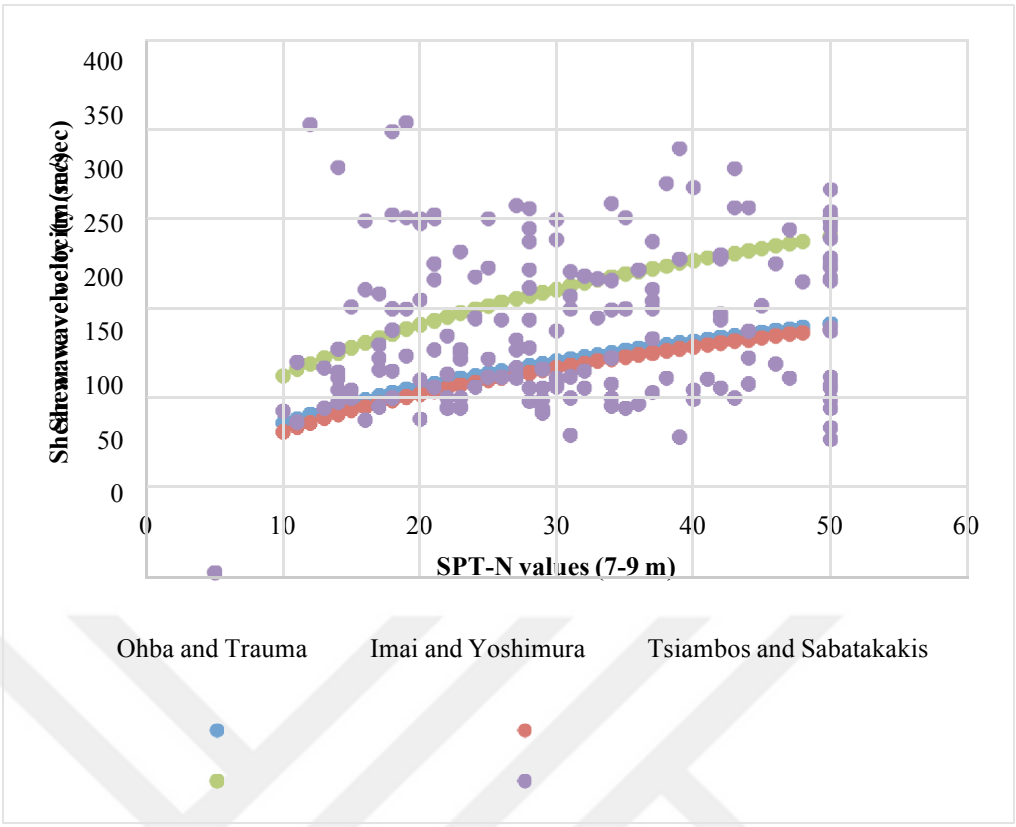

Figure 4.21 Comparison graph of shear wave velocity according to seismic measurements and SPT-N values 5-7 m depth

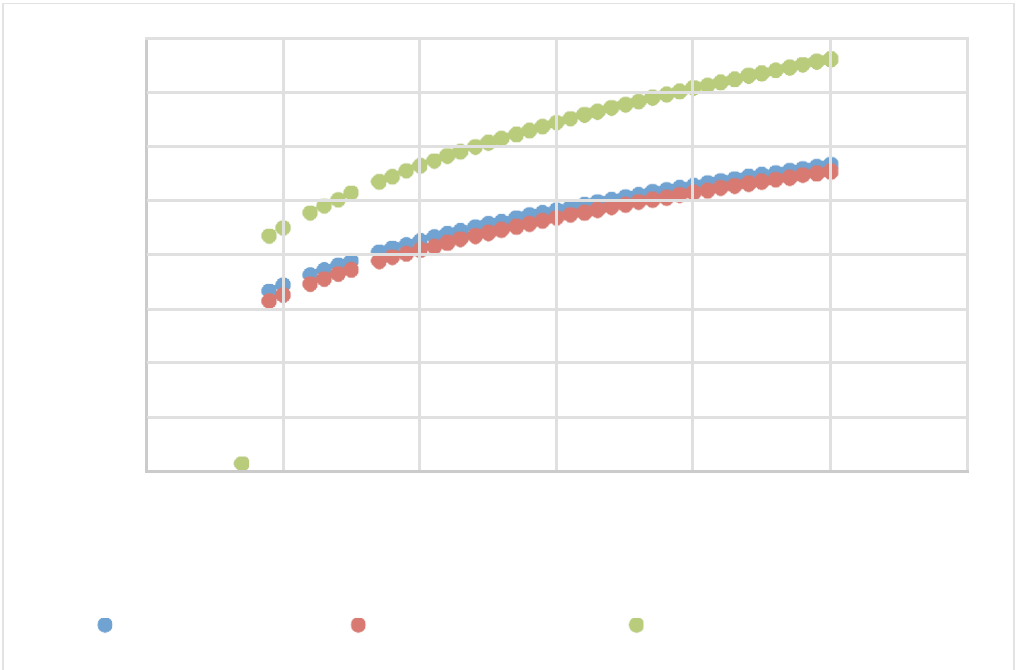

Figure 4.22 Comparison graph of shear wave velocity calculated results according to SPT-N values 7-9 m depth

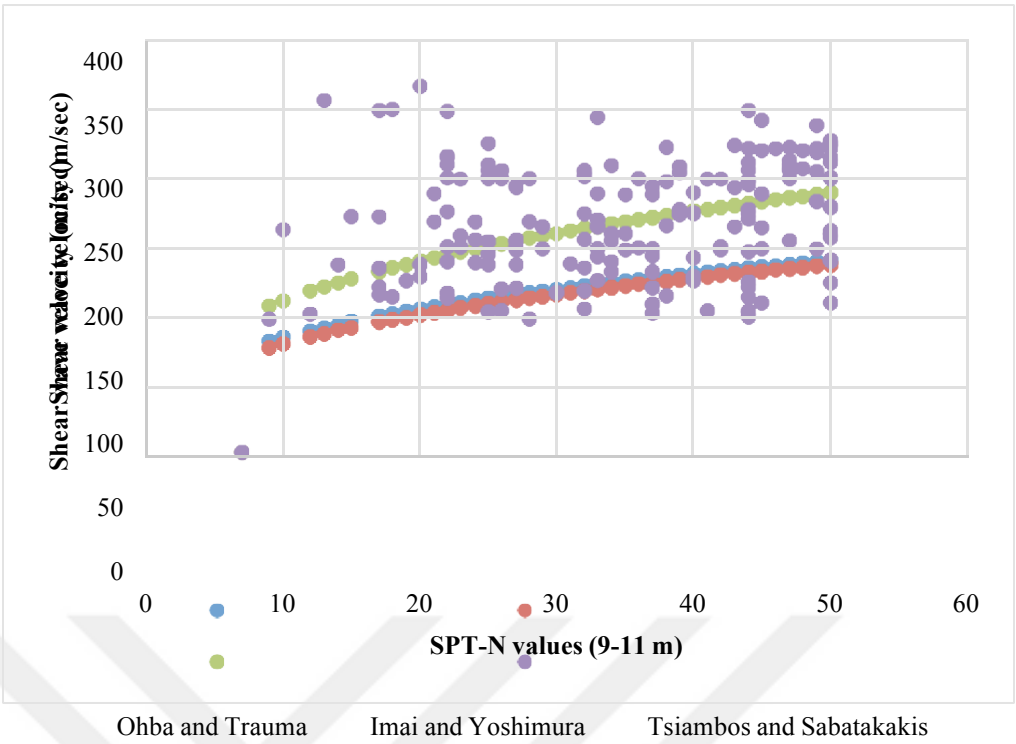

Figure 4.23 Comparison graph of shear wave velocity according to seismic measurements and SPT-N values 7-9 m depth

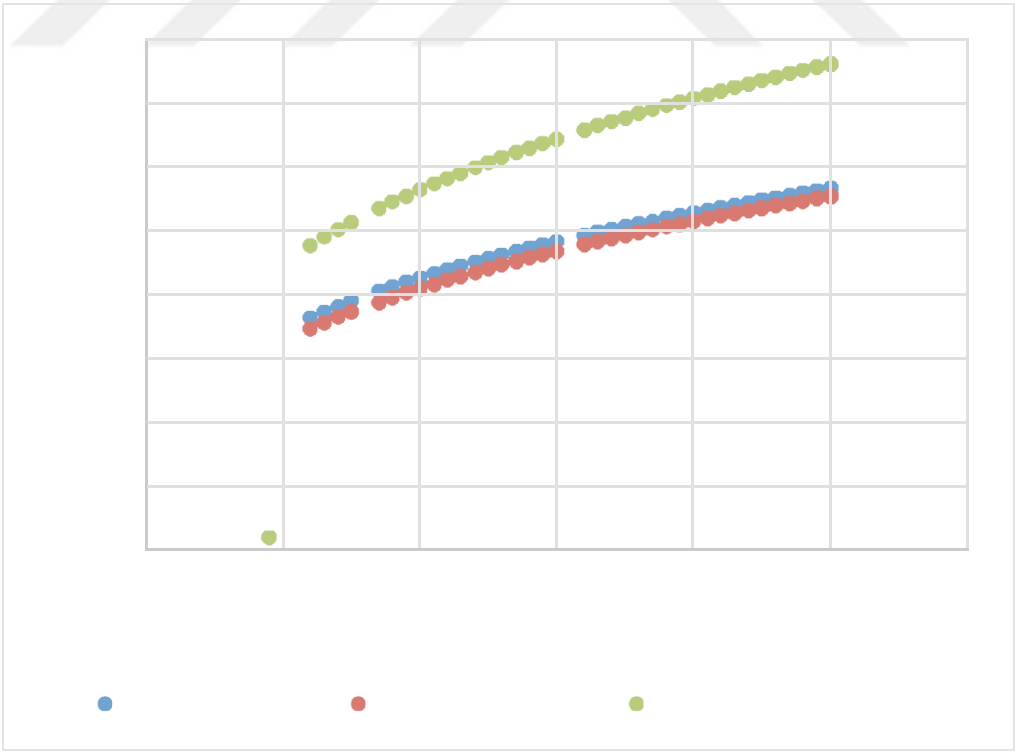

Figure 4.24 Comparison graph of shear wave velocity calculated results according to SPT-N values 9-11 m depth

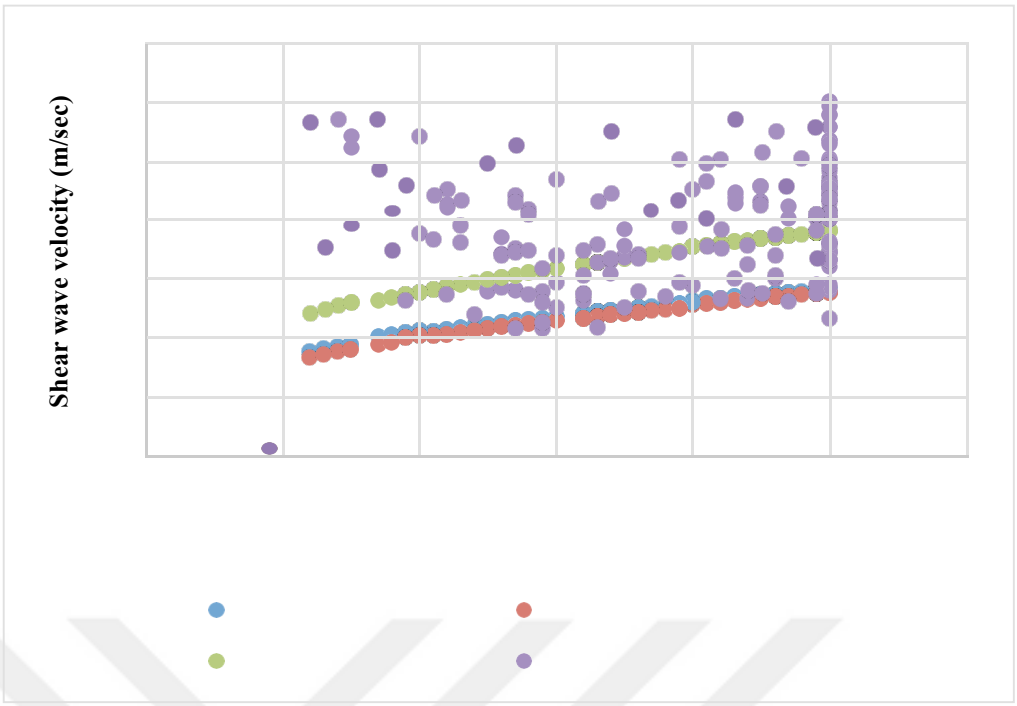

Figure 4.25 Comparison graph of shear wave velocity according to seismic measurements and SPT-N values 9-11 m depth

It has been observed that the results obtained from seismic measurement on graphs and the results of calculation methods obtained with SPT-N values are very different. When the results of the shear wave velocity found with the SPT-N values were examined between themselves, it was observed that the results obtained from the Imai and Yoshimura Method and the Ohba and Trauma Method were very close to each other.

The maximum and minimum values of the Vs value obtained by seismic measurements and the Vs value found from the calculations obtained with the SPT-N value were determined in the study area. The maximum Vs value obtained by the Ohba and Trauma Method is 282.5 m/sec, and the minimum Vs value is 138.3 m/sec. The maximum Vs value obtained by the Imai and Yoshimura Method is 276.4 m/sec, and the minimum Vs value is 129.2 m/sec. The maximum Vs value obtained by the Tsiambos and Sabatakakis Method is 276.3 m/sec, and the minimum Vs value is 178.9 m/sec. When the Vs values obtained as a result of seismic measurements are examined, the maximum is 598 m/sec, and the minimum is 135 m/sec.

Shear wave velocity data obtained from depths ranging from 1-3 m to 3-5 m, 5-7 m to 7-9 m, and 9-11 m were created using the ArcGis program as a result of seismic measurements taken in the study area. Figure 4.26 depicts the shear wave velocity map (1-3 m).

A shear wave velocity map obtained from seismic measurements in the study area for a depth of 1-3 m was investigated. The pink colored regions on the map have Vs values ranging from 100 m/sec to 150 m/sec. The Vs value of the yellow-orange colored regions that dominate most of the map is between 150 m/sec and 250 m/sec. The Vs value of the green zones on the map is approximately 250 m/sec and 400 m/sec. The maximum Vs value obtained at 1-3 m depth in the study area is 387 m/sec, and the minimum Vs value is 135 m/sec.

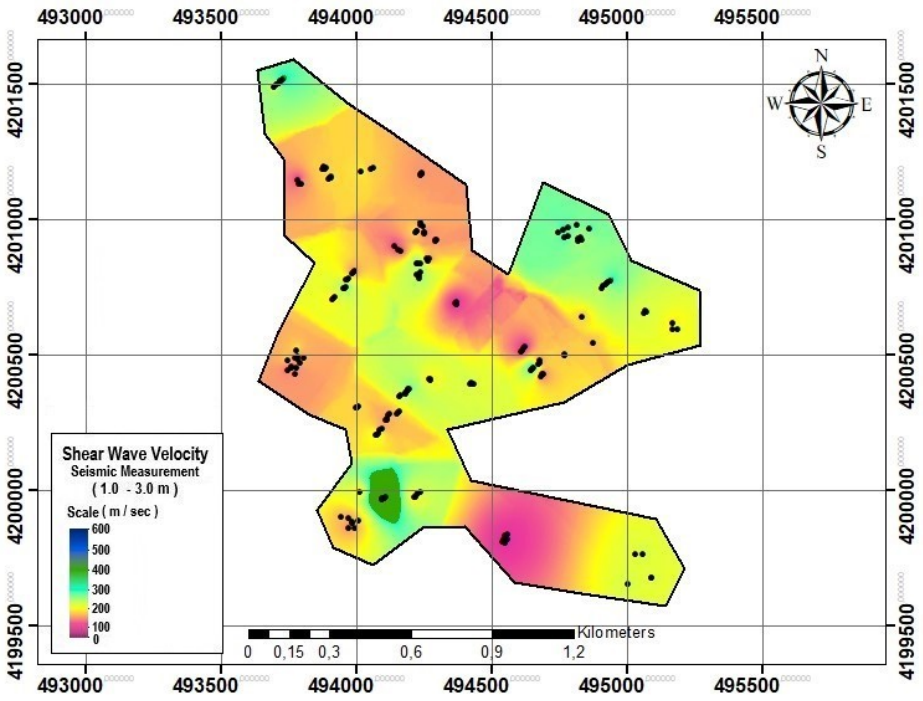

Figure 4.26 Shear wave velocity map obtained from seismic measurements (1-3 m)

Shear wave velocity map for 3-5m depth obtained from seismic measurements in the study area was examined. The Vs value of the pink areas on the map ranges between 100 and 150 m/sec. The Vs value of the yellow colored regions, which dominate a large portion of the map, is found to be between 150 and 250 m/sec. The Vs value of the green areas in the map is approximately 250 m/sec and 400 m/sec. The maximum Vs value obtained at 3-5 m depth in the study area is 400 m/sec, and the minimum Vs value is 142 m/sec. The shear wave velocity map (3-5 m) is given in Figure 4.27.

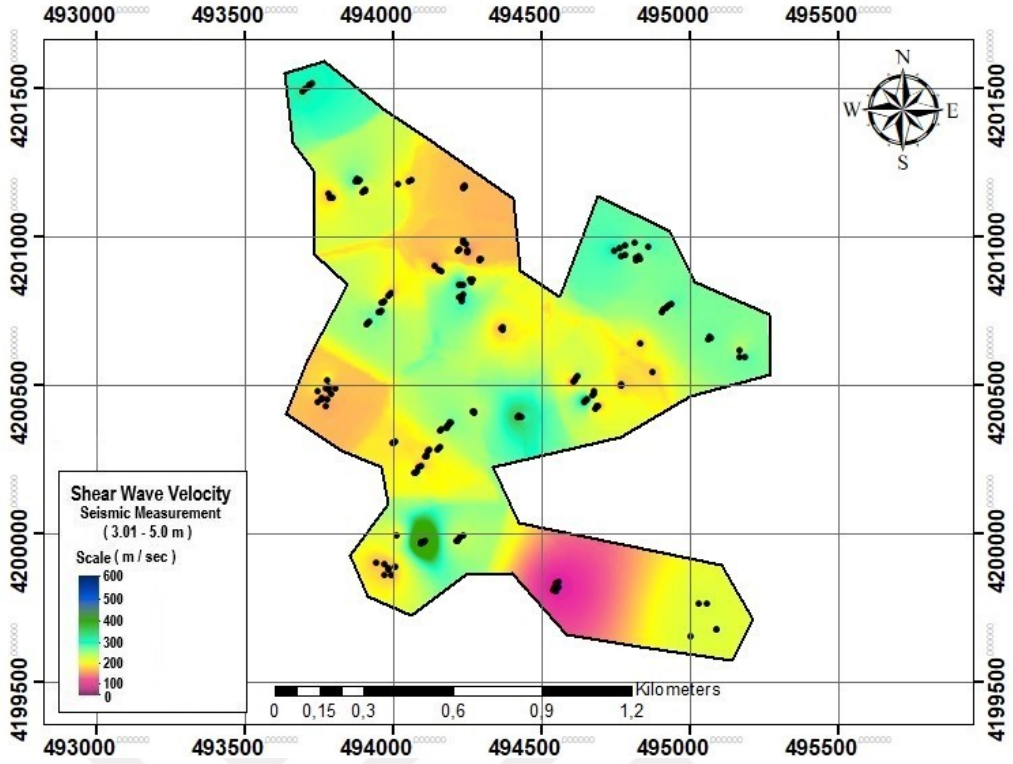

Figure 4.27 Shear wave velocity map obtained from seismic measurements (3-5 m)

The shear wave velocity map obtained from seismic measurements in the study area for 5-7 m depth was examined. The pink colored regions on the map have a Vs value of around 150 m/sec. The Vs value of the yellow colored regions on the map is observed to be between 150 and 250 m/sec. The Vs value of the green zones that dominate the majority of the map ranges from 250 m/sec to 400 m/sec. The Vs value of the blue colored region near the center of the map ranges between 450 and 550 m/sec. The maximum Vs value obtained in the study area at 5-7 m depth is 507 m/sec, and the minimum Vs value is 154 m/sec. Figure 4.28 depicts the shear wave velocity map (5-7 m).

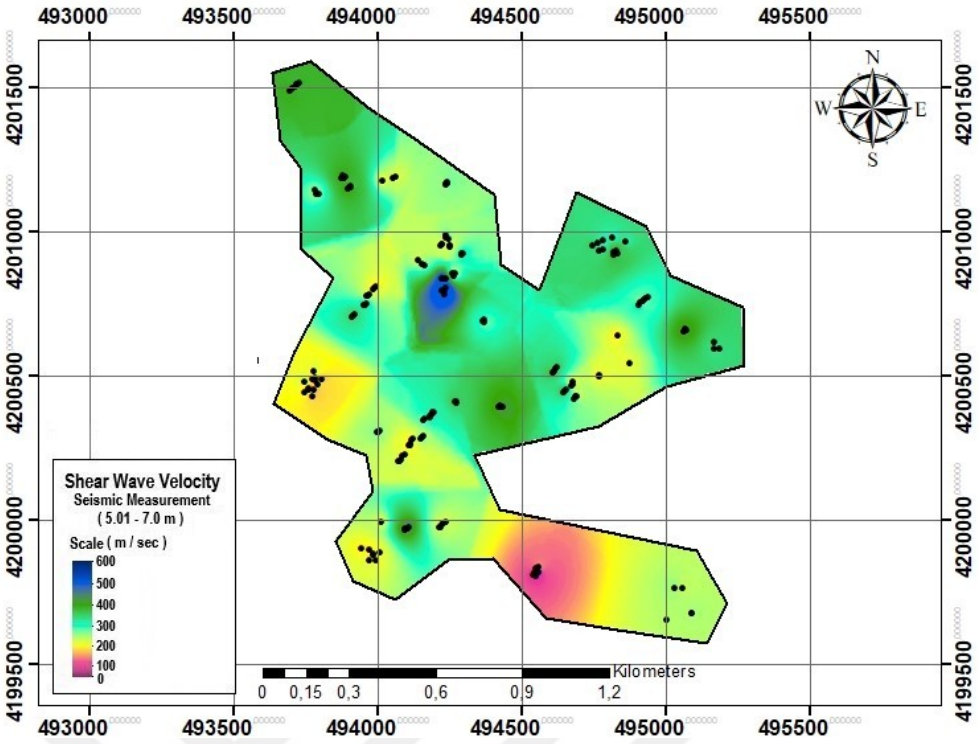

Figure 4.28 Shear wave velocity map obtained from seismic measurements (5-7 m)

Shear wave velocity map for 7-9m depth obtained from seismic measurements in the study area was examined. The Vs value of the pink areas on the map ranges between 150 and 250 m/sec. The Vs value of the yellow colored regions, which dominate a large portion of the map, is found to be between 300 and 400 m/sec. The Vs value of the blue colored regions on the map is found to be between 450 and 550 m/sec. The maximum Vs value obtained in the study area at 7-9 m depth is 533 m/sec, and the minimum Vs value is 199 m/sec. Figure 4.29 depicts the shear wave velocity map (7-9 m).

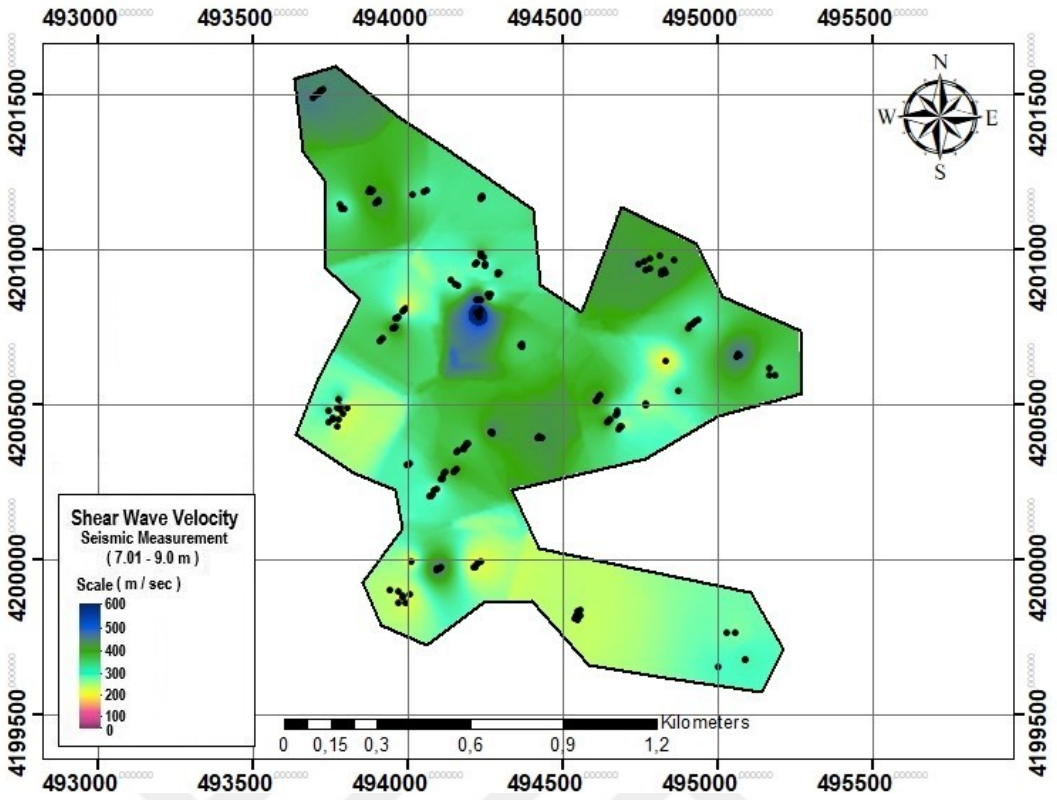

Figure 4.29 Shear wave velocity map obtained from seismic measurements (7-9 m)

Shear wave velocity map for 9-11 m depth obtained from seismic measurements in the study area was examined. The Vs value of the green colored regions that dominate most of the map is between 200 m/sec and 450 m/sec. The Vs value of the blue colored regions forming the remaining area of the map is between 450 m/sec and 600 m/sec. The maximum Vs value obtained at 9-11 m depth in the study area is 598 m/sec, and the minimum Vs value is 220 m/sec. The shear wave velocity map (9-11 m) is given in Figure 4.30.

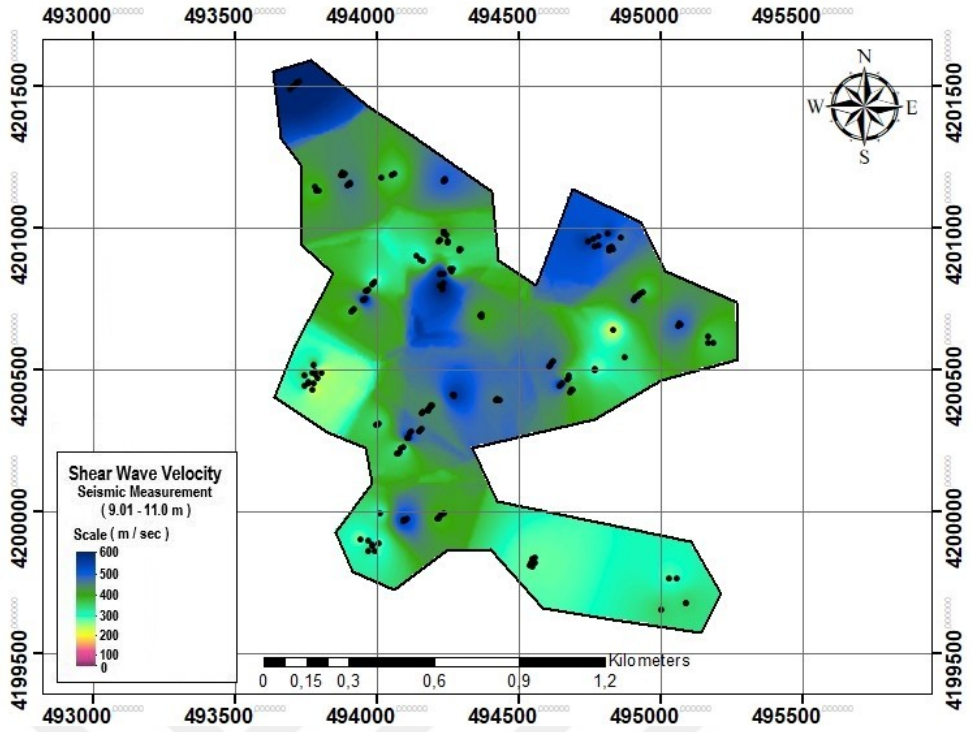

Figure 4.30 Shear wave velocity map obtained from seismic measurements (9-11 m)

4.3.1 Shear Wave Velocity Analysis 30 m

The strength of the ground is reflected in shear wave velocities. As a result, soil classification is based on shear wave velocity. Vs_{30} represents the average value of shear wave velocities obtained from on-site seismic studies up to a depth of 30m. The Vs_{30} values obtained from the measurements were evaluated in order to contribute to the GIS in the studies carried out for the Central District of Siirt, and the map was created using the mapping system's ArcGis program. As a result of the map, the soil classification for the Siirt Central District was obtained.

When the study area is examined, the pink colored regions seen on the Vs_{30} map have values ranging from 240 to 330 m/sec. The yellow-green regions of the map have Vs_{30} values ranging from 350 to 534 m/sec. In the study area, the maximum Vs_{30} value is 534 m/sec, and the minimum Vs_{30} value is 240 m/sec.

Velocity classifications were made in order to be able to conduct soil classification analysis of the velocity data obtained for 30 m depth in the study area with the seismic measurements made in the study area. 0% value of working area Vs>1500

m/sec, 0% value 760< Vs < 1500 m/sec, 45% value 360< Vs < 760 m/sec, 55% value 180< Vs < 360 m/sec, 0% Vs< 180 m/sec was determined. The map prepared in this context is presented in Figure 4.31.

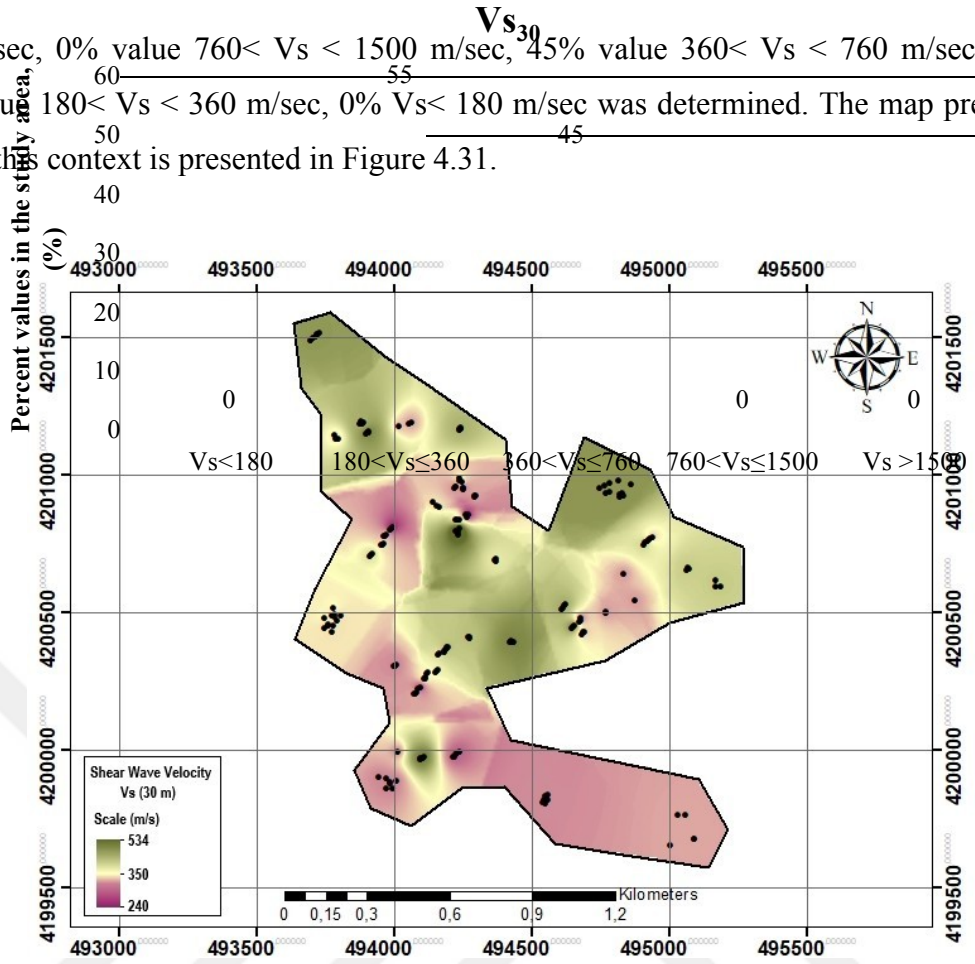

Figure 4.31 Map of shear wave velocity according to 30 m

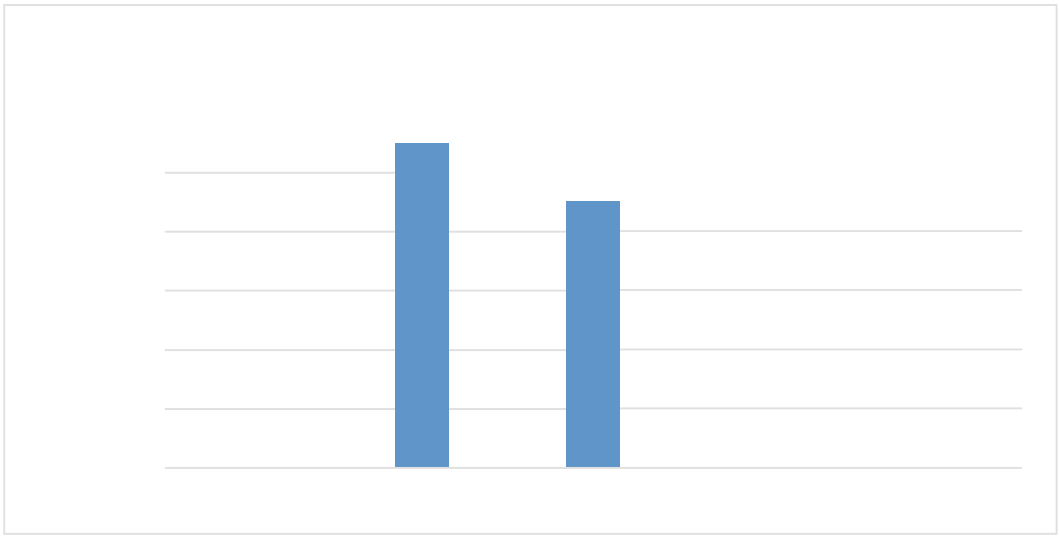

Figure 4.32 Distribution of Vs_{30} values in the study area

4.4 NEHRP (U.S.A.) Soil Classification Analysis According to Earthquake Code

The soil class is related to the average velocity of the shear wave velocity Vs_{30} up to a depth of 30 m, according to the NEHRP Earthquake Code. By using the data obtained by seismic measurements carried out in the study area, the necessary map for GIS analysis was created. While creating the map, ArcGis program was used and estimated maps of soil class values were created. In the prepared map, C and D soil class types were encountered in the study area.

With the seismic measurements carried out in the study area, it has been determined that 0% of the area is in A, 0% in B, 67% in C, 33% in D, and 0% in E soil class. The map prepared in this context is presented in Figure 4.33.

When the map is examined in general, the C soil class is more prevalent in the western part of the study area, while the D soil class is more prevalent in the eastern part. The blue colored areas on the map represent the C soil class, while the water green colored areas represent the D soil class.

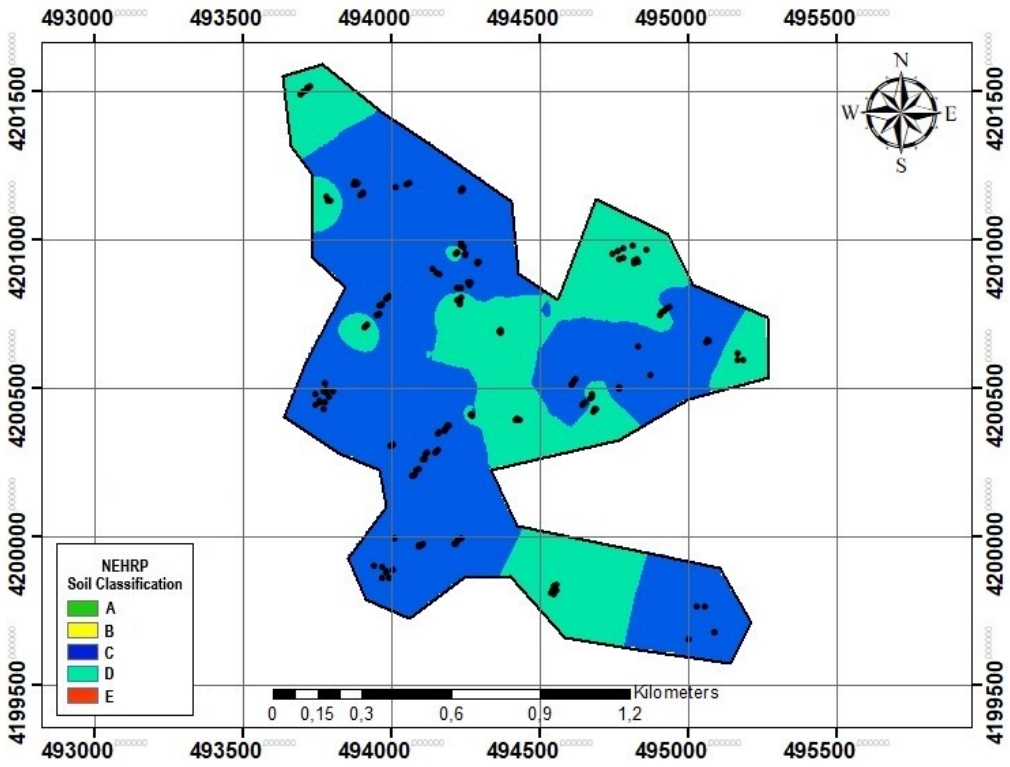

Figure 4.33 Map of NEHRP soil classification

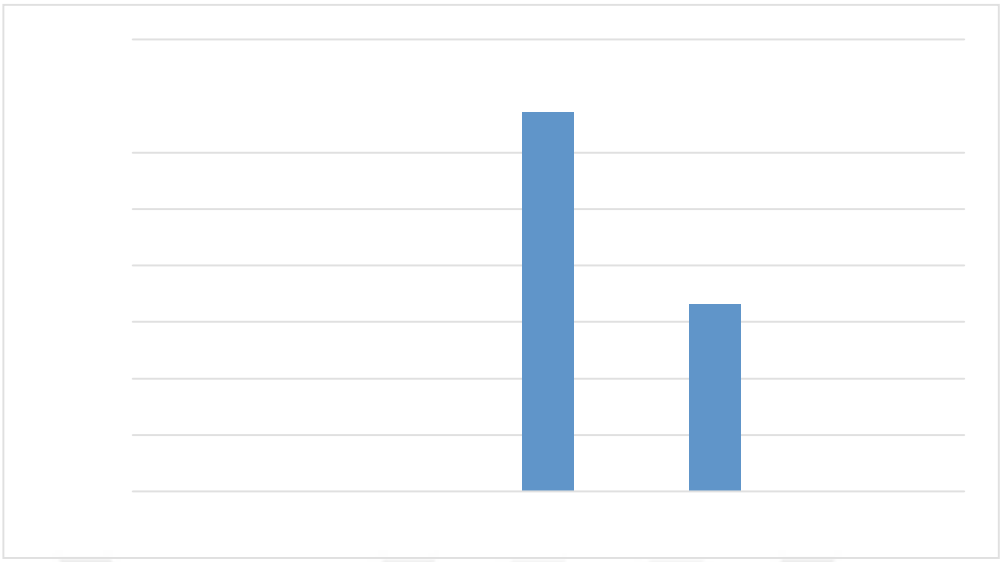

Figure 4.34 Distribution of soil classification values in the study area according to NEHRP

4.5 Earthquake Hazard Level Analysis According to Soil Amplification Calculation

Determining the soil ground effects and the construction of structures taking into account the determined soil effects is very important to prevent damage caused by possible earthquakes. In the study area, seismic studies were carried out to determine the local soil effect and data were obtained.

With the soil amplification values obtained from 178 boring points in the study area, estimated soil class maps were created using the ArcGis program. The data required for GIS analysis were obtained and processed on the map. The maximum soil amplification of the study area was determined as 2.46 and the minimum soil amplification was determined as 1.57. While creating the map, it was reflected as A (high hazard), B (medium hazard), C (low hazard).

As a result of the necessary calculations, it has been determined that 0% of the study area is A (high hazard), 52% is B (medium hazard), 48% is C (low hazard). The map prepared in this context is presented in Figure 4.35.

When the soil amplification assessment of the study area is made, it is observed that the B (medium hazard) and C (low hazard) classes are close to each other in value. While C (low hazard) class dominates in the northern region of the map, B (medium hazard) class dominates in the southern region.

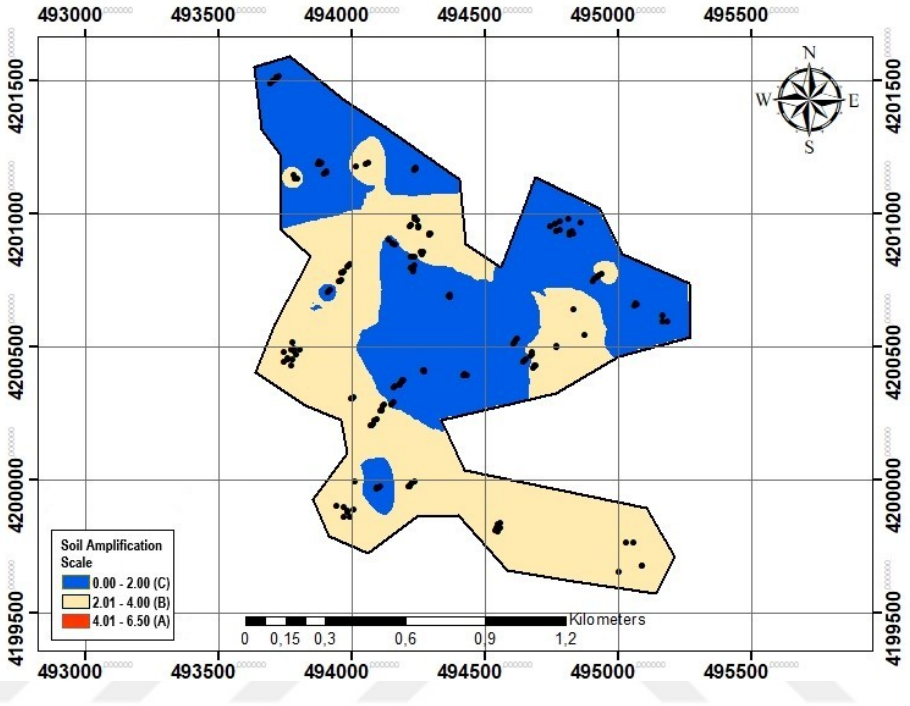

Figure 4.35 Hazard map according to soil amplification results

Figure 4.36 Distribution of hazard values in the study area according to soil amplification criteria

4.6. Dominant Vibration Period Analysis

The dominant vibration period represents the natural vibrational properties of the soil layers on the bedrock as a whole.

Dominant Vibration Period values were determined using data from 178 boring points in the study area, and estimated maps were created using the ArcGis program. On the maps, the maximum dominant vibration period is 0.89sec and the minimum dominant vibration period is 0.37sec. The map prepared in this context is presented in Figure 4.37.

The data obtained in order to observe the dominant vibration period were examined within themselves at certain intervals. When the dominant vibration period data obtained from the study area is classified within itself; Between 0.00sec - 0.37sec is 2%, between 0.37sec - 0.57sec 59% and between 0.57sec - 0.89sec 39%.

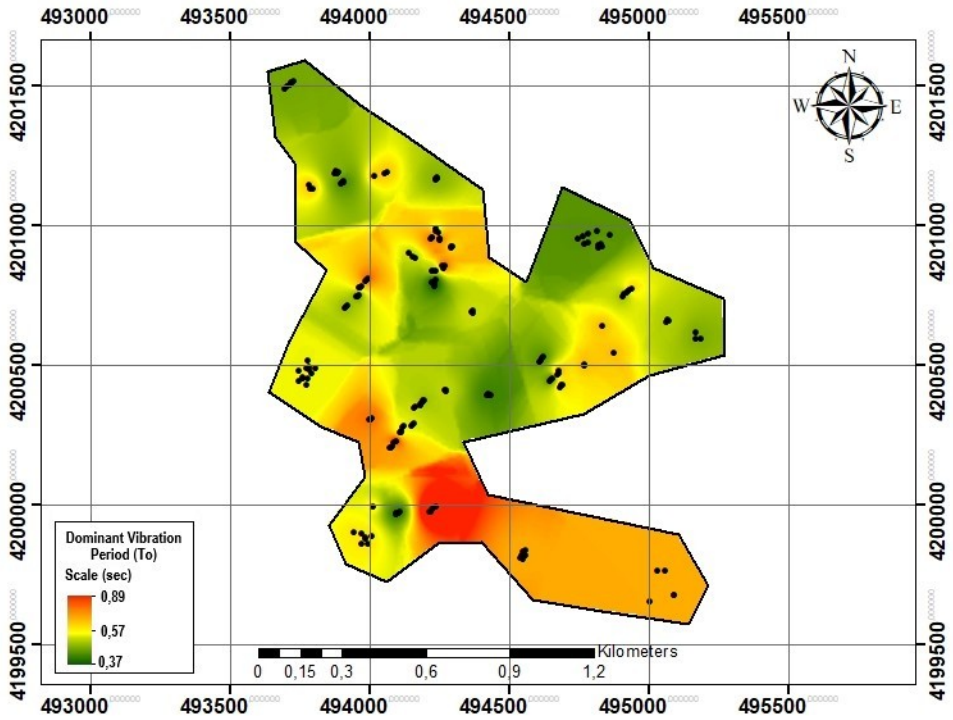

Figure 4.37 Map of dominant vibration period

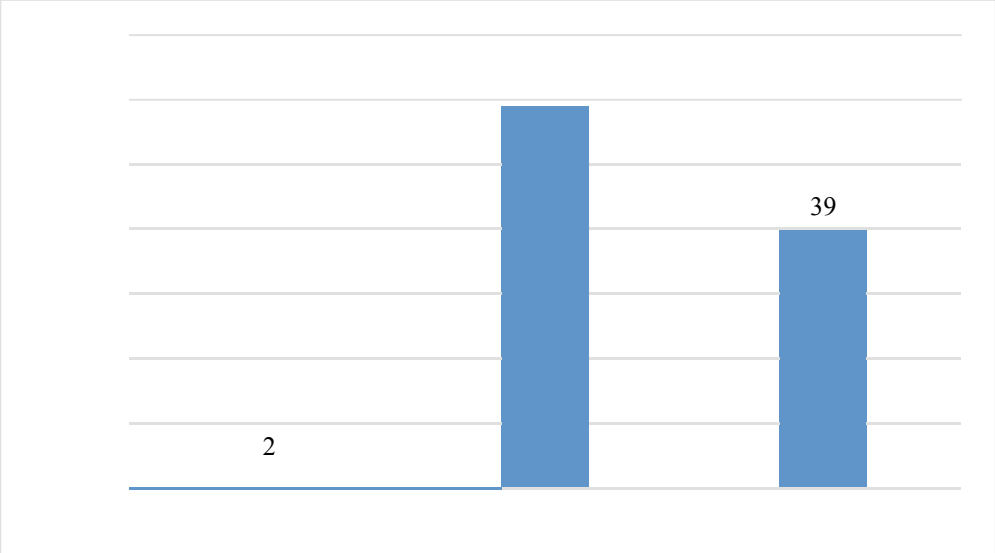

Figure 4.38 Distribution of dominant vibration period

4.7. Soil Classifications Analysis According to Eurocode 8

The soil class according to Eurocode 8 is based on the average velocity (Vs_{30}) of the shear wave velocity up to 30 m depth. The necessary maps for GIS analysis are prepared within the scope of the data obtained by measurements made in the field (Seismic Methods). The maps of soil class values according to Eurocode 8 using ArcGis program are created maps of A, B, C, D soil classes are determined in the prepared map.

As a result of the seismic data obtained from the study area, 0% consists of A, 67% B, 33% C and 0% D soil classes. The map prepared in this context is presented in Figure 4.39.

When looking at the general study area on the soil classification map prepared for Eurocode 8, it is clear that the western part is dominated by the B soil class, while the eastern part is dominated by the C soil class.

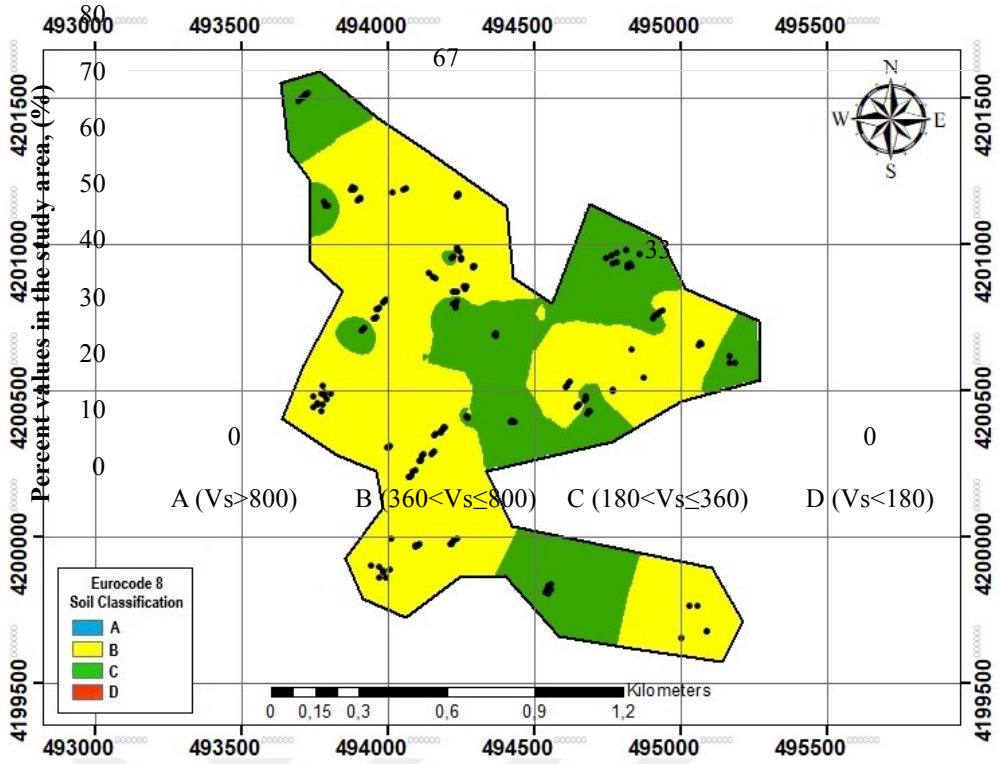

Figure 4.39 Soil classification map according to Eurocode 8

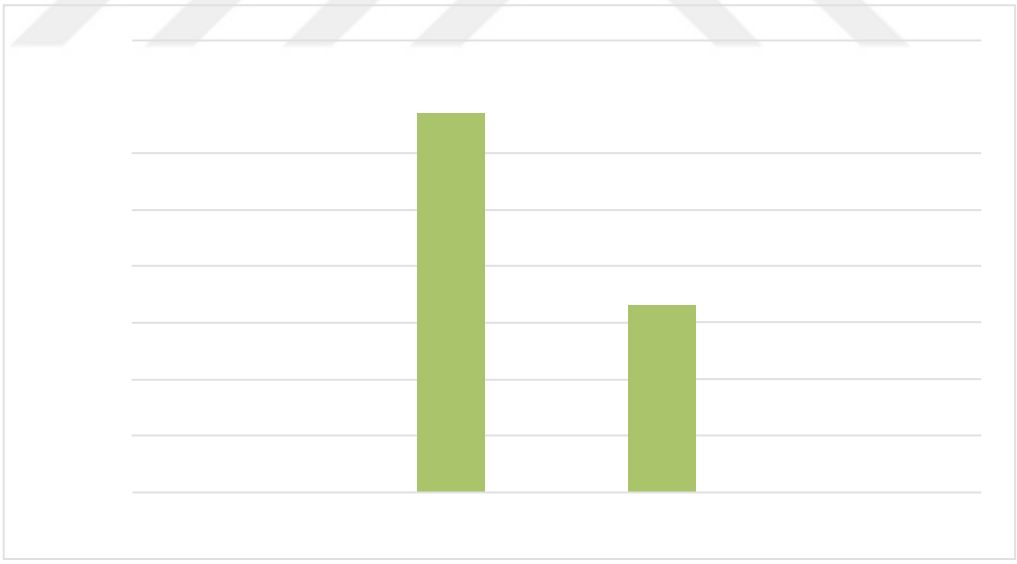

Figure 4.40 Distribution of soil classification values in the study area according to Eurocode 8

4.8. Local Soil Class According to TBDY-2019

The soil class is related to the average velocity of the shear wave velocity Vs_{30} up to a depth of 30 m, according to the TBDY-2019. By using the data obtained by seismic measurements carried out in the study area, the necessary map for GIS analysis was created. While creating the map, ArcGis program was used and estimated maps of soil class values were created. In the prepared map, ZC and ZD soil class types were encountered in the study area.

With the seismic measurements carried out in the study area, it has been determined that 0% of the area is in ZA, 0% in ZB, 67% in ZC, 33% in ZD, %0 in ZE and 0% in ZF soil class. The map prepared in this context is presented in Figure 4.42.

When the map is examined in general, the ZC soil class is more prevalent in the western part of the study area, while the ZD soil class is more prevalent in the eastern part. The purple colored areas on the map represent the ZC soil class, while the water green colored areas represent the ZD soil class.

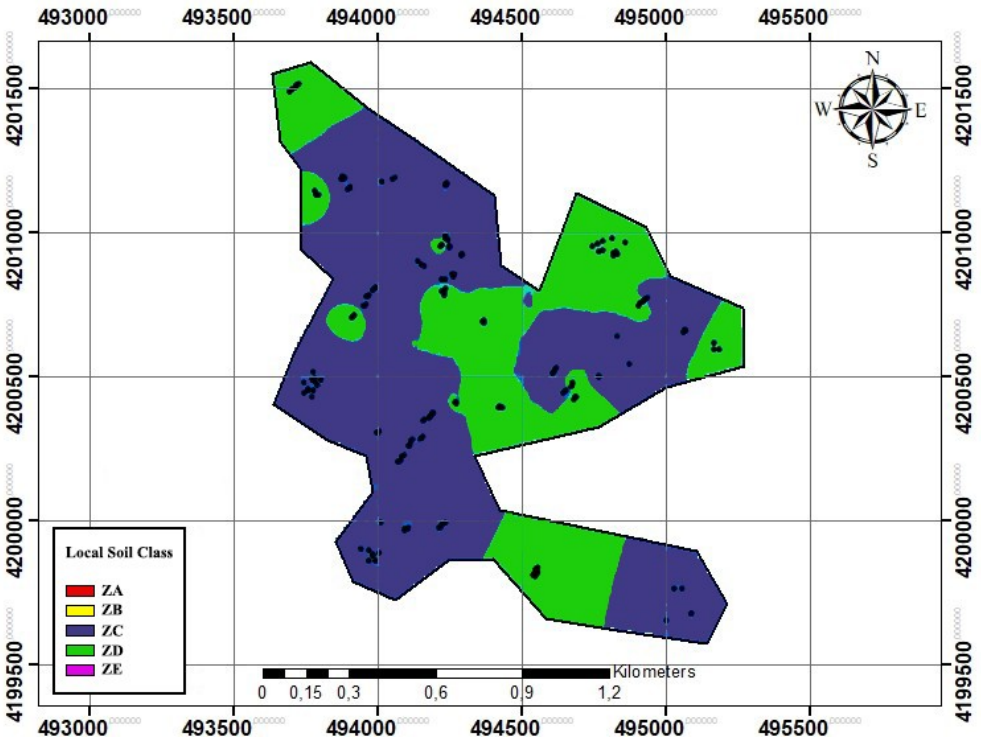

Figure 4.41 Local soil classification map according to TBDY-2019

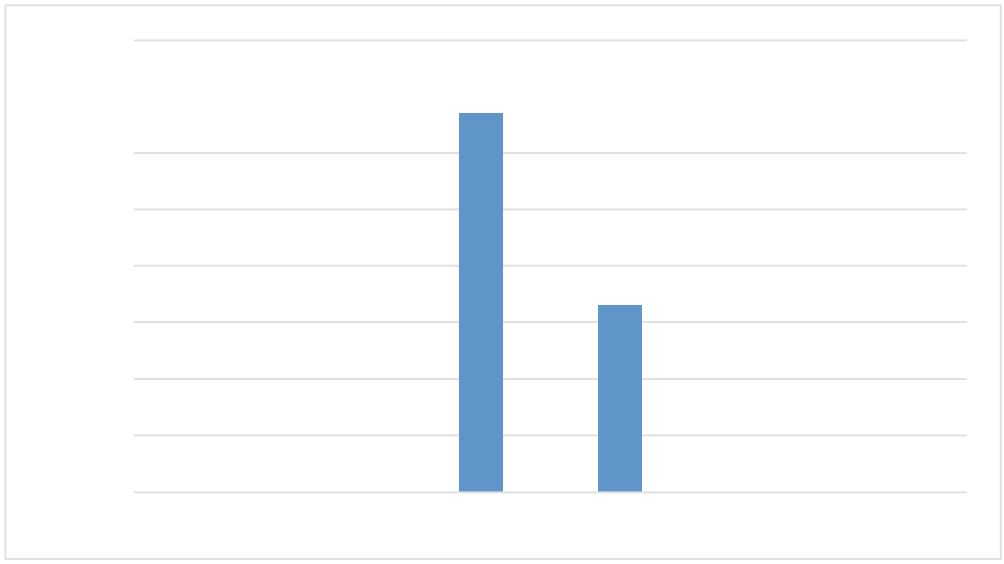

Figure 4.42 Distribution of local soil class values in the study area according to TBDY-2019

CHAPTER 5

CONCLUSIONS AND RECOMMENDATIONS

The values obtained from the field and laboratory test results in the soil survey reports obtained from the archive of the Siirt Environment and Urbanization Directorate used to create a database in this study. A total of 178 drilling points were obtained from the ground survey reports of Siirt Merkez District. Using the geotechnical data in the database, using the GIS-based ArcGis program, for the depths determined in the study area within the boundaries of Siirt Merkez District, SPT maps, bearing capacity maps, shear wave velocity map, NEHRP soil class map, soil amplification map, soil dominant vibration period map, soil classification map according to Eurocode 8 and local soil class map according to TBDY-2019 were created. These maps allow visual evaluation of geotechnical data in the study area. Thus, the digitilization of the data obtained for a part of Siirt Central District will provide information regarding that region in any study to be carried out in that region in the future. In other words, as a result of this study, it is now possible to obtain information about the soil properties in the region while also having easy access to the data. Furthermore, this data, which is available online, is a study that will save time and help the workforce.

- SPT-N data were collected from the obtained drilling points for depths of 1-3 m, 3-5 m, 5-7 m, 7-9 m, and 9-11 m, and maps were created using ArcGIS. It is well known that the SPT-N value is low on loose soil and higher on firm soil. When the maps were examined, it was observed that the SPT-N value increased with depth. In other words, as the depth of the study area increases, so does the firmness of the soil.

- It was determined that 24% of the SPT-N data obtained from 178 drilling points were between 1-20, 31% between 21-30, and 45% between 31-50.

- Many methods are used when calculating the bearing capacity of an area. These methods can be considered as land experiments and geophysical methods. Bearing capacity maps were created by using the Keçeli Method and Tezcan et al. Method, which are geophysical methods. Bearing capacity maps were obtained by using Meyerhof Method and Terzaghi-Peck Method from field experiments.

- In the results obtained by geophysical methods, it has been observed that the bearing capacity of Tezcan et al. Method is greater than that of the Keçeli Method. In the results obtained from the field experiments, it was observed that the bearing capacity of the Meyerhof Method was greater than the Terzaghi-Peck Method.

- Shear wave velocity maps and comparison graphs were created using data obtained from the study area. Shear wave velocities obtained by seismic measurements from soil survey reports were determined. The results of the shear wave velocity obtained by the methods formulated using the SPT-N values were obtained.

- Of the formulated methods, the Imai and Yoshimura Method, the Ohba and Trauma Method, and the Tsiambos and Sabatakakis Method were used. It has been observed that the results obtained from the Imai and Yoshimura Method and the Ohba and Trauma Method are very close to each other.

- It has been observed that the results obtained from seismic measurement in the study area and the results of the methods determined with SPT-N values are different.

- Shear wave velocities reflect the strength of the ground. When seismic measurements of shear wave velocity in the study area were examined, it was discovered that shear wave velocity increased with depth. In other words, as the depth increases, the strength of the soil also increases.

- Vs_{30} is the average value of the shear wave velocities obtained as a result of on-site seismic studies up to a depth of 30m. While the maximum Vs_{30} value is 534 m/sec in the study area, the minimum Vs_{30} value is 240 m/sec.

- 0% of study area Vs_{30}>1500 m/sec, 0% between 760 <Vs_{30} <1500 m/sec , 45% between 360<Vs_{30} <760 m/sec, 55% between 180<Vs_{30} <360 m/sec, and 0% between Vs_{30}<180 m/sec.

- The soil class is related to the average velocity of the shear wave velocity (Vs_{30}) up to a depth of 30 m, according to the NEHRP Earthquake Code. With the seismic measurements carried out in the study area, it has been determined that 0% of the area is in A, 0% in B, 67% in C, 33% in D, and 0% in E soil class.

- An earthquake hazard level map was created according to the soil amplification value obtained from the ground survey reports. It has been determined that 0% of the study area is A (high hazard), 52% is B (medium hazard), 48% is C (low hazard).

- The dominant vibration period represents the natural vibrational properties of the soil layers on the bedrock as a whole. The maximum dominant vibration period on the map is 0.89sec and the minimum dominant vibration period is 0.37sec. When the dominant vibration period data obtained from the study area is classified within itself; 2% between 0.00sec - 0.37sec, 59% between 0.37sec - 0.57sec and 39% between 0.57sec - 0.89sec.

- Soil class maps were created according to Eurocode 8. As a result of the seismic data obtained from the study area, it was observed that 0% A, 67% B, 33% C, 0% D soil class.

- Soil class map was created according to TBDY-2019 with the data obtained from the study area. With the seismic measurements carried out in the study area, it has been determined that map is 0% in ZA, 0% in ZB, 67% in ZC, 33% in ZD, %0 in ZE and 0% in ZF soil class.

Our country is located on many fault lines. As a result, having easy access to soil properties in any part of our country is extremely valuable and important. As the studies conducted in this context are of such importantance and so beneficial to us. The goal of this study is to contribute to the Geographic Information System by analyzing a region in the central district of Siirt in the geotechnical area, and the

study area can be expanded in the future by adding more data analyses that will contribute to this thesis work. Contribution to the Geographic Information System can be made with similar studies for other regions of Siirt Province.

REFERENCES

AFAD (2018), https://deprem.afad.gov.tr/depremkatalogu/deprem-bolgeleri-haritasi

Akın, M.K., Kramer, S.L. and Topal T. (2011). Empirical correlations of shear wave velocity (Vs) and penetration resistance (SPT-N) for different soils in an earthquake prone area (Erbaa-Turkey). *Engineering Geology*, 119, 1–17.

Akkaya, İ., Özvan, A., Akın, M., Akın, M., Övün, U., "Evaluation of Liquefaction Potential of Erciş (Van) Settlement Area Using Shear Wave Velocity (Vs)", Çukurova University Journal of Engineering and Architecture Faculty , 32(3), p. 55-68, 2017.

Alan İ. and Aksay, A, 2002, 1:1000, Scale Geological Maps of Turkey Siirt, Diyarbakır, Van Cizre Maps. 28. MTA. Department of Geological Studies

Ansal, A. M., "Effects of Geotechnical Factors and Behaviour of Soil Layers During Earthquakes", State-of-the-Art Lecture, Proc. of 10th European Con. on Earthquake Engineering, Wien, Austria, (1):467-476, 1994.

Arca, D. and Keskin Çıtıroğlu, H. (2011). Geographic Information System and Application Areas in Geology. Volume 4, Issue 1, 48 – 57.

BDTİM, (2018). Kandilli Observatory and Earthquake Research Institute from past to present, http://www.koeri.boun.edu.tr/new/tr/ tarihce

Bowles, J. E. (1996). Foundation analysis and design 5th. The McGraw-Hill Companies Inc. New York, USA.

Cabalar, AF., Karabas, B., Mahmutoğlu, B., Yildiz, O. (2021). An IDW-based GIS application for assessment of geotechnical characterization in Erzincan, Turkey. *Arabian Journal of Geosciences*, 2129, 2-4.

Chandler A.M., Lam N.T.K., Sheikh M.N., (2002), Response spectrum predictions for potential near-field and far-field earthquakes affecting Hong Kong: soil sites, *Soil Dynamics and Earthquake Engineering*, 22(6), 419-440.

Coduto DP (1994). Foundation design principles and practices. Prentice Hall, Englwood Cliffs

Crampton, J.W., 2011. *Mapping-A critical introduction to cartography and GIS*. UK: John Wiley & Sons Ltd.

Crooks, A.T. and Castle, C.J.E. 2011. The integration of agent-based modelling and geographical information for geospatial simulation. In: Agent-Based Models of Geographical Systems, A.J. Heppenstall, *et al*. (eds), 219–251.

Dejphumee S., 2021. Evaluation of Uncertainties in Site Response Analysis of Deep Soil Profiles in South Carolina Coastal Plain. *Bulletin of the Seismological Society of America* (2021) 111 (4): 1974–1988.

Dinç, S. and Keskin, F.(2017). Petrographic Properties of Units Around Hasankeyf (Batman). *Batman University Journal of Life Sciences.* Volume7, Issue 2/2

Dogruyol, M. (2021). Siirt Province Earthquake Analysis. *Journal of Natural Hazards and Environment.* 7(1), 149-158

Duran, O., Şemşir, D., Sezgin, İ. and Perincek, D. (1988). Stratigraphy, sedimentology and oil potential of the Midyat and Silvan groups in Southeastern Anatolia. TPJD Bulletin, v.1/2, p. 99-126

Erol, A. O. and Çekinmez, Z. (2014). Field tests in geotechnical engineering. Yüksel Proje Publications, Nu: 14-01, Ankara, Turkey

Grants Pass, What is GIS? https://www.grantspassoregon.gov/908/What-is-GIS, 20.02.2022

Goodchild, M.F., 1992. Geographic information science. *International Journal of Geographical Information Systems*, 6 (1), 31–45.

Goodchild, M.F., 2009. Geographic information systems and science: today and tomorrow. *Annals of GIS*, 15 (1), 3–9.

Goodchild, M.F., 2018. Reimagining the history of GIS. *Annals of GIS*, 24 (1), 1–8.

Güzel, M. (2009). Integrated use of geological, geophysical and geotechnical data in microzonation studys (northern adana case), Department of Geological Engineering Instıtute of Natural and Applıed Scıences Unıversıty of Çukurova, PhD.Thesis, Adana.

Halaç, B. (2016). Review of the soil classification criteria in earthquake regulations with respect to amplification, İstanbul Technical University Institute of Science, M.A. Thesis, İstanbul.

Hunter, J.A., et al., 2002, Surface and Downhole Shear Wave Seismic Methods for Thick Soil Site Investigations, Soil Dynamics and Earthquake Engineering, 22, 931-941

Kanai, K., Engineering Seismology, IIESEE Lecture Note, IEESS Japan, 1983.

Kanai, K., "Semi Empirical Formula for the Seismic Characteristic of the Ground", Bull. Earthq. Res. Ins., Vol.35, Part 2, 1965

Karabaş, B. 2019. Use of geographic information system for evaluating the some geotechnical properties in Malatya, Turkey. Master Thesis, Hasan Kalyoncu University.

Kaya A.C. 2008. The Usage of Midyat Stone as A Covering and Building Material Researching. Master Thesis, Cukurova University.

Keçeli, A. (1990). The determination of the dynamic permissible bearing capacity and Settlement by means of the seismic method. Jeofizik 4(2): 83-92.

Kurnaz, T.F. (2011). Geotechnical microzonation of Istanbul Esenler soils based on geographical information systems, Sakarya University Graduate School of Natural and Applied Sciences, Ph.D. Thesis, Sakarya.

Lemmens, M (2011): Geo-information – Technologies, Applications and the Environment, Delft University of Technology, The Netherlands, pp 85-99.

Lin, H., Chen, M., and Lu, G.N., 2013. Virtual geographic environment: a workspace for computer-aided geographic experiments. *Annals of the Association of American Geographers*, 103 (3), 465–482.

MAF, Ministry of Agriculture and Forestry
https://siirt.tarimorman.gov.tr/Menu/90/Siirt-Ili (20.12.2021)

Maptriks, Geographical Information System. https://maptriks.com (13.03.2022)

Mark, D.M., *et al*., 1999. Cognitive models of geographical space. *International Journal of Geographical Information Science*, 13 (8), 747–774.

Nixon, I.K., "Standard penetration test: State-of-the-art report", Proceedings of the 2nd Europen Symposium on Penetration Testing, Amsterdam, Netherlands, 3-21, May 1982.

O'Sullivan D. and Unwin D.J., 2010. Geographic Information Analysis and Spatial Data. Geographic Information Analysis, Second Edition (pp.1 - 31)

Qayum A. (2015). GIS Based Traditional Knowledge Mapping of Natural Resources towards Identifying Malarial Hotspots and Antimalarials, Jawaharlal Nehru University, New Delhi-110067.

Republic of Turkey Ministry of Environment, Urbanization and Climate Change General Directorate of Meteorology. https://www.mgm.gov.tr/veridegerlendirme/il-ve-ilceler-istatistik.aspx?m=SIIRT (07.01.2022)

Rošer, J. dan Gosar, A., 2010. Acta Geotechnica Slovenica 7 (1) 61–76

Sarkar, A (2019): Practical Geography- A systematic Approach, Orient Blackswan Private
Limited, Hyderabad, pp 395-415.

Shaw, S.L., Yu, H.B., and Sombom, L.S., 2008. A space-time GIS approach to exploring large individual-based spatiotemporal datasets. *Transactions in GIS*, 12 (4), 425–441.

Shi, J.Y. and Liu, P., 2014. An agent-based evacuation model to support fire safety design based on an integrated 3D GIS and BIM platform. *Computing in Civil and Building Engineering*, 2014, 1893–1900.

Siirt Municipality Directorate of Reconstruction and Urbanization SMDRU (2020). Survey report on the development plan of Siirt, Siirt municipality settlement area and revised development plan. Siirt, Turkey.

Sivrikaya, O. 2021. Foundation Construction in Civil Engineering I, Istanbul: Birsen Broadcast Distribution Limited Company

Subramaniama P., Yunhuo Z., Danovan W. and Ku T., 2020. Modal analysis of Rayleigh waves using classical MASW-MAM approach: Site investigation in a reclaimed land. *Soil Dynamics and Earthquake Engineering*, Vol.128, 105902

Şengül, T., Karabaş, B. (2021). Investigation of Liquefaction Potential in Kütahya Central District with Geographical Information System. *BSEU Journal of Science*, 8(2), 817-825.

Terzaghi, K. 1943. Theoretical Soil Mechanics. Wiley, New York.

Tezcan, S. S., Keçeli A. and Özdemir, Z. 2010. Determination of safety stresses in soils and rocks by seismic method. *Tübav Science Journal*, 3, 1-10.

Töreyen, G., Özdemir İ. and Kurt. T. (2010). ArcGIS 10 Desktop Application Document

Tsang H.H., Chandler A.M., Lam N.T.K., (2006), Estimating non-linear site response by single period approximation, *Earthquake Engineering & Structural Dynamics*, 35(9), 1053-1076.

Tsutomu Sato, Y.N. and J.S., 2004. 13th World Conf on Earthquake Engineering, Vancouver, B.C., Canada August 1-6, 2004 Paper No. 862

Tuladhar, R., Yamazaki, F., Warnitchai, P. and Saita, J., 2004. Earthquake Engineering and Structural Dynamics 33 (2) 211–225

Ulusay, R. (2000). Soil liquefaction, Blue Planet Popular Science Magazine, TMMOB Chamber of Geological Engineers Publication, 1, 34-45.

Yasobant, S., Vora, K.S., Hughes, C., Upadhyay, A. and Mavalankar, D.V., 2015. Geovisualization: A newer GIS technology for implementation research in health. *Journal of Geographic Information System*, 7:20-28

Yasobant S., Vora K. S., Upadhyay A., (2019) Geographical Information System Applications in Public Health: Advancing Health Research.

Yıldırım, A. and Karadoğan S. (2005). Geomorphology of the Tigris Valley among the Raman-Gercüş Anticlines. National Geography Congress, Turkish Geographical Society - Istanbul University, 29-30 September, 421 - 432, Istanbul

Youd, T. L., Idriss, I. M., Andrus, R. D., Arango, I., Castro, G., Christian, J. T., Dobry, R., Liam Finn, W. D., Harder Jr., L. F., Hynes, M. E., Ishihara, K., Koester, J. P., Liao, S. S. C., Marcuson III, W. F., Martin, G. R., Mitchell, J. K., Moriwaki, Y., Power, M. S., Robertson, P. K., Seed, R. B. and Stokoe II K. H. (2001). Liquefaction resistance of soils: summary report from the 1996 NCEER and 1998 NCEER/NSF workshops on evaluation of liquefaction resistance of soils, Journal of Geotechnical and Geo-environmental Engineering ASCE, 127, 817-832.